Cloning and *in vitro* expression of ferredoxin-I from *Capsicum annuum* L.

A thesis submitted in fulfillment of the requirements for the degree
Master of Applied Science

Linh B. Ton

B.Biotech.

School of Applied Science

Science, Engineering and Technology Portfolio

RMIT University

March 2010

Declaration

I certify that this thesis contains my work that was completed under the supervision of Assoc. Prof. Trevor Stevenson and Dr. Gregory Nugent at School of Applied Science, RMIT University, Australia and Dr. Tran Thi Dung at Nong Lam Univeristy, Vietnam from the period March 2008 to March 2010; except where due acknowledgement has been made, the work is that of the author alone; the work has not been submitted previously, in whole or in part, to qualify for any other academic award.

Linh B. Ton

Date: March 2010

Acknowledgements

First, I would like to thank Vietnamese Ministry of Education and RMIT University Australia as the sponsors for my study.

I would like to express my gratitude for my supervisors Assoc. Prof. Trevor Stevenson, Dr. Gregory Nugent and Dr. Tran Thi Dung for their guidance, supports and encouragements which offered me confidence and persistence to finish my research work.

My special thank goes to Prof. Dave Stalker for his short conversations that helped speed up my research.

I would like to thank Nong Lam Univeristy for offering me the chance to study. Thanks also to Prof. Neil Furlong, Prof. Peter Cole, Assoc. Prof. Nguyen Ngoc Tuan and Ms. Kathryn Thomas for their great patience, immediate support and advice as the scholarship administrators.

I would also like to thank previous and present staffs of Plant Biotech lab, RMIT Univeristy, Dr. Chitra Raghavan, Kim Stevenson, Dr. Kavitha Kuchimanchi, Dr. Yit Heng Chooi and Dr. Veera Chikkala for their support throughout my resrearch. I am really appreciate the encouragement, instructions and support for the protein work from Dr. Van Thi Thu Hao, Joy Tharasuk and Hasmath Hussein.

Thanks to my colleagues in Department of Biotechnology, Nong Lam Univerisy Ho Chi Minh city and friends in Plant Biotech Lab, Biotech Lab, and Teaching Lab of RMIT University, Melbourne for their technical help and friendships.

My sincere thank and hug for my dear friends who helped me through difficulties and shared happiness from the first day till the last day of my stay in Melbourne.

Last, but not least, I am greatly indebted to my grandmoms, parents, brother and relatives for their unconditional love, deeply sympathy, persistent encouragement and support. Finally, I would like to thank my parents for their sacrifice and belief in my science career.

List of Abbreviations

Amp	Ampicilin
AOS	active oxygen species
BLAST	Basic Local Alignment Search Tool
BME	β-mercaptoethanol
bp	base pair
cDNA	complementary DNA
Cm	Chloramphenicol
CPS	Chemiluminescent Peroxidase Substrate
CV	column volume
EDTA	ethylenediaminetetraacetic acid
Fd	ferredoxin
Fe-S	iron-sulfur
FRN	Ferredoxin –$NADP^+$ reductase
Gfp	gene coding for GFP
GFP	Green Fluorescent Protein
H_2O_2	hydrogen peroxide
HR	hypersensitive response
IPTG	isopropyl-β-D-thiogalactopyranoside
JA	jasmonic acid
kb	kilobase
kDa	kilodalton

LB	Luria-Bertani
LRR	Leucine-rich repeat
MAMP	microbe-associated molecular pattern
MCS	multicloning sequence
mM	millimolar
mRNA	messenger RNA
min	minute
µg	microgram
µL	microliter
NADP	nicotinamide adenine dinucleotide phosphate
Ni-NTA	nickel-nitrilotriacetic acid
Ni	Nickle
NO	nitric oxide
O_2^-	superperoxide
PAMP	pathogen-associated molecular pattern
PCR	polymerase chain reaction
Pflp	gene coding for plant ferredoxin-like protein
PFLP	plant ferredoxin-like protein
PR	pathogenesis –related protein
RC	reverse complement
ROI	reactive oxygen intermediate
ROS	reactive oxygen species
rpm	revolutions per minute

SAR	systemic acquired resistance
sec	second
SDS-PAGE	sodium dodecyl sulfate-polyacrylamide gel electrophoresis
SOB	Super optimal broth
TBE	Tris-borate EDTA
Tet	Tetracycline
T-PFLP	PFLP without transit peptide
T-*Pflp*	signal-truncated *Pflp*
UV	ultraviolet
w/v	weight per volume
w/w	weight per weight
X-Gal	5-bromo-4-chloro-3-indolyl-β-D-galactopyranoside

List of databases/softwares

BioEdit	biological sequence alignment editor
Clone Manager	Molecular Biology software package
ClustalW	multiple sequence alignment
EMBL	European Molecular Biology Laboratory
ExPASY	Expert Protein Analysis System
NCBI	National Center for Biotechnology Information

Table of contents

List of figures

List of tables

Thesis abstract

Ferredoxin is a ubiquitous protein among living organisms involving in many fundamental metabolic processes. The contribution of plant ferredoxin-I in bacterial disease resistance of plants has been proved with the emphasis on the iron binding domain. Iron accumulation by ferredoxin-I may play an important role in limiting the growth of the invading bacteria. The N-terminal signal peptide of the protein may have effect on the anti-microbial activity of the protein as directing the protein into chloroplasts instead of maintaining in the cytoplasm.

The objective of this study was to clone the ferredoxin gene from Capsicum leaves and investigate the expression of the cloned genes in *E. coli*. The gene isolation was done based on the published nucleotide sequence for the plant ferredoxin-like protein AF03662. Isolated sequences of ferredoxins with and without signal sequence (*Pflp* and T-*Pflp*, respectively) were sub-cloned into pGEM-T Easy vector and sent for sequencing. The sequence analysis results suggest the isolated ferredoxins are 100% homology in sequences and differs from the polypeptide coding by AF03662. The expression vectors for these gene sequences were constructed with the use of pRSET B expression system. The protein expressions that utilized BL21(DE3)pLysS as the host cells were inducted with 1 mM IPTG for 6 hour before the cell lyse with the sonicator. The His-tagged proteins were purified from 6-hour cell lysate through PolyPrep conlumn containing Ni-NTA under native conditions with the use of immidazole. The protein expressions and purifidations were evaluated by SDS-PAGE analysis followed by either Coomassie staining and immunodetection.

Chapter 1 Literature review

1.1 Bacteria and plant diseases

Bacteria can be found everywhere including in cold, dry valleys of Antarctica or in water near boiling temperature (Dube *et al.,* 2001). Some are beneficial to humans and the environment through diverse metabolic processes such as carbon catalytic, and nitrogen fixation. On the other hand, pathogenic bacteria cause severe to fatal diseases in humans, animals and plants (Ellis *et al.,* 2008). Bacteria account for around 5-10% of plant diseases of which 50-65% caused by fungi and 10 - 20% caused by viruses. There are also genetic and abiotic factors that cause diseases in plants such as genetic defects, pollution, extremes of temperature or pH, and mineral deficiency (Table 1.1) (Sigee, 1993). Plant pathogenic bacteria are present in five major genera – *Agrobacterium, Erwinia, Pseudomonas, Xanthomonas* and the coryneform bacteria including the genera *Arthrobacter, Clavibacter* and *Curtobacterium* (Sigee, 1993). In relation to plants, bacteria may be considered in two main groups: epiphytic bacteria which are present on plant surfaces and aerial (phyllosphere) regions, and internal bacteria which infect plant tissue (Sigee, 1993). Fungi are the cause of almost all diseases in plants and losses in agriculture. However, bacteria with their rapid development inside host plants and variety ways of dispersal has become a major economic concern in agriculture. Fire blight has been known as the most destructive disease of pome fruit caused by *Erwinia amylovora* and was reported to be present in 31 countries (van der Zwet, 1993; van der Zwet & Bonn, 1999). Citrus canker which is one of the most severe diseases of citrus crops caused by the bacteria *Xanthomonas axonopodis* pv. *citri* originated from tropical areas

of Asia and later emerged in South America, South Africa and Australia (Das, 2003). Banana Xanthomonas Wilt (BXW) disease which is caused by *Xanthomonas campestris* pv. *musacearum*, from 2001 to 2007, spread from the central part of Uganda to more than 35 districts in areas of intensive banana production (Mugira, 2009). In the case of BXW disease, the causal bacteria are dispersed by insects, wind-driven rainfall, infected planting materials and contaminated planting tools (Mugira, 2009). They are also the common means for the spread of plant pathogenic bacteria of economic concern. There are currently no long–termed effective treatment for plant diseases caused by bacteria (McManus & Stockwell, 2001).

Table 1.1 Percentage occurrences of different agents in lists of named diseases of crop plants

	Soft fruit	Cereals	Root crop	Ornamentals
Biological agents				
Fungi	49	58	55	64
Bacteria	6	6	9	8
Mollicutes	2	1	2	1
Viruses	14	15	12	8
Graft-transmissible	4	_	_	3
Nematodes	13	20	17	16
Algae	*1			
Higher plant (*Cuscuta*)	*1	_	_	1
Genetic defects	2	*1		
Physical agents				
Pollution	_	*1	*1	_
Physical	3	_	2	_
Mineral deficiency	1	*1	*1	_
Cause unknown	4	*1	2	_

*1, less than 0.5% of total list

Data are collected from Hansen (1985) for soft fruit (apple, citrus, pear, tomato), cereals (barley, corn, oats, wheat), root crops (beet, potato, onion, sweet potato) and ornamentals (rhododendron, rose, carnation, chrysanthenum) by Sigee (1993).

1.2 Plant loss by pathogenic bacteria

A number of bacterial diseases challenge important crops with direct economic loss due to reduction in yield and quality of harvest and indirect loss due to expense for disease control. Post-harvest damage of agricultural product caused by plant pathogenic bacteria is also of major concern (Sigee, 1993). The loss and its effect may extend to social issues where crops are main sources of food or important export commodities. Since 2001 the Banana *Xanthomanas* Wilt epidemic in East and Central Africa destroyed 60% of the bananas leading to the total economic loss of between 2 to 8 billion USD in the last 10 years (Mugira, 2009). However, the loss by Xanthomonas is of more concern for food security aspect than economic issues as banana is the most important staple food crop in Uganda and many countries in the East African Great Lakes region (Biruma *et al.*, 2007). Fire blight spread in Michigan in 2000 caused the death of over 220,00 apple trees with a total loss of 42 million USD. The estimated losses to fire blight and cost of disease control in US are over 100 million USD (Norelli *et al.*, 2003). Bacteria of economic concerns with their host, causal diseases and geographic distribution are summarized in the following table (Sigee, 1993).

Table 1.2 Economically important bacterial plant pathogens

Bacterium	Host	Disease	Geographic location
Agrobacterium tumefaciens	Rosaceae, chrysanthemum, grapevine	Crown gall	Temperate & mediterranean regions
Erwinia amylovora	Apples, pears & some ornamentals	Fireblight	World - wide in temperate zones
Erwinia carotovora	Potato	Soft rot	Temperate zones
Pseudomonas solanacearum	Over 200 species, e.g. banana, potato, tobacco, tomato	Bacterial wilt	World-wide in tropics & subtropics
Xanthomonas campestris pv. *citri*	Citrus fruit	Citrus canker	Asia, South America, North America (Florida), New Zealand
Xanthomonas campetris pv. *oryzae*	Rice	Leaf blight	Asia, South & North America, Australia, China

1.3 Bacterial structures and functions

1.3.1 Size and shape

Bacteria are single-celled, microscopic, prokaryotic organisms. Bacterial cell shape can be found in forms of spherical cells (coccus), ovoid cells (coccobacillus), straight/curved rod (vibrio), spiral rod i.e. spirillae, flexible rod (spirochetes) or filament (Actinomycetes). The normal morphology of the bacteria may change due to the available source of nutrition. Cocci generally have a diameter of about 0.1-1μm and rod shaped cells have a length of 1-2 μm. The size of cyanobacteria is much lager than the average size of bacteria (Janse, 2005).

1.3.2 Nucleoid

Nucleoid region of bacteria involves the central nucleoid and the peripheral ribosomal region. The central nucleoid contains a major part of the bacterial genome, which is present as highly condensed strands of supercoiled DNA. The peripheral ribosomal area may contain extensions of central nucleoid, granular inclusions, mesosomes, refractive bodies, polar bodies, bacteriophage particles and plasmids. Granular inclusions are composed of poly-β-hydroxybutyrate (PHB) and detectable in heat-fixed smear preparations of bacterial cells under light microscope. The presence of granules is a defined characteristic that is useful in bacterial classification. There are no reports on the relationship between the peripheral area and pathogenicity of plant pathogenic bacteria so far (Sigee, 1993).

1.3.3 Outer and inner (cytoplasmic) membrane

Outer and inner membranes of Gram-negative bacteria are generally identical with clear lipid bilayer structure except their lipopolysaccharide and protein composition. The outer membrane comprises of rigid peptidoglycan basal layer, attachment of lipopolysaccharides, lipoproteins and specialized porin proteins on the outerside of the outer membrane (Ghuysen & Hakenbeck, 1994; Janse, 2005). These features make the outer membrane the main barrier that protects the cell from toxic substances and interacts with the outside environment. The inner membrane is the barrier between the cytoplasm and the outside part of the cell, which is the site of biochemical and signal transduction reactions and transport activities.

1.3.4 Lipopolysaccharide (LPS)

Lipopolysaccharides (LPS) forming the outermost layer of Gram-negative bacterial cell are amphipathic molecules (Newman *et al.*, 2001). Each LPS consists of three main regions, an inner lipid region (lipid A), a core region of polysaccharide and an outer region of polysaccharide (O-antigen). Lipid A consists mainly of a glucosamine disaccharide and fatty acid. The O antigenic chain is primarily composed of a chain of repeat units of oligosaccharides. It is the major determinant for surface characteristics of bacterial cell and mainly responsible for antigenic properties of the bacterial strain, however, it is neither essential for viability nor pathogenicity of bacteria. LPS has been proved to involve plant defensive responses (Dow *et al.*, 2000; Newman *et al.*, 2001). Pathogenic bacteria with defective LPS show increased *in vitro* sensitivity to antibiotics and antimicrobial peptides and declined number of viable bacteria in plant (Titarenko *et*

al., 1997). Purified LPS is believed to induce accumulation of certain pathogenesis-related proteins (PRs) in plants (Newman *et al.,* 1995). Infiltration of LPS preparations from different kinds of bacteria including non-pathogenic and plant pathogenic bacteria *e.g. Erwinia* spp., *Pseudomonas* spp. can suppress the hypersensitive response induced by bacteria containing avirulent or virulent gene (Mazzucchi & Pupillo, 1976; Mazzucchi *et al.,* 1979; Dow, 2000).

1.3.5 Membrane lipids and membrane proteins

The membrane lipid composition of plant pathogenic bacteria can be an important taxonomic feature. In Gram-negative bacteria, there are approximately 50 and 300 different proteins in the outer and the inner membrane, respectively. The outer membrane possesses a small number of major proteins compared to a large variety of proteins of the inner membrane (Ghuysen & Hakenbeck, 1994). Outer membrane proteins act as channels supporting transport activities and receptors as signal translators from the outside environment.

1.3.6 Periplasmic space

Periplasmic space is the space between outer and cytoplasmic membrane. It is an important reservoir of about 100 proteins and cell wall materials. Periplasmic proteins mainly function in nutrient uptake and catabolism. The cell wall materials contained within the periplasm are important for the rigidity of bacterial cells due to the cross-linking between the peptides of adjacent peptidoglycan chains (Figure 1.1).

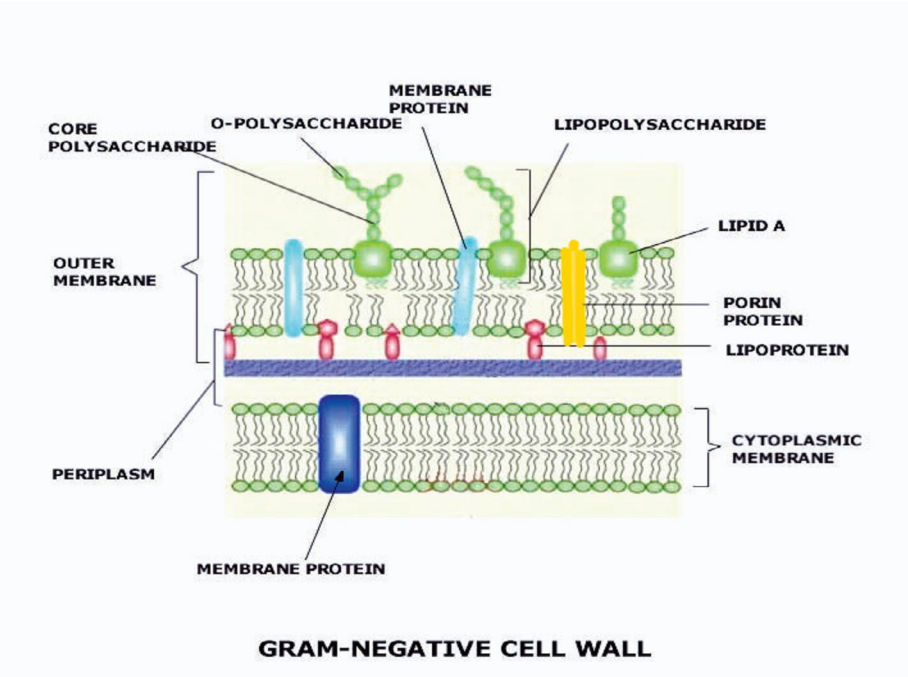

Figure 1.1 Cell wall structure of Gram-negative bacteria. Taken from Janse (2005)

1.3.7 Capsule

Capsule is a slime layer covering the bacterial cell, which partly present as a well-defined capsule and partly diffuses into the surrounding environment. Bacterial capsule may be visible with a light microscope using negative-stain method and under transmission electron microscope using ruthenium red stain. Composition of capsule is primarily a matrix of polysaccharides, possibly polypeptide and glycopeptides. Polysaccharide content of the slime presents in different forms (*e.g.* homo/hetero – polysaccharide, neutral/acidic molecules) depending on genera of bacteria. However, the production of capsule sometimes depends on culture conditions (Sigee, 1993). Extracellular polysaccharides produced by plant pathogenic bacteria form a protective barrier for the bacterial cell and is believed to be involved directly in host-pathogen interactions as virulence factors (Dow *et al.,* 1995).

1.3.8 Flagella

Bacterial flagella may be divided into three major parts: the filament which is 50-100 μm in length and 20 nm in diameter, connected to the basal body by the hook; and the motor (Macnab & Aizawa, 1984; Janse, 2005). Flagella have a simple structure comprised of glycoprotein protein (Taguchi *et al.,* 2009). It functions as means for bacterial motility that is controlled by genes coding for stimuli receptors, transducers and flagella motion (Macnab & Aizawa, 1984; Manson, 1990).

1.3.9 Fimbriae and pili

Fimbriae and pili are nonflagellar filamentous proteinaceous appendages that widely occur among various types of bacteria (Ottow, 1975; Romantschuk, 1992). Their size is around 0.2-20 μm in length, and 3-14 nm in width (Ottow, 1975). The filament is made up with helically arranged subunits of a protein whose size is different depending on fimbrial types. Both fimbriae and pili have specific sites for adhesion on the target surface and viral recognition (Ottow, 1975; Bauer, 1986; Romantschuk *et al.*, 1993). Pili have an additional function in sexual conjugation (Romantschuk, 1992; Sigee, 1993).

1.4 Materials of plant cover

1.4.1 Plant cell wall

Access to intercellular space of plant cells is the first step in infection process of phytopathogenic bacteria (Huang, 1986; Strange, 2003). Thus, the plant epidermis and plant cell wall act as barriers to protect plant cells from pathogens as well as interacting with the extracellular environment. Each plant cell is surrounded by two kinds of cell walls, the outer primary wall and the inner secondary wall (Strange, 2003). Primary cell walls of higher plants comprise of polysaccharides (up to 90% of the dry weight), structural glycoprotein (2-10%), phenolic esters (up to 2%), bound minerals (1-5%), and enzymes (O'Neill & York, 2003). Macromolecular components of primary walls include cellulose, hemicellulose and pectic polysaccharides (O'Neill & York, 2003). When most of cell growth has ended, secondary walls are formed with primary deposition of lignins

and suberin (Boudet, 2003; Strange, 2003). The presence of secondary walls leads to the rigid structure of the plant body (Boudet, 2003). Middle lamella lies between cells and composed of pectic compounds including, usually, chains of galacturonic acid residues and proteins (Strange, 2003). Divalent cations (*i.e.* Ca^{2+}) are involved in the combination of polygalacturonic chains and form the gel properties of pectin (Strange, 2003).

1.4.2 Cuticle

Plant cuticle is collectively composed of cutin, a biopolyester composed of hydroxyl and epoxy fatty acids, and wax, a complex mixture of soluble lipids. Cuticle is attached by pectin layer to the epidermal cell walls of the aerial parts of plant such as fruits and leaves (Figure 1.2) (Kolattukudy, 1980; Kolattukudy, 2001).

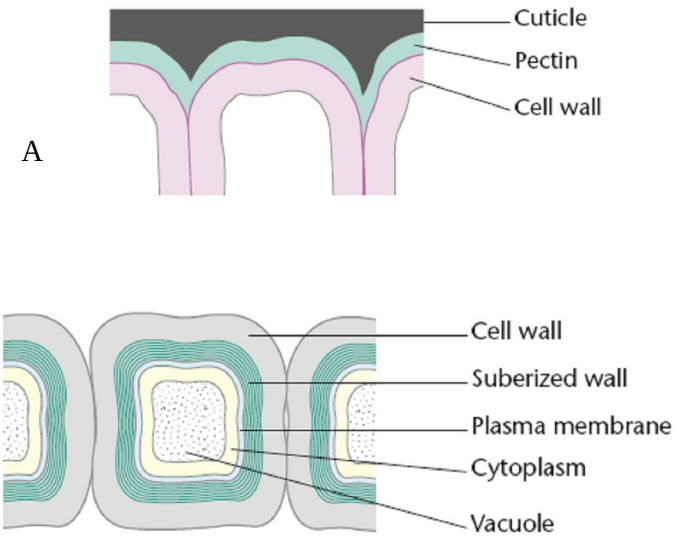

Figure 1.2 Plant cuticle.

(A) Plant cell wall; (B) Suberized wall. The figure is taken from Kolattukudy (2001).

1.4.3 Suberin

Suberin, a polymer containing aromatics and polyesters, is synthesized in cells from the innermost layer the outermost layer of the underground parts *e.g.* root, tubers (Kolattukudy, 1980). Suberin is formed in wounded surfaces on aerial parts of plants and is considered a wound-induced polymer (Kolattukudy & Dean, 1976; Garrod *et al.*, 1982; Mohan *et al.*, 1993) .

1.4.4 Lignin

Lignin is a polymer of aromatic subunits usually derived from phenylalanine (*e.g.* coniferyl alcohol and monolignols) (Whetten & Sederoff, 1995). This polymer is present in the middle lamella and inner side of the secondary wall (Donaldson, 1992; Fromm *et al.*, 2003). Lignification can be induced in many cell types by disease or wounding (Whetten & Sederoff, 1995).

1.5 Natural openings

1.5.1 Stomata

Stomata are pores bordered by two semicircular guard cells, present in the epidermis of leaves, especially on the undersurface, and young shoots (Schulze-Lefert & Robatzek, 2006). The movement of guard cells that is sensitive to atmospheric conditions controls stomata aperture and facilitates gas exchange with the atmospheric environment as well

as water transport from roots to the upper parts of plants (Torii, 2006; Schulze-Lefert & Robatzek, 2006).

1.5.2 Hydathodes

Hydathodes are pores present in the epidermis or margins of leaves of certain plants, and surrounded by two crescent-shaped cells like stomata. However, the size of their aperture is not regulated. The inside of the pore is composed of loosely arranged thin walled parenchyma cells, the epithelium (Rajan, 2003). The process of water secretion through hydathodes under conditions that transpiration is inhibited (*e.g*. high humidity) is called guttation (Singh *et al.,* 2009). Guttation water is known to contain various compounds in dissolved state including various kinds of enzymes, sugars, amino acids, vitamins and mineral elements (*e. g.* P, K, Na, Mg, Fe) (Rajan, 2003). This fluid contains a variety of potential nutrients and growth factors for epiphytic bacteria and fungi (Goatley & Lewis, 1966; Blakeman & Fokkema, 1982; Frossard & Oertli, 1982).

1.5.3 Flower

Pollens, stigma and nectaries provide short-term habitat for certain plant bacteria (*e.g*. *Pseudomonas syringae* pv. *syringae* and *Erwinia amylovora*) (Sigee, 1993). Pollens contain lipids, proteins, pigments, and aromatic compounds. Stigmas, the receptive portions of the female tissues, are generally classified into two groups: wet stigma covered with a viscous surface secretion from epidermal cells containing proteins, lipids, polysaccharides and pigments; and dry stigmas that have intact surface cells (Edlund *et al.,* 2004). Nectary, a common secretory tissue in angiosperms that produces nectar,

which may be situated in vegetative parts or reproductive parts of plants (Vesprini *et al.*, 1999). Nectar secretion occurs in different ways through pores in the epidermis or after rupture of the cuticle under nectar pressure (Vesprini *et al.*, 1999). Nectar is mainly composed of sucrose, fructose and glucose (less than 5% of the sugar), proteins and lipids, which attracts both pollinators and certain epiphytic microorganisms (Vesprini *et al.*, 1999; Bubán & Orosz-Kovács, 2003).

1.5.4 Lenticels

Lenticels originate from cells beneath stomata with porous structure comprised of parenchyma cells (Beck, 2005); epidermis components of stems, roots, leaves and fruits (Neish *et al.*, 1995; Everett *et al.*, 2008). They provide means for gas exchange between the internal tissues and the atmosphere (Kenoyer, 1903).

1.6 Bacterial access into plant tissue

1.6.1 Migration

Phytopathogenic bacteria are transmitted by vectors, in a huge variety of ways, as means for bacterial survival, dissemination, and penetration into plant tissue (Sigee, 1993). Flagellar motility of bacteria is beneficial to their survival in a wide range of environments, especially in which essential factors *i.e.* nutrition, oxygen become limiting (Kelman & Hruschka, 1973; Panopoulos & Schroth, 1974; Macnab & Aizawa, 1984; Turnbull *et al.,* 2001). In plant-associated bacteria, motility enables them to reach favorable sites of infection through chemical (chemotaxis) or oxygen (aerotaxis) stimuli (Chet *et al.,* 1973; Panopoulos & Schroth, 1974; Huang, 1986). Chemotaxis and motility are reported to enhance the initial contact and adsorption of symbiotic rhizobia to the host root surface, increase in the efficiency of nodule initiation as well as the rate of infection development (Caetano-Anolles *et al.,* 1988). However, the systemic invasion of bean leaves by *Pseudomonas phaseolicola* is independent of flagellar motility (Panopoulos & Schroth, 1974). In most of studied cases, the motile strain of studied bacteria actively reaches favorite plant surfaces, while the non-motile strain is randomly passively distributed or slower in movement to the sites of infection (Panopoulos & Schroth, 1974; Romantschuk, 1992; Turnbull *et al.,* 2001). Movement of bacteria is directed by flagella towards or away from attractants or repellents (Panopoulos & Schroth, 1974; Caetano-Anolles *et al.,* 1988). Receptors on cell envelop and cytoplasmic proteins co-ordinate the movement of flagella upon chemotaxis or aerotaxis (Manson, 1990).

1.6.2 Attachment and entry

Attachment of bacterial cells to foliage and root surfaces is an early and significant step in the infection process in certain disease and may contribute to the increase of pathogenic bacteria on plant surfaces (Lippincott & Lippincott, 1969; Romantschuk *et al.*, 1993; Dulce *et al.*, 2007). Successful attachment to plant surfaces of plant-associated bacteria facilitates their epiphytic growth or the initial phase of colonization (Romantschuk *et al.*, 1993; Turnbull *et al.*, 2001; Dulce *et al.*, 2007). In some plant pathogenic bacteria, fimbriae contributes to the attachment to their host surfaces, for example, in case of *Pseudomonas syringae* pv. *phaseolicola* (Romantschuk, 1992) *Pseudomonas solancearum* (Young *et al.*, 1985) and *Agrobacterium tumefaciens* (Dulce *et al.*, 2007). Bacteria gain access into plant tissue through natural openings: stomata (Melotto *et al.*, 2006), hydathodes (Staub & Williams, 1972), nectarhodes (Bubán & Orosz-Kovács, 2003), or through wounds (Lippincott & Lippincott, 1969).

1.7 Plant-bacteria interactions

1.7.1 Locations and conditions

Plant pathogenic bacteria usually undergo two phases of colonization, external phase on plant surfaces and internal phase inside plant tissue (Beattie & Lindow, 1995; Hallmann, 2001). Internal growth phase of plant pathogenic bacteria usually occurs in intercellular spaces of plant tissue or cell apoplasts, less frequently in vascular tissue and leaf parenchyma tissue, and intracellular spaces (Staub & Williams, 1972; Hallmann, 2001; Rico *et al.*, 2009). Plants recognize bacterial presence when bacterial population reaches a certain concentration which is about 10^4 cells/mL in tobacco tissue (Sigee, 1993).

1.7.2 Compatible and incompatible interaction

Interactions between plant and bacteria happen at different level depending on the plant specificity or recognition of bacteria and bacterial exposure to plant. Many studies on plant-microbe interactions have been performed on popular plant pathogenic bacteria of genera *Pseudomonas*, *Erwinia*, and *Xanthomonas* (Montesinos *et al.*, 2002). Plants can only recognize a certain group of pathogens and a strain of bacteria is able to invade a limited number of host species. Specificity in interaction between pathogen and host plants is based on gene-for-gene elicitor-receptor model (Baker *et al.*, 1997; Montesinos *et al.*, 2002). According to this model, the compatibility of the combination beween avirulence (*avr*) genes in pathogen and resistance (*R*) genes in the host plant accounts for their specific interactions. A non-complementary combination of this gene pattern results

in compatible interactions and plant failure to recognize the pathogens. Thus, the pathogens have chance to continue their invasion causing disease development. By contrast, a non-compatible combination of *avr* and *R* genes results in an incompatible interaction and activation of defense responses in plant (Montesinos *et al.*, 2002). These responses can be localized or systemic involving the recognition of pathogen by the host plant, signal transduction and expression of several genes.

1.7.3 Plant innate immunity

Natural openings, especially stomata, were believed as passive port for the entry of foliar bacteria. However, recent findings have recognized that stomata can actively limit bacteria passage (Melotto *et al.*, 2006; Melotto *et al.*, 2008). Guard cells have leucine-rich repeat (LRR) receptors that are sensitive to pathogen-associated molecular patterns (PAMPs) or activated microbe-associated molecular patterns (MAMPs). This reaction leads to the induction of stomata closure (Melotto *et al.*, 2008). MAMPs or PAMPs are defense elicitors are evolutionary stable and reported to improve plant resistance (Bent & Mackey, 2007).

1.7.4 Hypersensitive response (HR)

Incompatible interaction between pathogen and plant cell results in hypersensitive response (HR) (Goodman, 1978; Sigee, 1993) characterized by rapid localized cell death and activation of defence genes in the surrounding cells (Watanabe & Lam, 2006). The dead cell region is dehydrated quickly and becomes a barrier limiting the growth of

pathogen within the infected site (Watanabe & Lam, 2006). The apoptosis in HR is believed to initiate with rapid accumulation of reactive oxygen intermediates (ROI), superoxide (O_2^-), hydrogen peroxide (H_2O_2), and nitric oxide (NO) (Langebartels *et al.*, 2002; Watanabe & Lam, 2006). Production of reactive oxygen species (ROS) and a number of phosphorylation events activate the signal network relating to systemic acquired resistance (SAR) (Langebartels *et al.,* 2002; Nawrath *et al.,* 2006). The feature of this response is the production of signal molecule such as salicylic acid (SA), jasmonic acid (JA), nitric oxide (NO) and ethylene; and the expression of defence genes including pathogenesis-related (PR) genes (Montesinos *et al.,* 2002; Nawrath *et al.,* 2006).

1.8 Active defense

1.8.1 Systemic acquired resistance (SAR)

Induced resistance is an active defense mechanism of plants and is also a feature of incompatible interactions of plants and pathogens (Hutcheson, 1998). There are two types of induced resistance including systemic acquired resistance (SAR) and induced systemic resistance (ISR) (Hammerschmidt, 1999; Heil & Bostock, 2002). SAR is characterized by an accumulation of salicylic acid (SA) and pathogenesis-related proteins (PRs) following an occurrence of necrotic lesion caused by a pathogen (fungi or bacteria) (van Loon, 1997; van Loon *et al.,* 1998; Hammerschmidt, 1999; Maldonado *et al.,* 2002). The resistance develops both locally and systemically based on SA signalling pathway (Durner *et al.,* 1997; Hammerschmidt, 1999). The enhancement and translocation of SA lead to an increase in the endogenous level of H_2O_2 and other reactive oxygen species due to the capacity of some catalase isoenzymes to inhibit the H_2O_2 degrading activity

(Durner *et al.,* 1997; Molinari & Loffredo, 2006). Hydroxyperoxide has been believed to be a signal that causes activation of family 1 of pathogenesis-related proteins (PR-1) gene expression (Durner *et al.,* 1997; Molinari & Loffredo, 2006). PRs play important roles in limiting pathogen growth, indirectly by helping to reform host cell walls at wounded sites, or directly, by their antimicrobial and enzymatic activities (Durner *et al.,* 1997; Hammerschmidt, 1999). These proteins include cell wall polymers (lignin and suberin), phenylpropanoids and phytoalexins (Durner *et al.,* 1997; van Loon, 1997). HR with generation of ROS also induces several families of PRs (Durner *et al.,* 1997; van Loon & van Strien, 1999). There have been 14 families of PRs recognized in various crop plants which were classified based on their amino acid sequences, serological relationships and enzymatic or biological activity (van Loon & van Strien, 1999; Edreva, 2005). Inducible PRs are usually acidic proteins secreted into intercellular spaces (van Loon, 1997; Heil, 2001; Heil & Bostock, 2002). Basic PRs expressed at a low level mainly located in the vacuole (van Loon, 1997; Heil & Bostock, 2002). SAR can also be induced by exogenous application of salicylic acid (SA) or synthetic compounds such as CGA-245704 (a benzothiadiazole derivative) and CGA-41396 (2,6-dichloroisonicotinic acid) (Hammerschmidt, 1999).

1.8.2 Induced systemic resistance (ISR)

Another kind of systemic resistance which is similar to SAR induced by nonpathogenic rhizobacteria is categorized as induced systemic resistance (ISR) (van Loon *et al.,* 1998; Choudhary *et al.,* 2007). ISR and SAR share some similarities as systemic resistance in providing plants a non-specific, local and systemic protection (van Loon *et al.,* 1998). In both types of induced resistance, it generally takes from a few days

to a week for the plants to reach the induced state after the induction (van Loon *et al.,* 1998). Besides, plant induced resistance is only activated with the inoculation of a bacterial dosage that exceeds a threshold population size; and it is maintained during the lifetime of the plant (van Loon *et al.,* 1998). Unlike SAR initiation by pathogen that causes necrotic lesions, there are not any visible symptoms on the host during ISR (van Loon *et al.,* 1998). Rhizobacteria can activate plant resistance in varied ways by their lipoplysaccharides, siderophores, and SA (van Loon *et al.,* 1998; Newman *et al.,* 2001). Some rhizobacteria induce resistance through SA-dependent SAR pathway, while the others require jasmonic acid (JA) or ethylene signalling compounds for ISR to develop (van Loon *et al.,* 1998; van Loon *et al.,* 2006). The type of systemic resistance activated in plants and the associated signalling transduction pathway depends on the strain of inducing bacteria, the host plants, and the pathogen (van Loon *et al.,* 1998; Kloepper *et al.,* 2004). Defensive capacity of plants through ISR may be due to the accumulation of antimicrobial compounds such as phytoalexins and β-1,3-glucanase (van Loon *et al.,* 1998). Rhizobacteria associated ISR are also referred to as plant growth-promoting rhizobacteria (PGPR) (Kloepper *et al.,* 2004). The direct enhancement of plant growth by PGPR may result from the supply of the bacterial metabolites (Shoda, 2000; Montesinos & Vilardell, 2001; Saleem *et al.,* 2007). PGPR can also indirectly stimulate plant growth by suppressing plant pathogens through antagonism as well as through activation of plant defence (van Loon *et al.,* 1998; Kloepper *et al.,* 2004; Saleem *et al.,* 2007).

Figure 1.3 Model for elicitation of active defense responses in plants.

Products of avirulence genes (Avr) are secreted by the pathogen into the apoplast. Reversible binding of avirulence products to resistance gene products (R1-3) are indicated by the two-headed arrows. Leucine- rich repeat (LLR) domains are indicated by the small linked circles. Plant cells may have more than one member of each family and not every family will be present in a cell. Dashed lines represent possible pathways and hypothetical components indicated by the question marks. Coincident events with induced gene expression include opening of Ca^{2+} and K^{+} channels and accumulation of H_2O_2. Abbreviations: K, protein kinase; nls, nuclear localization signal; SA, salicylic acid; LZ, TIR,, signal transduction domain; Ptix, Pti1, Prf, NADPH; PCD, programmed cell death (Hutcheson, 1998)

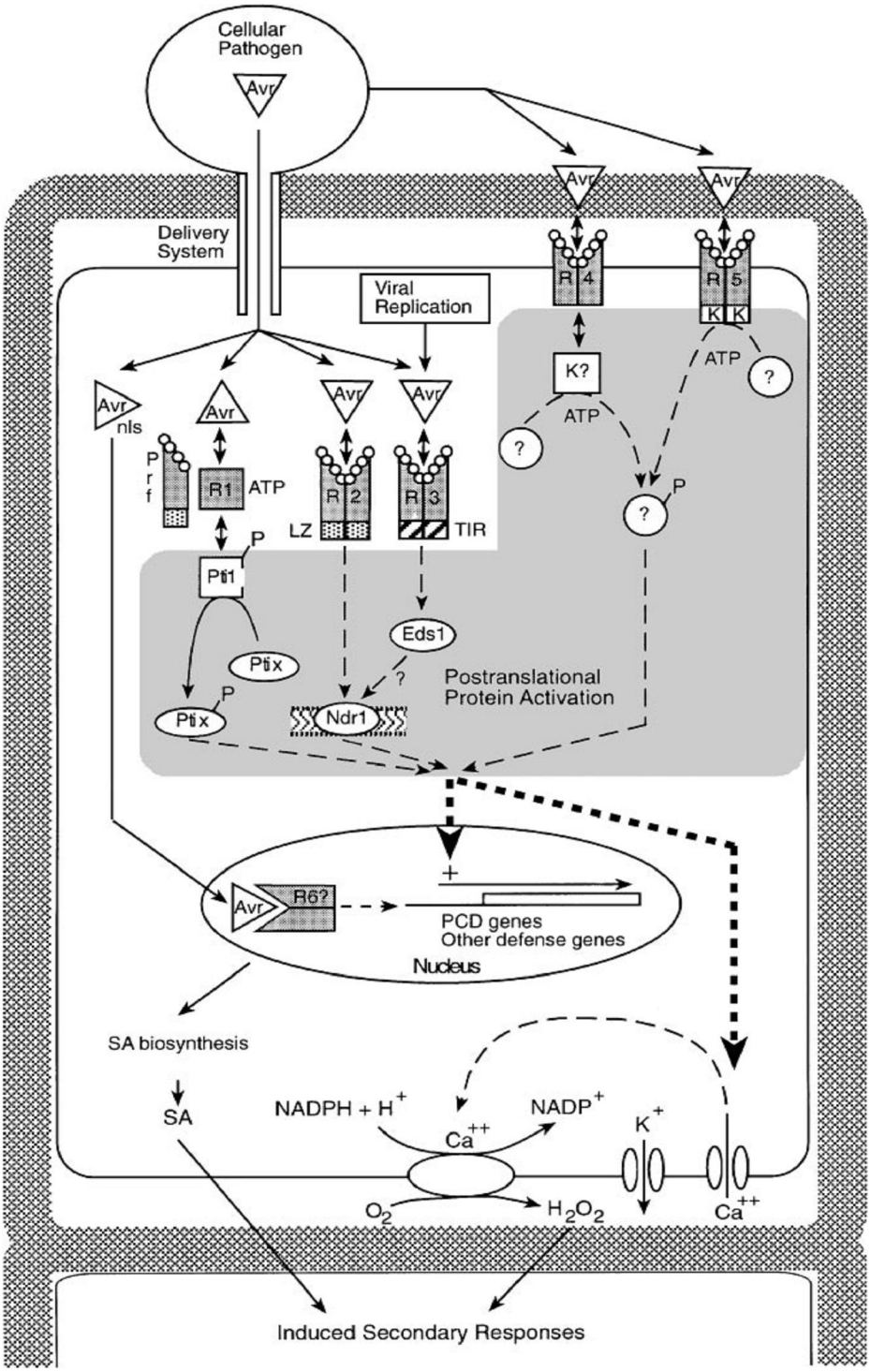

Figure 1.3 Model for elicitation of active defense responses in plants

1.9 Suppression of host plant defense

Despite physical and chemical barriers as well as inducible immune system of host plants, pathogenic bacteria are able to suppress plant defence by expression of proteins that interact directly with host cell component to alter the host cell signal transduction or that are unrecognized effectors escaping protective barriers of the host (Bent, 2007; Hueck, 1998; Gohre & Robatzek, 2008). Most of plant pathogenic bacteria possess type III secretion system that facilitates injection of bacterial proteins or effectors through the cell wall and plasma membrane of the host to gain access to the intracellular nutrient (Hueck, 1998; Gohre & Robatzek, 2008). Effectors capable of suppression of plant defence from plant pathogens reviewed by Gohre and Robatzek (2008). Also in the review, suppression actions of *Pseudomonas syringae* were most reported targeting at minimizing or overcoming plant defence triggered by bacterial flagella, host cell death and cell wall deposition.

1.10 Disease control

1.10.1 Principles

Management of a disease is based on relating knowledge about etiology, epidemiology, pathogenesis and vector biology (Scholthof, 2007; Forbes *et al.*, 2009). Disease control usually relies on six traditional principles as follows in descending order of priority: 1. avoidance of disease by choosing a period of time or environment condition unfavourable for infection; 2. preventing the introduction of the pathogen; 3. elimination of the inoculum; 4. maintain protective barrier to infection; 5. utilization of

cultivars that are resistant to pathogen; 6. cure for infected plants (The American Phytopathological Society, 2010). However, the first four principles are a prerequisite for prevention of plant diseases caused by bacteria. Protective measures applied on plants so far includes: cultural practices and sanitary procedure, chemical control, biological control, and breeding of resistant cultivars (Sigee, 1993).

1.10.2 Cultural practices and sanitary procedures

Location to grow a crop should be far from infected fields, absent of pathogen habitat. The environmental characteristics, the nature of soil, and water also need to be considered (Ogle & Dale, 1997). Inoculums of disease can be control by using disease-free plant materials and removing any infected parts during plant growth. Proper culturing practices have to avoid creating wounds and potential spread of bacteria, for example, when watering or handling with seeds and rootstocks. It is also necessary to sterilize planting equipment with disinfectants (Sigee, 1993).

1.10.3 Chemical control

Chemical agents for phytobacterial disease control include two main types: bactericides (synthetic organic and inorganic compounds) and antibiotics (microbial derived products). Organic bactericides are mostly composed of aromatic compounds (*i.e.* phenazine mono-oxide, probenazole) and used in powder form. Inorganic bactericide, Bordeaux mixture, is used for spraying or soaking. $Cu2^{+}$ mixture directly cause bacterial cell death, while the other agents have indirect affect on bacteria by

interacting recognition of plant (Sigee, 1993). The use of antibiotics is limited as there are a small number of commercially available compounds, unstable under natural conditions. In addition, antibiotic application in bacterial control apparently enhances resistance of bacteria to the antibiotic. Despite their rapid action and efficient in prevention of epiphytic growth, chemical control have disadvantages regarding to cost-ineffectiveness, environment, toxicity and antibiotic resistance of phytopathogenic bacteria (Sbragia, 1975; Sigee, 1993).

1.10.4 Biological control

Biological control has currently been the first choice in plant disease control as it overcomes the limitation of chemical control. Application of competitive micro-organism (antagonists) and biological control agents is the characteristic of the disease control. Compared to chemical control antagonists have more specific affect on the pathogen and less environmental and host plant effects. The introduced antagonists may compete with plant pathogens for nutrients, or colonize entry sites of pathogenic bacteria (Shoda, 2000; Kloepper *et al.*, 2004). In some cases, antagonists produce antimicrobials, for example, bacteriocins and novel antibiotic compounds (Vidaver, 1976; Sigee, 1993; Montesinos *et al.*, 2002). The action of biological control may also be deleterious in case bacteriophages are used (Vidaver, 1976; Sigee, 1993). The presence of antagonists or their interaction with host plants sometimes results in activation of HR and systemic acquired resistance (Montesinos *et al.*, 2002).

1.11 Anti-microbial compounds

1.11.1 Bacteriocins

Many bacteria produce bacteriocins which are proteinaceous compounds or excluded peptide compounds (Holtsmark *et al.*, 2008). Bacteriocins perform various inhibitory effects on closely related bacteria (Sigee, 1993; Holtsmark *et al.*, 2008). The best characterized bacteriocin is colicin produced by *E. coli*, which effects on target cells by pore-formation, inhibition of cell-wall synthesis, DNAse and RNAse activity (Holtsmark *et al.*, 2008). Anti-microbial activity of bacteriocins affects only a small group of bacteria, thus, there is limitation in the choice of antagonists based on these compounds (Sigee, 1993).

1.11.2 Siderophores

Siderophores are low molecular weight compounds produced under iron-limiting conditions (Loper & Buyer, 1991; Sigee, 1993; Shoda. 2000). Iron-sulfur clusters within structure of siderophore are able to uptake and transport Fe^{3+} into microbial cell. Siderophore production has been detected in popular plant-associated microogarnisms (Loper & Buyer, 1991). However, siderophore production is very important in biological control in the rhizosphere, especially pyoverdines produced by *Pseudomonas* spp. (Loper & Buyer, 1991; Sigee, 1993).

1.12. Ferredoxin

1.12.1 Overview

Ferredoxin (Fd) was first discovered in the non-photosynthetic anaerobic bacterium *Clostridium pasteurianum* in 1962, (Mortenson *et al.*, 1962), and later was found in spinach chloroplasts (Tagawa & Arnon, 1962). In both of species, ferredoxin was found to be involved in nitrogen fixation and in photoreduction of NADP+ (Sticht & Rösch, 1998). Ferredoxins are soluble iron-sulfur (Fe-S) proteins with exclusive iron-sulfur clusters (Sticht & Rösch, 1998; Meyer, 2001; Meyer, 2008). Ferredoxins function in electron transfer activity of a variety metabolic processes in bacteria, plants and animals (Sticht & Rösch, 1998). These ubiquitous proteins are divided into three phylogenetic families. The first kind comprises of around 55 or up to over 100 residues with 1 or 2 clusters of [4Fe-4S] or [3Fe-3S]. These are high potential iron proteins that are widely distributed in bacteria. The second type is more popular in plants and consists of 90-130 residues containing one [2Fe-2S] cluster. These proteins have low redox potentials between -305 and -455 mV (Cammack *et al.*, 1997 cited by Sticht and Rösch, 1998) and very acidic (pI 3-4) (Sticht & Rösch, 1998). The third family of Fds are thioredoxin-like [2Fe-2S] proteins isolated from the aerobe *Azotobacter vinelandii* (Shethna *et. al.*, 1964 cited by Meyer, 2001) and the anaerobe *Clostridium pasteurianum* (Hardy *et. al.*, 1965 cited by Meyer, 2001).

1.12.2 Plant ferredoxin-like protein (PFLP)

Lin *et al.* (1997) discovered of a HR delay caused by a plant amphipathic protein, later referred to as PFLP. The protein was found to suppress bacterial growth in the initiation of HR, and affect the interaction between an elicitor from *Pseudomonas syringae* pv. *syringae* ($harpin_{Pss}$) and the corresponding receptor in the tobacco plant .

1.12.3 PFLP = plant Fd I

Proteins derived from amphipathic extraction of healthy cotton, tomato and sweet pepper leaves show the same molecular weight of 22 kDa. Comparison of the N-terminal amino acid sequences of these peptides showed high conservation (Lin *et al*., 1997). PFLP sequence showed identity to *Lycopersicon esculentum* Fd I (72%), pea Fd I (52%), *Arabidopsis thaliana* Fd A (54%), *Spinacia oleracea* Fd I (52%), *Oryza sativa* Fd I (56%) and maize Fd (48%). Characteristics of PFLP sequence suggest that it is a Fd I (Dayakar *et al.*, 2003).

1.12.4 Pflp and PFLP

The sweet pepper (*Capsicum annuum* L.) *Pflp* is 662 bp in length (Dayakar *et al*., 2003; NCBI accession number AF039662.1). The encoded plant ferredoxin-like protein (PFLP) contains the N-terminal signal peptide (the leading 47 residues) and the mature

chain (97 residues) (Dayakar *et al.*, 2003; NCBI accession number Q9ZTS2). The cystein residues at positions 86th, 91th, 94th and 124th are believed to be iron binding sites and of potential [2Fe-2S] clusters (Dayakar *et al.*, 2003).

1.12.5 PFLP induction of harpin-mediated HR

$Harpin_{Pss}$ mediated HR was increased when co-infiltrated into tobacco leaves with recombinant PFLP from *E.coli*. Transgenic tobacco plants expressing a PFLP also showed enhanced HR via inoculation of virulent bacteria *Erwinia carotovora* subsp. *carotovora* and *Pseudomonas syringae* pv. *syringae* (Huang *et al.*, 2004). The $harpin_{Pss}$-induced cell death of *pflp* transgenic tobacco was dependent on AOS and Ca^{2+}, while wild-type tobacco suspension was independent on AOS and Ca^{2+} (Dayakar *et al.*, 2003). The later finding demonstrated that H_2O_2 production was induced during HR and light dependent (Huang *et al.*, 2004).

1.12.6 PFLP as an antimicrobial peptide

Beside the capability to interfere with bacteria growth *in vivo*, PFLP expressed in *E.coli* showed an anti-microbial activity against *E. coli*, *Erwinia carotovora* and *Pseudomonas syringae* in iron defective medium (XCM medium) (Huang *et al.*, 2006). Growth of *E. carotovora* was improved with supplement of 0.01mM $FeSO_4$ in XCM medium, but was diminished by the addition of 0.2μM PFLP. The protein solution failed to inhibit the bacterial growth in XCM medium with 0.1mM $FeSO_4$. Limited growth of infiltrated bacteria in the transgenic plants was believed, partly, to be due to the iron-

binding activity of PFLP. Anti-microbial activity of PFLP was thought to rely on the 86th cystein residue in [2Fe-2S] domain. Huang *et al.* (2007) demonstrated that PFLP (Fd I) amount in transgenic tobacco were regulated during pathogen infection, which might influence the bacterial pathogen. The research also revealed the ability of harpin to activate kinases for phosphrylation of PFLP *in vitro* that might relate to the stabilization of this protein as well as its involvement in the activity of other metabolic enzymes (Huang *et al.*, 2007). The enhanced resistant to soft rot bacteria in transgenic plants containing gene for PFLP have been reported (You, 2003; Yip, 2007).

1.12.7 Aims of the present study

The evident for the antimicrobial activity of PFLP suggests this is the potential peptide for plant protection applications. However, the mechanism by which PFLP accelerate HR and interfere the growth of bacteria is still inadequate explained. As mentioned above PFLP is highly similar in sequence with Fd from rice and Solanaceae plants which possess the highly conserved iron binding domain. Thus, the activity of PFLP that relies on the [2Fe-2S] cluster of the proteins might not be exclusive to Capsicum Fd-I. Moreover, the research on enhancement plant defense of PFLP by Dayakar *et al.* (2003) utilized the full-length peptide which contained the chloroplast targeting signal peptide. Thus, part of the produced protein might be directed to locate in the chloroplasts. In this case, the amount of PFLP located in the chloroplast of the transgenic plants and the wild-type plants is apparently different. The increased amount of Fd-I in tobacco in response to bacterial inoculation was reported by Huang *et al.* (2007). There is possible the contribution of the native PFLP located chloroplast in the interaction between host plants and invading bacteria. More exact observation on the

activity of PFLP will be obtained with the use of its full-length and its signal peptide – truncated forms in parallel experiments.

This study aims to isolate a ferredoxin gene from *Capsicum annuum* L. and confirm its sequence. The ferredoxin gene fragments with and without the signal sequence will be used for protein expression. The produced protein will be used for bioassays to determine their antimicrobial activities. The overall research is comprised of the following research aims:

1. Isolation and confirmation of a ferredoxin gene from Capsicum leaves

PFLP or ferredoxin will be isolated from Capsicum genomic DNA and cDNA with the specific primers developed from the published data. The amplified sequences will be analysed by sequencing and alignments. Based on the sequence comparison either nucleotide template will be used for amplification of the signal sequence truncated form of the Fd (T-*Pflp*).

2. Construction of expression vector

The protein expression will be carried out by using pRSET vector system. The cloned ferredoxin fragments will be ligated into pRSET vector in the downstream region of the polyhistidine sequence and transformed into *E.coli* TOP10F' for sequence confirmation.

3. Protein expression and the whole cell lysis analysis

The correct constructs of pRSET/ferredoxin will be expressed in BL21(DE3)pLysS with IPTG induction. Samples collected at different time points of the induction will be lysed and analysed on polyacrylamide gels by SDS-PAGE. The induction duration for scaling up the expressions will be determined from the electrophoresis results.

4. Protein purification and Western blotting

The expressed proteins will be purified and analysed by SDS-PAGE and Western blotting. Besides the target proteins confirmation conditions for expression, extraction and purification of the two versions of Capsicum ferredoxin genes will be identified to obtain high yield of ferredoxin for utilization in upcoming bioassays *i.e*. *in vitro* and *in vivo* antimicrobial assays.

Chapter 2 Materials and methods

2.1 Capsicum DNA extraction

Leaves of *Capsicum annuum* L. were weighed, frozen in liquid nitrogen and stored at -80^{o}C. For each DNA extraction 100 mg of leaf tissue was ground to fine powder in liquid nitrogen using a mortar and pestle. The total DNA isolation was performed with the QIAgen DNeasy Plant Mini kit (Qiagen) according to the manufacturer's instruction. The DNA concentration of the extracts was estimated by agarose gel electrophoresis.

2.2 Capsicum RNA extraction and cDNA synthesis

Total RNA from Capsicum leaf tissue was extracted by using QIA RNeasy kit (Qiagen) and the manufacturer's instruction including on-column Dnase digestion step. Complementary DNA (cDNA) from capsicum RNA extract was generated with Transcriptor High Fidelity cDNA Synthesis Sample Kit (Roche, Germany) and the supplied anchored-oligo$(dT)_{18}$ primer, following the standard procedure (Roche). The RT-PCR product was used as template for later amplification by PCR.

2.3 Bacterial strains and competent cell preparation

2.3.1 Bacterial strains

Escherichia coli strains used for cloning, transformation, and gene expression with their genotypes are listed, as follows:

SURE: *e*14^{-}(McrA^{-}) Δ.(*mcr*CB-*hsd*SMR-*mrr*)171 *end*A1 *sup*E44 *thi*-1 *gyr*A96 *rel*A1 *lac rec*B *rec*J *sbc*C *umu*C::Tn5 *(*Kan^{r}*)* *uvr*C [F´ *pro*AB *lacI*^{q}ZΔM15 Tn10(Tet^{r})] (Stratagene, La Jolla, CA).

DH5α: [F^{-}φ80*lacZ*ΔM15 Δ.(*lac*ZYA-*arg*F)U169 *rec*A1 *end*A1 *hsd*R17 (r_k^-, m_k^+) *pho*A *sup*E44 *thi*-1 *gyr*A96 *rel*A1 λ^{-}] (Invitrogen, Carlsbad, CA).

TOP10F': F′ {*lac*I^{q}, Tn*10*(Tet^{R})} *mcr*A Δ(*mrr-hsd*RMS-*mcr*BC) Φ80*lacZ*ΔM15 Δ*lac*X74 *rec*A1*deo*R *ara*D139 Δ(*ara-leu*)7697 *gal*U *gal*K *rps*L (Str^{R}) *end*A1 *nup*G (Invitrogen, Carlsbad, CA).

BL21 (DE3) pLysS: F^{-}, *omp*T *hsd*SB (r_B^- m_B^-) *gal dcm* (DE3) pLysS (Cam^{R}) (Invitrogen, Carlsbad, CA). This strain of *E.coli* was used for gene expression.

2.3.2 Conditions for *E. coli* growth and storage

Except specified notifications, all of *E. coli* incubations were carried out at 37^{o}C in a static incubator (Labmaster, Australia) for culture on agar plates or in rotation incubator (Ratek, Australia) at 210 rpm for broth culture. Incubation time depended on the specific use of bacteria. Media for *E. coli* culture was either LB or SOB supplemented with appropriate antibiotics (Sambrook & Russell, 2001). Details of LB and SOB media are summarized in **Table 2.1**. Specific maintenance media for TOP10F' and BL21(DE3)pLysS strains was LB containing 10 μg/mL tetracycline (LB/Tet 10) and 35 μg/mL chloramphenicol (LB/Cm35), respectively. The bacterial cultures were kept either at 4^{o}C for frequent use or at -80^{o}C in 30% glycerol for a long term storage.

Table 2.1 Component of LB and SOB media (Sambrook & Russell, 2001)

	LB , w/v	**SOB,** w/v
Trypton (Sigma, USA)	1%	2%
Yeast extract (PhytoTechnology Laboratories, USA),	0.5%	0.5%
NaCl (Merck, Australia)	1%	0.5%
MgCl2 (BDH Chemicals, Australia), added just before use.	-	10 mM
KCl (UniLab, Australia)	-	0.186‰
Agar (OXOID, UK)	1.5%	1.5%

2.3.3 Competent cell preparation

Electrocompetent cells of *E.coli* strains including SURE and DH5α were supplied by Plant Biotech Laboratory, RMIT University. TOP10F' and BL21 (DE3)pLysS electrocompetent cells were prepared according to the online protocol of California Institute of Technology (2005). Overnight LB broth culture of *E. coli* was inoculated into 250 mL of LB media contained in a 1L flask. The incubation condition in the rotator shaker as mentioned in **2.4.1** was maintained until the absorbance at 600 nm (OD_{600}) of the culture reached 0.6-0.9. After alternate steps of resuspension in deionised water and pelleting with a Beckman centrifuge (Beckman Allegra 21R), the cell pellet was finally resuspended in 1 mL of pre-chilled 10% glycerol and divided into pre-chilled 500 μL tubes.

2.4 Plasmids for cloning and gene expression

2.4.1 pGEM-T Easy Vector Systems (Promega)

pGEM-T Easy Vector Systems (Promega) with 3 kb pGEM-T Vector was used for cloning of PCR products as its convenience for screening and sequencing of recombinant plasmids (Figure 2.1). The single 3'-T overhangs at the insertion site allows the ligation of an A-tailed PCR product into the plasmid while preventing self-ligation of the vector. Sequencing of the recombinant plasmid is facilitated by using primers developed from T7 RNA polymerase promoter and SP6 RNA polymerase promoter sites. The insertion of a PCR product into the MCS located within the α-peptide coding region of β-galactosidase

inactivates expression of this gene. Transformed colonies are selected based on color indicator, being unable to convert the X-Gal substrate into a blue colored precipitate. However, successful ligation can also be found in blue colonies in some cases.

2.4.2 pRSET B (Invitrogen)

pRSET B (Invitrogen) is a 2.9 kb pUC-derived expression vector designed for enhancement of protein expression and purification of the cloned genes in *E. coli*, especially in BL21(DE3)pLysS cells (Invitrogen) (Figure 2.2). The T7 promoter enables high-level protein expression from the inserted gene which is in frame with the N-terminal fusion peptide. The polyhistidine (6X His-tagged) sequence facilitates the purification of fusion protein by using metal-chelating resin and the detection of recombinant protein with a commercially available antibody *eg*. Anti-HisG. The enterokinase cleavage recognition site between the 6X His-tagged region and multiple cloning sites allows the removal of the N-terminal fusion peptide from the purified recombinant protein.

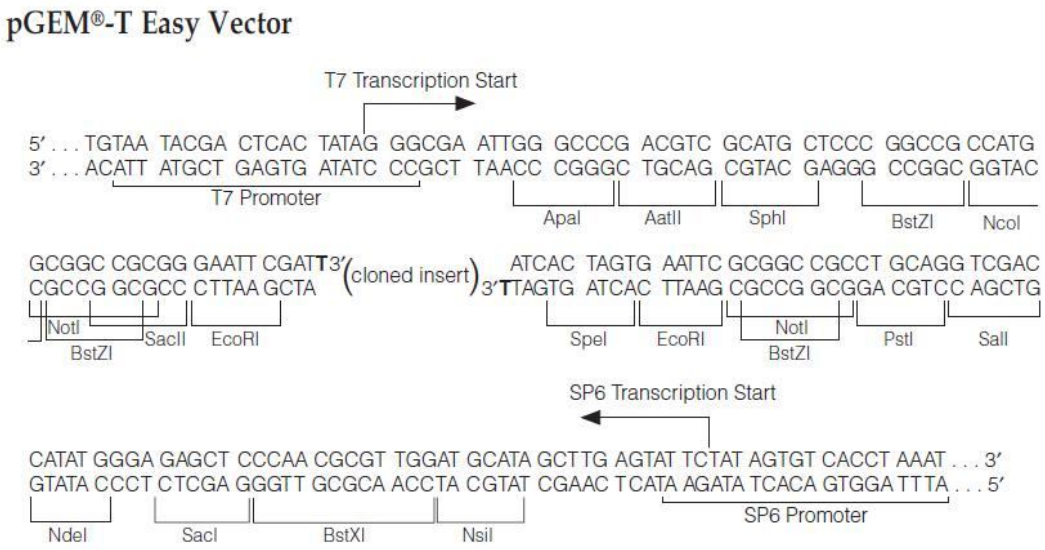

Figure 2.1. The multiple cloning sequence of pGEM-T Easy Vector.

Figure was adapted from Promega Technical Manual for pGEM-T and pGEM-T Easy Systems (2009).

A

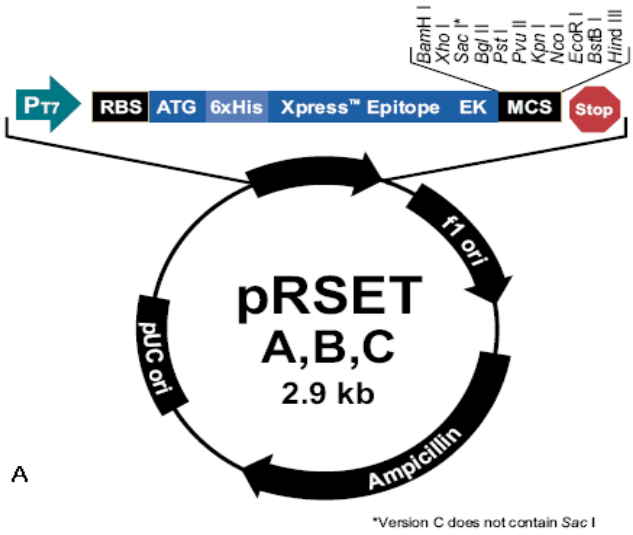

A

B

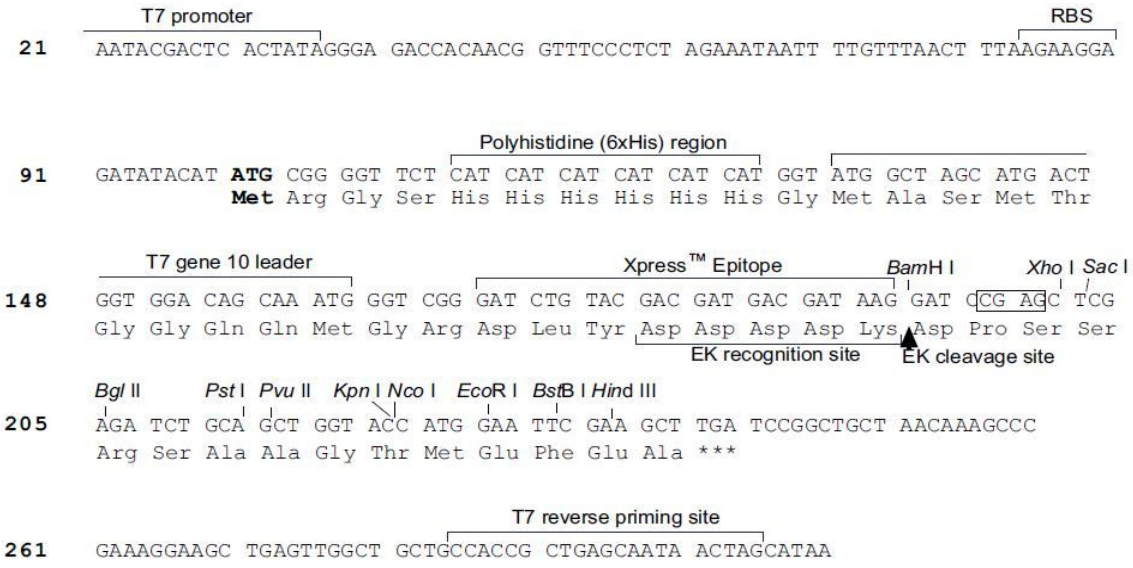

Figure 2.2 The map and the multiple cloning site of pRSET B. Taken from Invitrogen Manual Instructions for pRSET Expression Vector Systems.

2.5 Primers for gene cloning and confirmation

Primer design and analysis was performed by using Clone Manager Suite software version 7.0 (Scientific and Educational Software) and Primer - BLAST on NCBI (www.ncbi.nih.gov). Primers for isolation of *Pflp* or signal peptide - truncated *Pflp* (T-*Pflp*) was based on the published *Pflp* mRNA sequence (NCBI, AF039662). Primers included restriction sites, *Nco*I and *Eco*RI, respectively, in the forward primers (APF3 and APF4) and the reverse primer (APR3). For sequencing of the recombinant plasmid, T7 and SP6 promoter primers were applied on pGEM-T Easy derived vectors while T7 promoter primer and T7 Reverse primers were used for recombinant pRSET B vectors. These primers were designed to the relevant sequences of pGEM-T Easy and pRSET B vectors. Primers were synthesised by GeneWorks Pty. Ltd. (Hindmarsh, SA, Australia). The lyophilized primer stocks were resuspended in sterile milliQ water to the concentration of 100 μM from which 10 μM working stocks were made by dilution with sterile water. All of the primer stocks were stored at -20^{o}C. Details about the sequence of the nucleotides are listed in Table 2.2 with their respective functions.

Table 2.2 Primers used within this study for isolation of genes and analysis of recombinant plasmids

Oligo name	**Sequence (5' to 3' direction)/Function**	**Feature**
APF3	CGACGT**CCATGG**CTAGTGTCTCAGCTACCATGATTA	The forward primer for isolation of full-length *Pflp* with *Nco*I site in bold letters.
APF4	TCGAGTGCGC**CCATGG**CTTCATACAAAGTGAAAC	The forward primer for isolation of T-*Pflp* with *Nco*I site in bold letters.
APR3	AGCCTGC**GAATTC**TTAGCCCACGAGTTCTGCCTCTTTG	The reverse primer for isolation of either *Pflp* or T-*Pflp* with *EcoRI* site in bold letters.
SP6	TATTTAGGTGACACTATAG	Promoter sequences used as primers for sequencing of genes cloned into pGEM-T Easy vector
T7	TAATACGACTCACTATAGGG	
T7 Reverse	TAGTTATTGCTCAGCGGTGG	Sequencing of genes cloned into pRSET B in combination with T7 primer.

2.6 Polymerase chain reaction (PCR)

For isolation of genes from Capsicum genomic DNA, ACCUZYME DNA Polymerase (Bioline) and *Pfu* DNA polymerase (Bioline, Australia) were used with the supplied buffers and Mg^{2+} solutions according to the recommended protocols. ACCUZYME and *Pfu* DNA polymerase (Bioline, Australia) are high fidelity thermostable enzymes possessing 5'–3' DNA polymerase and 3'-5' proofreading exonuclease activities which produce blunt-ended PCR products of up to 5 kb in length. DNA amplification for detection or analysis of recombinant plasmids were performed using Gotaq Green Master mix (Promega, USA) to which sterile deionized water, primers and DNA template were added for the reaction mixture. Amplification reactions were performed in a final volume of 25 μL. PCRs were performed on one of the following PCR machines including PCR Express Thermal Cycler (ThermoHybaid, Middlesex, UK), GeneAmp 2400 (PerkinElmer, Waltham, MA) or G-Storm GS1 (GeneWorks, Australia). PCR cycles used within the research is outlined in Table 2.3 below.

Table 2.3 PCR protocol for different primer combination

Primers	**Denaturation**	**Cycle**	**Enlongation**	**Final step**
APF3/APR3	94°C/5 min	30X [94°C/30 sec, 60°C/30 sec, 68°C/1.5 min]	68°C/7 min	4 °C
APR4/APR3	95°C/2 min	30X [95°C/30 sec, 65°C/30 sec, 72°C/30 sec]	–	10 °C
SP6/T7	95°C/2 min	30X [95°C/30 sec, 52°C/30 sec, 72°C/30 sec]	72°C/1 min	10 °C
T7/T7 reverse	95°C/2 min	30X [95°C/30 sec, 55°C/30 sec, 72°C/30 sec]	72°C/1 min	10 °C

2.7 Agarose gel electrophoresis

Nucleotide samples were visualized after electrophoresis in agarose gels. One percent (w/v) agarose (Bioline, Australia) was prepared in 1X TBE which includes 89.2 mM Tris base (Sigma, US), 88.9 mM boric acid (Sigma, US) and 2.5 mM EDTA (pH 8.0). Agarose mixture dissolved by microwave heat and cooled to around 60^{o}C and supplemented with ethidium bromide (EtBr) to the final concentration of 0.2 μg/mL before being poured into the gel tray. The nucleotide samples were mixed with 6X loading dye (Fermentas, US) and loaded into agarose gels. Electrophoresis was performed in 1X TBE buffer with Sub Cell GT gel electrophoresis apparatus (Bio-Rad) and the voltage setting ranging from 80 to 100V depending on sample volumes used. A DNA standard, 1 kb DNA ladder (Fermentas), was used to estimate the molecular size and concentration of DNA samples. When the electrophoresis was completed, nucleotide bands on gel were visualized and photographed under UV light using Gel Document System (Bio-Rad).

2.8 Ligation

A 10 μL ligation reaction comprised of 10X ligation buffer (Promega) and a 1:3 molar ratio of vector to insert and T4 ligase (Promega). For ligation into pGEM-T Easy vector, the inserts were A-tailed *via* an A-tailing reaction prior to the ligation based on the Technical Manual for pGEM-T and pGEM-T Easy vector Systems (Promega). Ligation reactions were incubated overnight or 12 hours at 16^{o}C in an ice-box.

2.9 Transformation and screening

Electroporation of recombinant plasmid into *E. coli* electrocompetent cells followed the method described by Sambrook and Russell (2001). Two microliters of ligation reaction was added into each aliquot of electrocompetent cell which was placed on ice. The mixture was then transferred into a pre-chilled electroporation cuvette (Bio-rad). Electroporation was done with the apparatus settings as follows, 200 Ohm, 25 μF and 1.5 V. Immediately after the electroporation, the culture from the cuvette was pipetted into 1 mL of SOC broth (SOB broth with addition of 20 mM glucose). The transformed culture were proliferated in rotary incubator for 1 hour, then 200 μL of it was spread on selective LB plates containing only appropriate antibiotics or with 0.8 mM IPTG (Promega, USA) and 0.05 mg/mL X-Gal. Colonies that appeared on the selective plates on the next day were picked up with sterilized toothpicks, streaked on a new LB plate containing appropriate antibiotic(s) and inoculated into 3 mL of LB broth supplemented with 100 μg/mL Ampicillin (Sigma, USA) (LB/Amp100). The LB/Amp100 plate containing putative transformed cells, referred as master plates, was incubated overnight and stored at 4^{o}C. The 3 mL bacterial culture was incubated in shaking incubator overnight, which was used for plasmid isolation and restriction enzyme analysis to select the expected recombinant clones. Plasmid isolations were checked by gel electrophoresis.

2.10 Restriction enzyme analysis

Plasmids of the clones from the master plates were digested by restriction enzymes to check the presence of the inserts. Each of the digestion reactions involves 1X NEBuffer

(NEB, UK), plasmid, restriction enzymes (NEB, UK) and addition of sterilized milliQ water to the final volume of 20 μL. The reactions were incubated from 4 hours to 12 hours (overnight) at 37^{o}C in the incubator. The results of the digestion were visualized by agarose electrophoresis method (refer to **2.7**). The insert positive clones were further analyzed for the size and orientation of the inserts by PCR with appropriate primers (refer to **2.5**).

2.11 Sequencing and analysis of sequence data

The clones that contained the right size of the insert were selected for DNA sequencing. Plasmid purification of those clones was carried out with QIAprep Spin Miniprep Kit (Qiagen, USA). A sample for sequencing includes 300-600 ng of plasmid DNA sample, 1μL of 3.2 μM primer, and addition of milliQ water to the final volume of 15.5 μL. The mixture was prepared in a 200 μL tube, sealed with parafilm and sent to AgGenomics for sequencing service (AgGenomics Pty. Ltd., Aus). Sequencing results were analyzed with BioEdit V7.0.9 (Hall, 2005), Clone Manager Suit software version 7.0 (Scientific and Educational Software) and BLAST (NCBI, USA).

2.12 Preparation for expression

After confirmation by sequencing, recombinant pRSET B containing the correct inserted sequence was transformed into BL21(DE3)pLysS and transformants were screened on LB/Amp100 plates. The ampicillin-resistant clones were subsequently selected and streaked on LB/Cm35/Amp100 plates before proceeding with the expression. Chloramphenicol in culture media helps to maintain the pLyS plasmid that is

required for the expression of T7 lysozyme and ampicillin is for the maintenance of pRSET B vector.

2.13 In vitro expression

The i*n vitro* expression of pRSETB containing either *Pflp* or T-*Pflp* inserts was performed according to the standard instruction (Invitrogen). Two milliliters of SOB/Amp100/Cm35 broth was inoculated with a single recombinant colony which is BL21 (DE3)pLysS cells containing recombinant pRSETB with either Pflp or T-Pflp inserts. The culture was grown overnight at 37^{o}C with shaking, which was inoculated into 25 mL of SOB the next day. The culture was continued to grow at 37^{o}C with shaking until an OD_{600} of 0.4-0.6 was reached. 1 mL of the culture was collected in a 1 mL tube and was centrifuged at 9,000 rpm/10 min in an Eppendorf microcentrifuge at room temperature. The supernatant was removed and the cell pellet was stored at -20^{o}C. IPTG was added to the remaining culture to the final concentration of 1mM and the culture was continued to grow. Then, 1 mL of cell samples was collected at 1 hour intervals for 6 hours and was processed the same way as the first collection of 1mL sample. Samples of all time points were resuspended in 20mM Sodium Phosphate buffer (NaH_2PO_4 and Na_2HPO_4, pH 7.4), frozen in liquid nitrogen and thaw in water bath at 42^{o}C. The freeze-thaw was repeated for 5 times and the insoluble protein was pelleted by centrifugation at 9,000rpm for 10 min at room temperature. The clear lysate or soluble protein was transferred into new tubes. The soluble and insoluble protein samples were analyzed with protein analysis method (SDS-PAGE) and stored at -20^{o}C.

2.14 **SDS-PAGE** (Sodium dodecyl sulfate polyacrylamide gel electrophoresis)

Either 12% ClearPAGE gels (C.B.S Scientific, USA) or manually prepared polyacrylamide gels were used. Manually prepared gels comprised of 4% stacking gel and 12.5% resolving gel (Roskams & Rodgers, 2002). Loading samples for SDS-PAGE were prepared based on the standard instruction for pRSET B application (Invitrogen, USA). To 20 µL of soluble protein solution 5 µL of 5X SDS-PAGE sample buffer [0.225M Tris-Cl, pH 6.8; 50% (v/v) glycerol, 5% (w/v) SDS; 0.05% (w/v) bromophenol blue and 5% (v/v) β-mercaptoethanol or BME, (QIAGEN, 2003)] was added. Insoluble protein pellet was resuspended in 100 µL of 1X sample buffer which was diluted with milliQ water from the 5X solution. All of the samples were heated at 95^{o}C in a heat block for 5 min and loaded on SDS-PAGE gel. For observation of protein migration on gel, efficiency of blotting onto nitrocellulose membrane and estimation the sizes of protein on gel or Western Blot, a protein marker was used, such as SeeBlue Plus2 Pre-stained standard (Invitrogen, AUS), CLEARPAGE Prestained marker (C.B.S. Scientific, USA) and Precision Plus Protein Standards (Bio-Rad). Pre-cast gels were run at 90V for 20 min and at 120V for 90 min in Tricine SDS running buffer pH 8.5 [60mM Tris base, 40mM Tricine, 2% (w/v) SDS and 2.5mM sodium metabisulfite]. Manually prepared gels were run at 60V for 30 min and 90V for 60 min in Tris-Glycine-SDS running buffer [25 mM tris base, 192 mM glycine and 0.1% (w/v) SDS] (Mullick & Rodgers, 2007).

2.15 Staining and destaining

Separated proteins on SDS-PAGE gel were visualized with Comassie stain (25% methanol, 7.5% acetic acid, 0.1% Coomassie Brilliant Blue R 250) for 0.5 hour with shaking (50 rpm) at room temperature. After staining, the staining solution were replaced

with destaining solution which contained 5% methanol, 7.5% acetic acid and milliQ water (Roskams & Rodgers, 2002). The gels were destained overnight at room temperature with shaking.

2.16 Cell preparation for protein purification

A single colony of recombinant BL21 (DE3)pLysS on a LB/Amp100/Cm100 plate was inoculated in 5 mL of SOB/Amp100 broth and incubated with shaking overnight. The next day, the overnight culture was added into a 1 L flask containing 200 mL of SOB broth. The resultant culture had an OD_{600} of around 0.1 and the cells were proliferated until an OD_{600} of around 0.4-0.6 was reached. Before and after IPTG induction, 1 mL of the culture was removed as non-induced and induced controls. These controls were pelleted in a microcentrifuge at 9,000 rpm for 10 min at room temperature. The cells were stored at -20^{o}C or subsequently lysed by the "freeze-thaw" method described in section 2.13 and processed for SDS-PAGE gel analysis (refer to 2.14). After removing the non-induced control, the remaining culture was supplied with IPTG to the final concentration of 1 mM and continued to growth for 6 hours. When IPTG induction was completed, aliquot parts of the culture were pelleted in either Multifuge 1S-R (Heraeus, UK) or Beckman Allegra 21R (Beckman Coulter) centrifuge at the speed of 4,700 rpm for 15 min at 4^{o}C. The cell pellet was processed for protein purification or frozen in liquid nitrogen and stored at -80^{o}C. Recombinant BL21(DE3)pLysS containing 6X His-tagged Green Fluorescent Protein (GFP) in pRSETB (Invitrogen) was used as a control for evaluation of the methods used for cell lysis, protein purification and western blot.

2.17 Cell lysis for protein purification

Cell pellet from 200 mL of the culture (section 2.16) was resuspended in 8 mL of sodium buffer (50 mM NaH_2PO_4 and 300 mM NaCl) containing 20 mM BME and homogenized by thoroughly vortexing. The cell suspension was kept on ice and sonicated with Branson Digital Sonifier (Branson Ultrasonics Corporation, USA) for 6 min (30 sec pulses, 10 sec pauses) at 30% amplitude. On ice DNase I incubation followed with an addition of 100 µL DNase I (Grade II, Roche, Australia) and DNase I reaction buffer (10 mM Tris, pH 7.6; 25 mM $MgCl_2$, 5 mM $CaCl_2$) to the sonicated suspension. Subsequently, the cell solution was centrifuged at 4,700 rpm, 4^oC for 15 min in Multifuge 1S-R (Thermo Fisher Scientific Inc., USA) or Beckman Allegra 21R (Beckman Coulter Inc., USA) centrifuge. The clear lysate was transferred into a new tube, kept on ice, and was used immediately for purification.

2.18 Protein purification

Purified proteins were achieved due to the high affinity between Ni-NTA agarose (Qiagen, Australia) and the 6X His-tagged proteins. Ni-NTA agarose resin is supplied as 50% slurry with ethanol and can be re-used for purification of the same protein (Qiagen 2003). The purifications followed the instructions for Ni-NTA application and protein purification from Qiagen. The resin mixutre (2 mL)was added into a 10 mL Poly-Prep column (Bio-Rad) which was, then, capped and kept vertically until the resin was settled on the column. The volume of settled resin is referred as bed volume or column volume (CV). When most of storage ethanol went out, the column was washed with 10 CV or 10 mL of sterilized milliQ water and, then, equilibrated with 5 CV of sodium buffer (50 mM NaH_2PO_4 and 300 mM NaCl) containing 10 mM immidazole and 20 mM BME. After the

column equilibration, the column was filled with the clear lysate (section 2.17), blocked and horizontally incubated at 4^{o}C with gentle rotation (50 rpm) for 0.5 hour. Upon finishing incubation, the column was returned to the original vertical position for the resin to re-settle. The flow through from the on-column lysate was collected for later analysis. Non-specific binding to the resin was washed away with subsequent addition of wash buffers which comprised of sodium buffer, 20 mM BME and immidazole with increased concentrations (20 mM and 30 mM). Elution of 6X His-tagged proteins was performed with a sodium buffer containing 200 mM or 250mM immidazole and 20 mM BME. All of the flow-through collected from the column was stored at -20^{o}C and analyzed on SDS-PAGE gel (**2.15**) followed by Coomassie staining (**2.16**) or Western blotting (**2.19**). 6X His-tagged PFLP and T- PFLP expressed in BL21 (DE3)pLysS cells were purified along with 6X His-tagged GFP, of which detailed protocols are summarized in Table 2.4. Upon completion of purification, the column was subsequently washed with 3 CV of the buffer containing 250 mM immidazole (I 250), 0.5 M NaOH for 30 min, filled with 30% ethanol and stored at 4^{o}C.

Table 2.4 Protocols for purification of 6X His-tagged versions of PFLP, T-PFLP and GFP using Ni-NTA agarose

Proteins	**Equilibration**	**Washing**	**Elution**
	(I-concentration of immidazole used in the buffer(*)/volume)		
PFLP	I 10/5 CV(**)	I 20/20 CV, I 30/3 CV	I 100/2 mL
T-PFLP	I 10/5 CV	I 30/15 CV	I 200/2 mL
GFP	I 10/5 CV	I 20/15 CV; I 30/3 CV	I 200/2 mL

(*) *All of the buffers used in purification containing 50 mM NaH_2PO_4, 300 mM NaCl, 20 mM BME and varied concentrations of immidazole, thus they are briefly mentioned with the applied concentrations of immidazole.*

(**) *CV (column volume) is the bed volume.*

2.19 Western Blot

2.19.1 Trans-blotting

Except where notified, trans-blotting was performed using iBlot Gel Transfer System (Invitrogen) according to the manufacturer's instruction. Trans-blotting was also performed electrophoretically according to the standard instruction in a Mini Trans-Blot Electrophoretic Transfer Cell (Bio-Rad) (Figure 2.4). Upon trans-blotting, proteins on SDS-PAGE gel were transferred to nitrocellulose membrane. For electro-blotting method, after electrophoresis (section 2.14), the gel was equilibrated in transfer buffer [25 mM Tris (pH 8.3), 192 mM glycine, and 20% (v/v) methanol] for about 10 min. The nitrocellulose membrane, fiber pads, filter papers, which had the same size as the gel, were also pre-wetted with the transfer buffer prior to the assembly in a cassette as shown in Figure 2.3**.** The cassette was locked and placed in the transfer cell along with an ice-cooling unit. Pre-chilled transfer buffer was used for electro-transfer. A stir bar was added into the cell to help maintain the even temperature and ion distribution within the buffer. The stirrer was set at maximum speed. Transferring was carried out at 100 V for 1 hour.

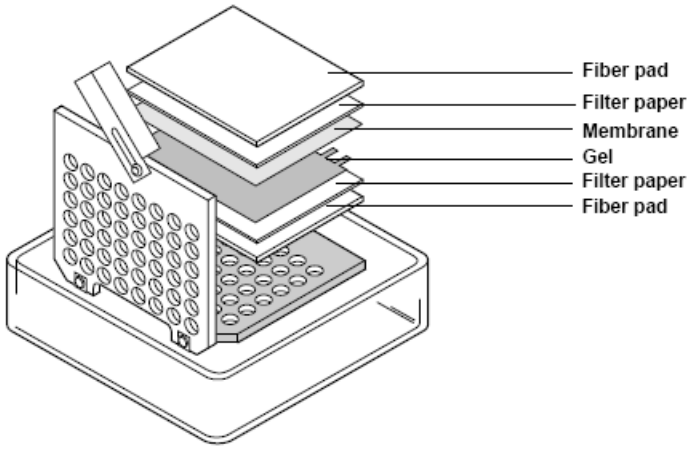

Figure 2.3 Assembly of the sandwich for electro-transfer of proteins from a SDS-PAGE gel to nitrocellulose membrane.

Figure was taken from Instruction Manual for Mini Trans-Blot Electrophoretic Transfer Cell (Bio-Rad).

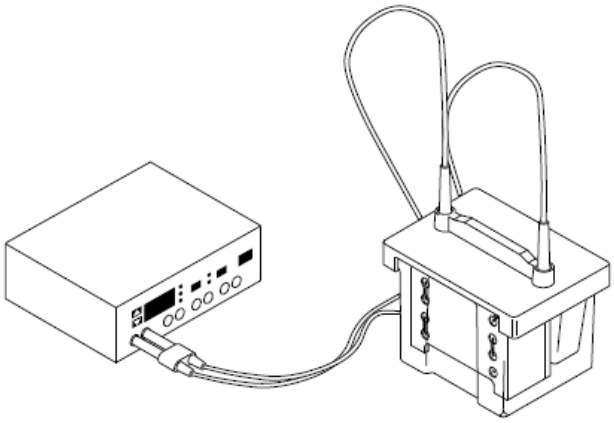

Figure 2.4 Mini Trans-Blot Electrophoretic Transfer Assembly.

Figure was taken from Instruction Manual for Mini Trans-Blot Electrophoretic Transfer Cell (Bio-Rad).

2.19.2 Blocking

On completion of the trans-blotting, the membrane was remove from the cassette and immersed in blocking solution or blotto for 1 hour with gentle shaking (50 rpm) at room temperature. The blotto, which involved 5% (w/v) skimmed milk in 1X TBST [20 mM Tris, 137 mM NaCl, 0.1% (v/v) Tween 20], was boiled at 95^{o}C with stirring for 2 hours, cooled to around 50^{o}C and filtered through Miracloth (CalBiochem) before use. The blotto was prepared and used within 3 days with the storage of the solution at 4^{o}C.

2.19.3 Detection

Anti-HisG Antibody (Invitrogen, USA) and Anti-mouse-antibody-HRP (Promega) were used as primary and secondary antibodies, respectively. Anti-HisG Antibody is able to specifically bind to the polyhistidine sequence of the recombinant proteins. As a mouse monoclonal IgG_{2a} antibody, Anti-HisG Antibody can be used in combination with Anti-mouse-antibody-HRP. For immuno-detection, the membrane after blocking was incubated with the primary antibody which was diluted 1:5000 in the blocking buffer. Incubation with primary antibody was done at room temperature with gentle shaking for 0.5 hour and continued with the overnight incubation at 4^{o}C. The blot was rinsed twice in 20 mL of 1X TBST for 10 min before and after the incubation with the secondary antibody (1:2500 ditlution in blotto). Chemiluminescent substrate (Chemiluminescent Peroxidase Substrate-3, Sigma) was added onto the blot which was subsequently placed between two sheets of transparent films and exposed to an Amersham Hyperfilm ECL chemiluminescent film for 2 min. Film development was carried out in the absence of white light and immersion of the film in solutions for development and fixing.

Chapter 3 Cloning and expression of ferredoxin from *Capsicum annuum*

3.1 Introduction

The cloning of *Pflp* gene and *Pflp* without signal sequence, T- *Pflp* from Capsicum DNA and synthesized cDNA was performed by PCR using the gene specific primers. The isolated genes were subcloned into pGEM – T Easy vectors that were selected, subsequently, through the screening on selective media and endonuclease digestions before gene sequencing. Sequencing results were analysed by alignments with the published sequence. After sequence confirmation, construction of the expression vectors were continued with the subcloning of *Pflp* and T-*pflp* genes from pGEM-T Easy vectors (Promega) to pRSETB vectors (Invitrogen). Confirmations of the expression vector constructs were done with screening on selective media, digestions and sequencing. Protein expression was performed in BL21 (DE3)pLysS with the confirmed recombinant pRSET B vectors followed by the protein purification and Western blotting.

3.2 Confirmation of Pflp gene sequence from sweet pepper

3.2.1 Isolation of *Pflp* gene from sweet pepper leaves

Capsicum genomic DNA and synthesized cDNA (Figure 3.1) were used as template for *Pflp* isolation by PCR. Amplification of *Pflp* with APF3 and APR3 primers resulted in a 456 bp product which underwent gel purification, A-tailing and ligation into pGEM-T Easy vectors. The product achieved through PCR with Capsicum genomic DNA and cDNA showed the same size on 1% agarose gel (Figure 3.2).

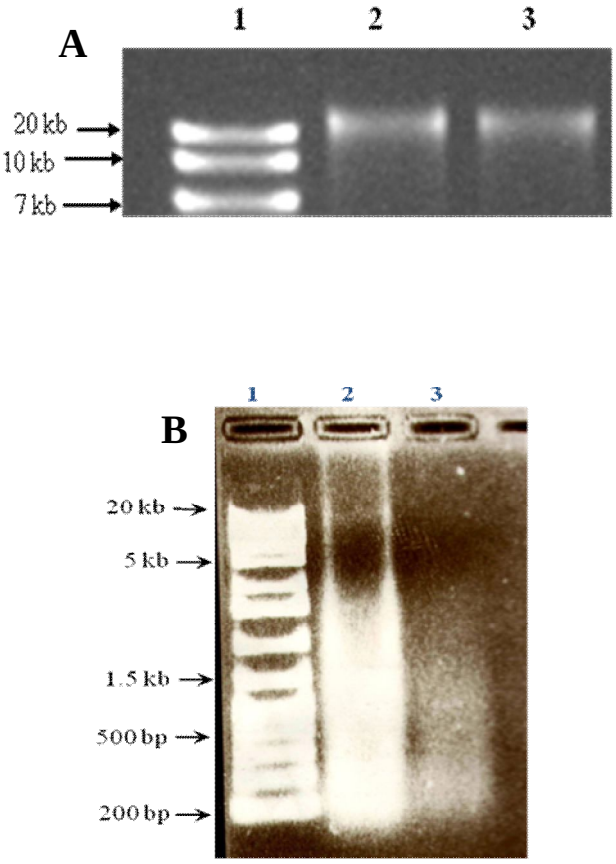

Figure 3.1 Total DNA and RNA extraction from sweet pepper leaves

(A) Lane 1: 1kb plus DNA ladder (Fermentas), Lane 2&3: Capsicum total DNA extraction. (B) Lane 1: 1kb plus DNA ladder, Lane 2&3: Capsicum total RNA extraction.

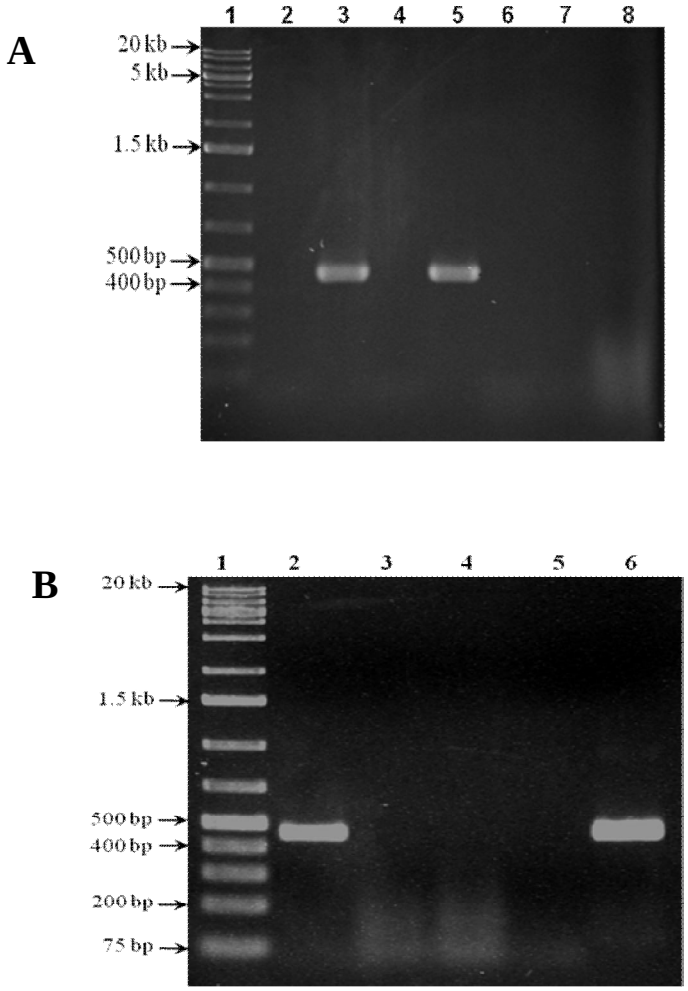

Figure 3.2 Agarose gel electrophoresis of *Pflp* amplified with APF3 and APR3 primers

(A) *Pflp* amplification from capsicum cDNA using GoTaq Green Master Mix (Promega, USA), lane 1: 1 kb ladder; lane 2 & 4: amplification with (-) cDNA control, lane 3 & 5: with cDNA, lane 6: with RNA extract, lane 7: without template; lane 8: 1 µL RNA extract. (B) PCR products of *Pflp* amplification from capsicum cDNA and total DNA using Accuzyme (Bioline, USA), lane 1: 1 kb ladder, lane 2: with total DNA, lane 3& 4: with (-) cDNA control, lane 5: without template, lane 6: with cDNA.

3.2.2 Cloning of *Pflp* into pGEM-T Easy Vector

Cloning of *Pflp* into pGEM-T Easy Vector was performed as the schematic description in Figure 3.3. Gel purification of amplified *Pflp* was followed by A-tailing reaction with incubation at 72^{o}C using PCR Express Thermal Cycler (ThermoHybaid, Middlesex, UK) for 20 min. The ligated construct was transformed into SURE cells by electroporation and was subsequently screened on selective LB/Amp100 plates containing IPTG and X-gal (refer to 2.9). There were only 3-10 colonies growth on each selective plate and more blue colonies were obtained. Both white and blue colonies were selected for plasmid miniprepation and restriction endonuclease analysis. The recombinant vectors were confirmed by double digestions with *Eco*RI and *Nco*I. The recombinant pGEM-T Easy vector contaning *Pflp* insert was supposed to release a 450 bp fragment and the 3 kb linearized backbone. Plasmid isolation and restriction enzyme digestion were visualized with gel electrophoresis and UV illumination. Digestions of candidate clones with *Eco*RI and *Nco*I released two fragments with the approximate sizes of 3 kb and 500 bp as shown in Figure 3.4.

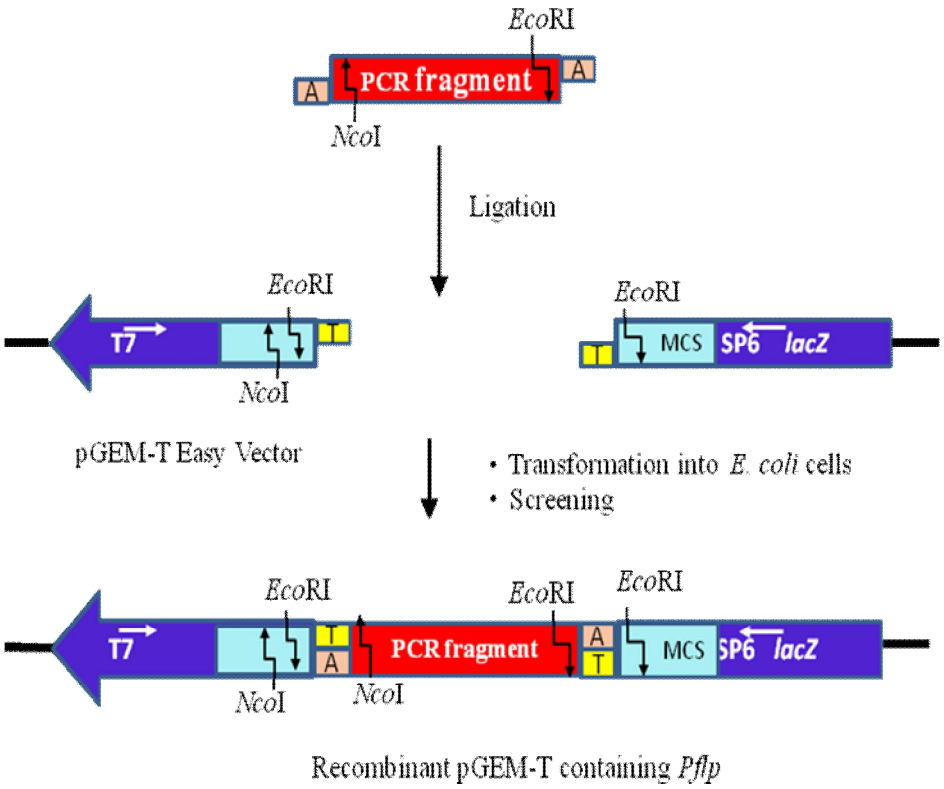

Figure 3.3 Schematic description of ligation of *Pflp* into pGEM-T Easy Vector

A-tailed PCR product ligated T-overhangs at the multi-cloning sites (MCS) located within *lac*Z coding sequence (dark blue). The ligation was transformed into *E. coli* cells for selection of the recombinant vectors. Orientations of T7 and SP6 RNA polymerase promoters are shown as arrows. Restriction sites resulting in cohesive ends by the specified enzymes are indicated with elbow arrows.

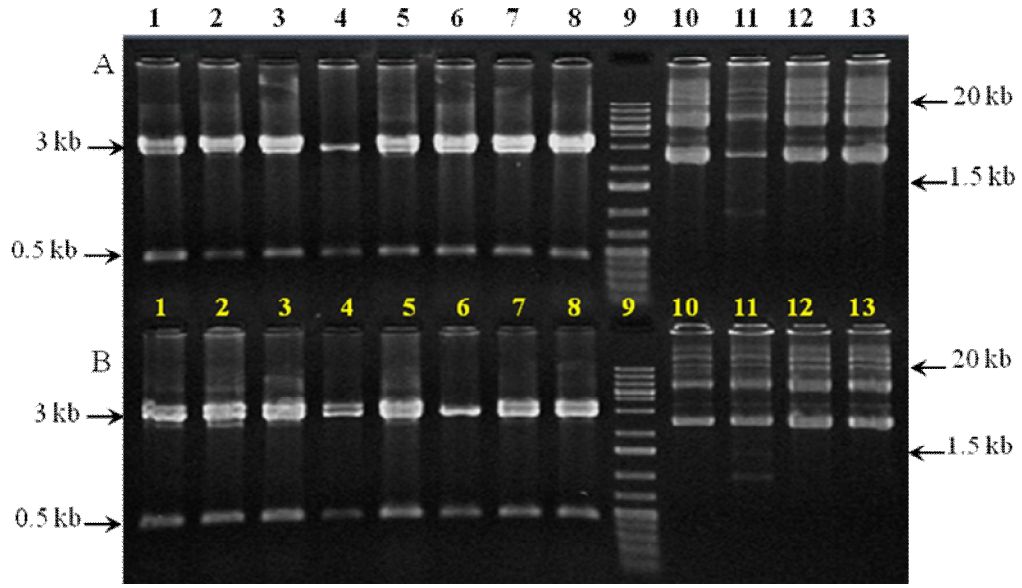

Figure 3.4 Plasmid minipreparation of *E. coli* clones containing recombinant pGEM-T Easy/*Pflp* vectors and restriction digestion of the putative recombinant vectors

Isolation and *Nco*I/*Eco*RI digestion of recombinant pGEM-T Easy vectors containing *Pflp* amplified with GoTaq Green Master Mix (Promega) from genomic DNA (A) and total cDNA (B). In (A) and (B), lane 1-8: linearized pGEM-T Easy (3 kb) + *Pflp* (450 bp), lane 9: 1 kb ladder, lane 10 – 13: plasmid isolation. The same size of PCR product (0.5 kb bands) were observed in amplifications of Capsicum genomic DNA and cDNA with the specific primers.

3.2.3 Sequence analysis

Six candidate pGEM-T Easy/*Pflp* vectors were sequenced with SP6 and T7 primers. Obtained sequences showed high squence idendity to the published *Pflp* sequence, AP1 (NCBI, AF039662) through multiple sequence alignment by ClustalW (EMBL - EBI). Figure 3.5 shows that all of the aligned sequences differ from the published sequence at nucleotide position 202. This change results in the substitution for asparagine (N) by aspartic acid (D) in the deduce polypeptide coding by the isolated *Pflp* compared to the translated sequence of AP1. Sequences of cDNA amplified *Pflp* (LT-7 and LT-8RC) contains guanine at position 100 which is adenine in the sequences of genomic DNA amplified *Pflp* and AP1, which leads to the presence of glycine residue in the deduced polypeptide chain instead of serine according to the published sequence. However, no nucleotide difference occurred in the conserved iron-binding domain which contains 4 functional cystein residues at positions 86th, 91th, 94th and 124th in the polypeptide chain (Figure 3.6). The sequences of the recombinant pGEM-T Easy vector containing *Pflp* amplified by Accuzyme from genomic DNA (LT17RC + LT18, LT21 RC + LT22, LT23 RC + LT24) matched the published *Pflp* sequence with only one nucleotide change indicated in the blue rectangle. Despite one base pair difference, the sequences of *Pflp* amplified from Capsicum genomic DNA and cDNA are the same. In addition, Capsicum *Pflp* was reported to possess no intron in its sequence, thus, genomic DNA can be used as template for *Pflp* and T-*Pflp* cloning.

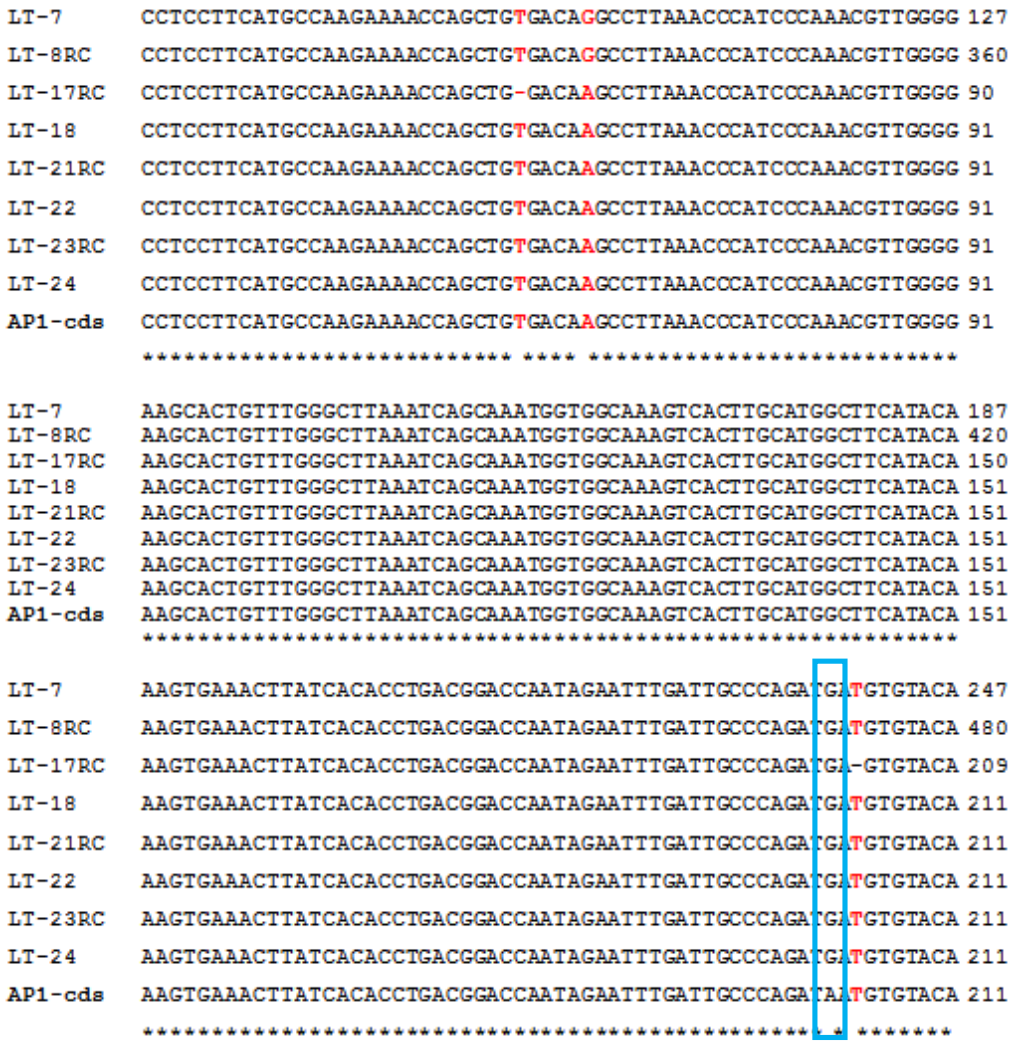

Figure 3.5 Aligment of *Pflp* sequences from recombinant pGEM-T/*Pflp*

Pflp sequences in the recombinant pGEM-T vectors were processed with BioEdit prior to alignment with ClustalW software. All of the sequenced samples contained *Pflp* from Capsicum genomic DNA except the *Pflp* sequence of LT-7 and LT-8 RC was amplified from Capsicum cDNA; the published sequence of *Pflp* (AP1). The identical alignment is marked by asterisks and differences were indicated with red letters and a blue rectangle.

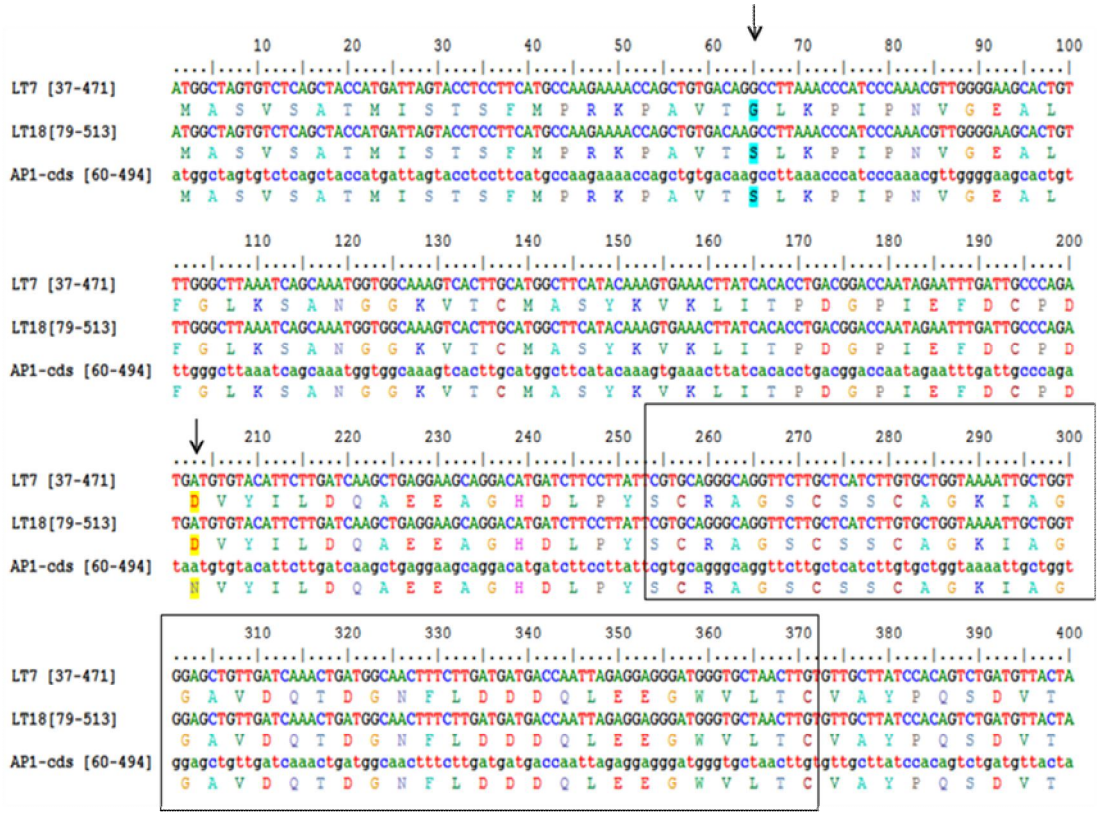

Figure 3.6 Amino acid sequence and the conserved domain of PFLP

Sequence alignment was performed using BioEdit v7.0.5. Nucleotide differences at position 64 and 202 of the published sequence (AP1; AF039662, NCBI) result in residue changes as indication by arrows. In the amino acid sequence of PFLP from Capsicum cDNA (LT7) glycine is present instead of serine in the polypeptide of PFLP from Capsicum genomic DNA (LT18) and AP1 protein. The conserved iron-sulfur cluster binding domain (in rectangle) was detected using CD search tool of NCBI with the query sequence Q9ZTS2 which is translated from AF039662. The iron-binding domain consists of 4 functional cysteine residues at positions 86th, 91th, 94th and 124th in the polypeptide chains.

3.3 Cloning of signal peptide –truncated *Pflp* (T-*Pflp*)

3.3.1 Cloning of T-*Pflp* into pGEM-T Easy vector

Signal sequence - truncated *Pflp*, T-*Pflp*, was amplified from genomic DNA using APF4 and APR3 primers and *Pfu* DNA polymerase (Bioline, Aus). Amplified T-*Pflp* was gel purified and A-tailed prior to ligation into pGEM-T Easy vectors. The ligated construct was transformed into TOP 10F' and selected on LB/Amp100/IPTG/X-Gal plates. White and blue colonies on LB/Amp100/IPTG/X-Gal plates were selected for restriction digestion analysis (Figure 3.7). A candidate vector is expected to release two fragments with the sizes of 3 kb and 313 bp after *Eco*RI digestion. The clones mentioned with their respective number on the master plate in Figure 3.7 were chosen for *Eco*RI digestions the results of which are presented in Figure 3.8. The negative controls for the digestion without addition of *Eco*RI of each analysed clone were set up to evaluate the efficiency of the restriction reaction. Clones resulted in unfavorable size of insert or without inserts (clones 1, 2, 8 and 10) were eliminated. Digestions of clones 4-7 resulted in three bands at approximately 3 kb, 1.8 kb and 320 bp. The 3 kb band is the linearized pGEM-T Easy vector and the 320 bp band is the possible *T-Pflp* insert. Incompletely digested vectors have sizes within 5 and 1.8 kb or the size range of intact plasmid in the negative controls. The presence of inserts in the candidate vectors of clone 4-7 was confirmed by PCR with SP6 and T7 primers. The PCR product of pGEM-T Easy/T-*Pflp* and pGEM-T Easy/*Pflp* vectors, as demonstrated in Figure 3.9 A, are 497 bp and 634 bp bands, respectively. The amplification result obtained in Figure 3.9 B showed the presence of bands of the predicted sizes in PCR of the candidate clones (lanes 1-4) and pGEM-T Easy/*Pflp* (lane 6). There was no bands in negative controls of PCR (lanes 7, 8).

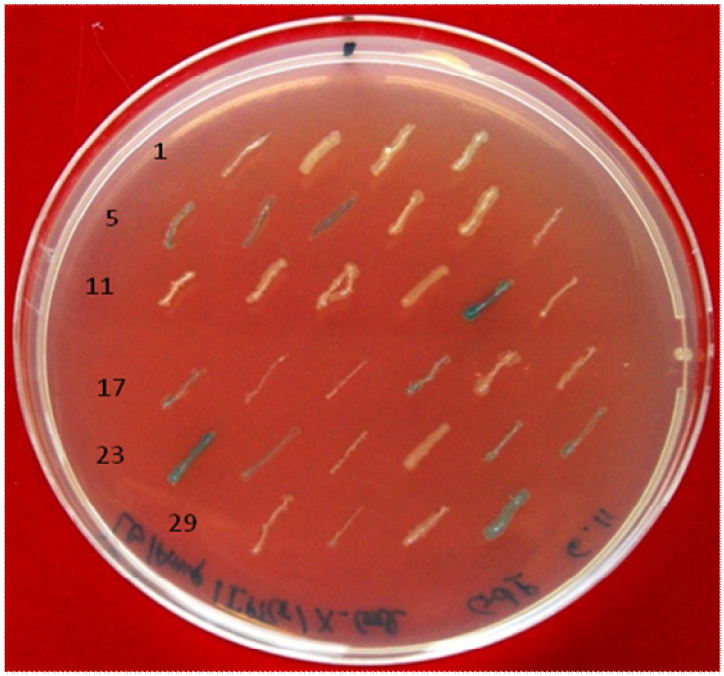

Putative clones containing pGEM-T/T-*Pflp* vectors

Figure 3.7 Transformed clones selected for pGEM-T/T-*Pflp* screening

White colonies on LB with IPTG and X-gal usually contain recombinant vectors. However, recombinant vectors with the right inserts sometimes may be obtained from the blue colonies on selective plates.

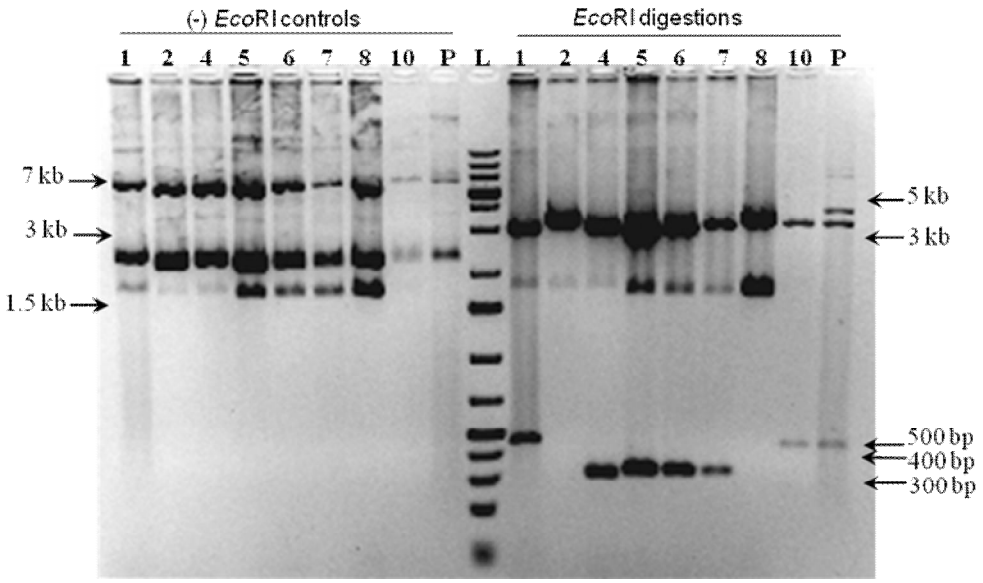

Figure 3.8 *Eco*RI digestion of putative pGEM-T Easy/T-*Pflp* vectors

The presence of T-*Pflp* in recombinant pGEM-T Easy was checked with *Eco*RI digestion which was expected to release a 313 bp insert and of the 3 kb vector. The negative controls for the digestions have the same component as the digestions but exclude *Eco*RI. The lane number indicates the respective number of clones on the master plate of which the plasmids were analysed. The digestion utilized pGEM-T Easy/*Pflp* vector (P) was aimed to facilitate the identification of T-*Pflp* insert in the digestions.

.

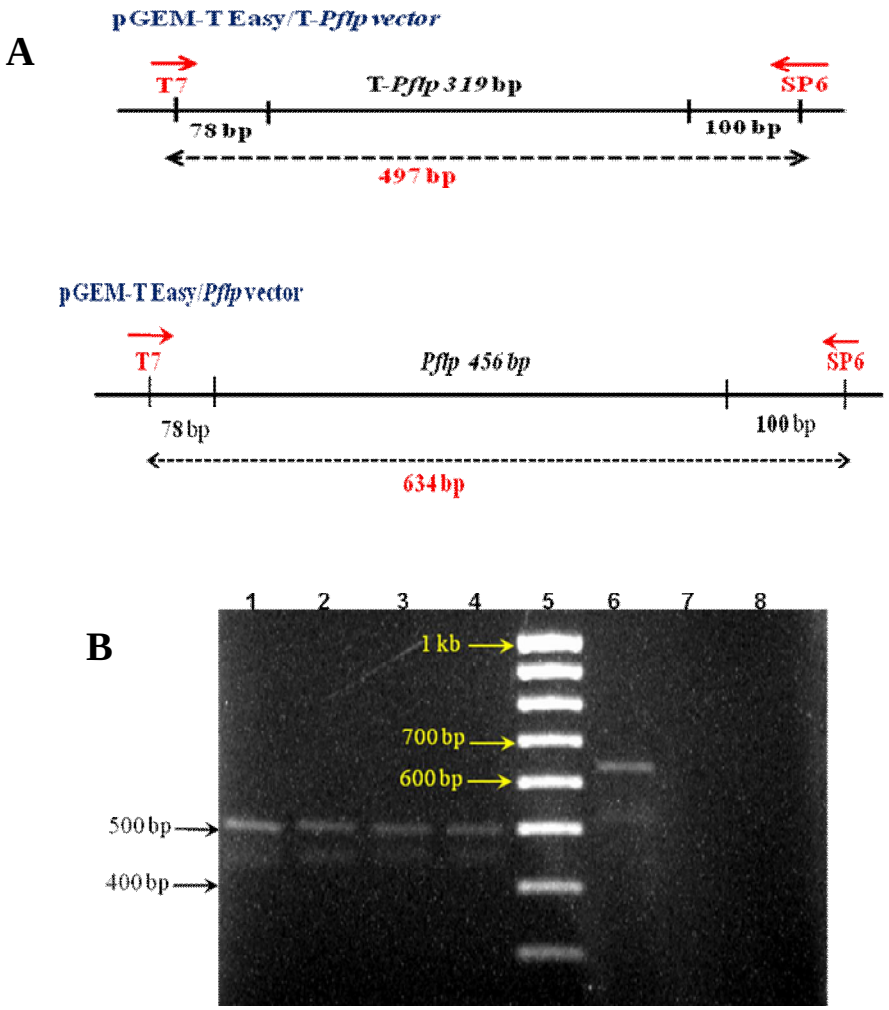

Figure 3.9 Confirmation of recombinant pGEM-T Easy/T-*Pflp* vectors by PCR with SP6 and T7 primers

Putative pGEM-T Easy/T-*Pflp* vectors which contain the right size of the inserts were futher confirmed by PCR using SP6 and T7. The amplification with a sequenced pGEM-T Easy/*Pflp* vector was perfomed in parallel to observe the difference between the two recombinant pGEM-T Easy vectors. A. The expected size of the amplified products from the recombinant pGEM - T Easy vectors. B. PCR results and the templates used for amplification as follows, lane 1 – 4: pGEM-T Easy/T-*Pflp*, lane 6: pGEM-T Easy/*Pflp*, lane 7: insert (-) recombinant pGEM-T Easy vector, lane 8: PCR reaction without DNA template; Lane 5: HyperLadder IV (Bioline, USA).

3.3.2 Sequence analysis

The obtained T-*Pflp* sequences with SP6 and T7 primers are the same as partial sequences of *Pflp* insert in pGEM-T Easy. The fittest alignment of *Pflp* derived sequences and the published sequence obtained with Gd-1 and Gd-2 –RC which were sequences of the same clone with SP6 and T7, respectively (Figure 3.10). There is also one base pair change in Gd-1 and Gd-2–RC at the position 202 of the published sequence (AP1) that is the same as in the alignment of *Pflp*. The nucleotide difference at position 32 of Gd-1 sequence is an error in sequencing which was confirmed by comparisons with the trace files and the reverse sequence (Gd-2) by T7 primer. The T-*Pflp* clone bearing Gd-1 and Gd-2-RC is 100% identical in sequence with the isolated *Pflp*, thus, it was used for subcloning into the expression vector.

Figure 3.10 Alignment of T-*Pflp* sequences in pGEM-T vectors with known sequences of *Pflp*

Gd 1 and reverse complement Gd2 (Gd2 –RC) are sequences of the same pGEM-T/T-*Pflp* vector derived from the sequencing with SP6 and T7, respectively. Sequences obtained from T7 reverse primer sequencing were complimentarily reverted by BioEdit software prior to sequence alignment with ClustalW. Sequences of the two analysed vectors as follows, LT-7 + LT-8RC, LT-17RC + LT-18. The identical alignment is marked by asterisks and differences were indicated with red letters. The single difference between the query sequences and the published sequence (AP1) was marked in blue rectangle.

3.4 Construction of expression vectors

3.4.1 Subcloning of *Pflp* and T-*Pflp* into pRSET B vectors

Pflp and T-*Pflp* amplified from genomic DNA which have the highest similarity with the published sequence (Figure 3.10) was selected to be subcloned from pGEM-T Easy vectors into pRSET B vectors (Invitrogen). The subcloning was schematically summarized in (Figure 3.11). The recombinant pGEM-T Easy vectors and pRSET B vectors were digested with *Nco*I and *EcoR*I. The resulted *Pflp* and T-*Pflp* fragments and linearized pRSET B with *Nco*I and *EcoR*I ends were isolated by electrophoresis and gel purification and combined in ligation reactions. The ligated product was transformed into TOP10F' cells and was screened on LB/Amp100 plates. Three candidate pRSET B/*Pflp* clones were selected for restriction analysis with *Nco*I, *Bam*HI and *EcoR*I (Figure 3.12).

Plasmid isolation of each clone was subsequently digested with *Bam*HI, *Eco*RI, combination of *Bam*HI with *Nco*I or *Eco*RI. Single digestion results in the linearized pRSET B. Double digestions of a pRSETB/*Pflp* with the correct orientation of the insert result in a visible 3.3 kb band in *Bam*HI and *Nco*I digest while two bands with sizes of 3kb and 467 bp are obtained in *Bam*HI and *Eco*RI digest (Figure 3.12). The electrophoresis result in Figure 3.12 shows the presence of 2.8 kb and 467 bp fragments in *Bam*HI and *Eco*RI digestions which are not detected in the negative controls and the remaining digestions. The reactions without addition of the restriction enzymes (-) and digestions of pRSET B were negative insert controls, while pGEM-T/Easy digests were positive insert controls.

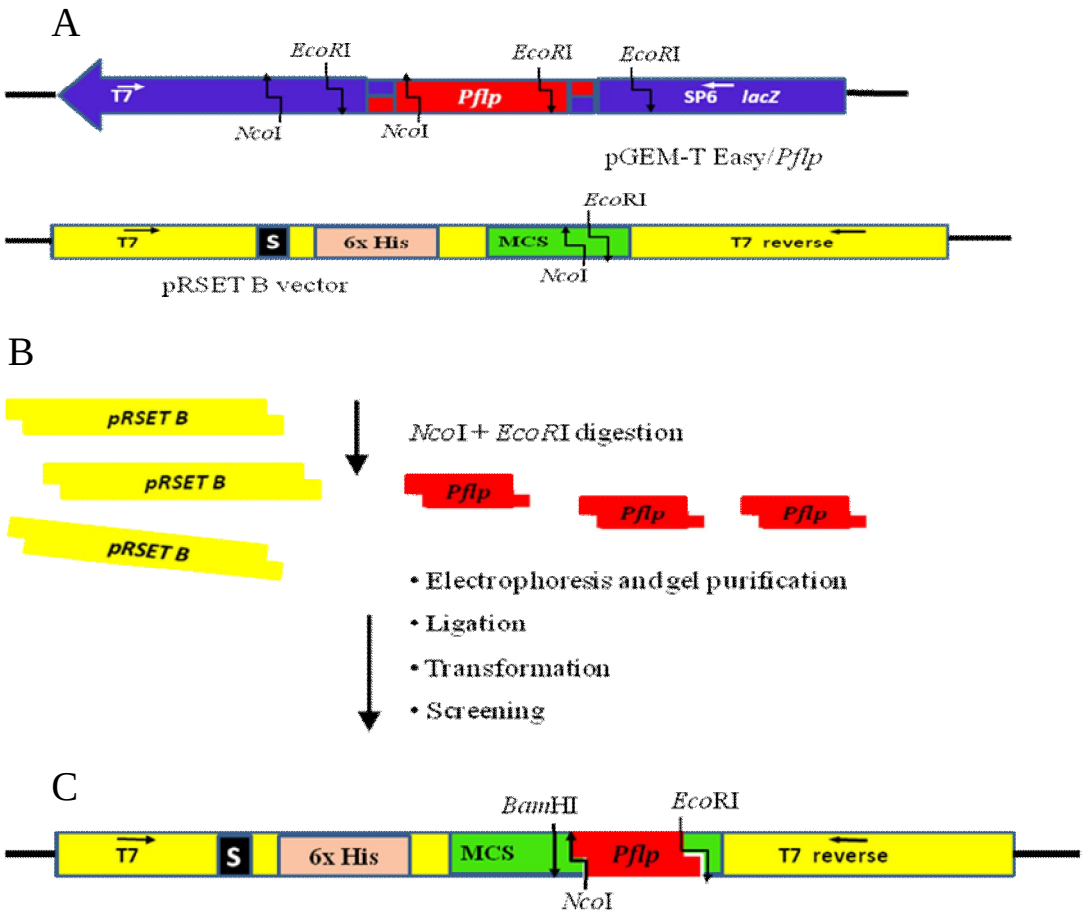

Figure 3.11 Construction of expression vector with pRSET B

Digestion with *Eco*RI and *Nco*I was applied for pGEM-T Easy/*Pflp* and pRSET B vectors (A) before isolation of the inserts and vectors for ligation, transformation and screening for the expression vector pRSET B/*Pflp* (B). The expression vector (C) was confirmed based on its reference points *e g*. restriction sites, position of the start codon (S), in which *Pflp* inserts with correct orientation are not released by *Bam*HI and *Nco*I digestion. PCR confirmation can be applied using *Pflp* specific primers, T7 and T7 reverse primers. The coding region of the fusion protein contains polyhistidine (6x His) region and the insert. Elbow arrows indicate restriction sites with cohesive ends while the straight one describes the blunt end.

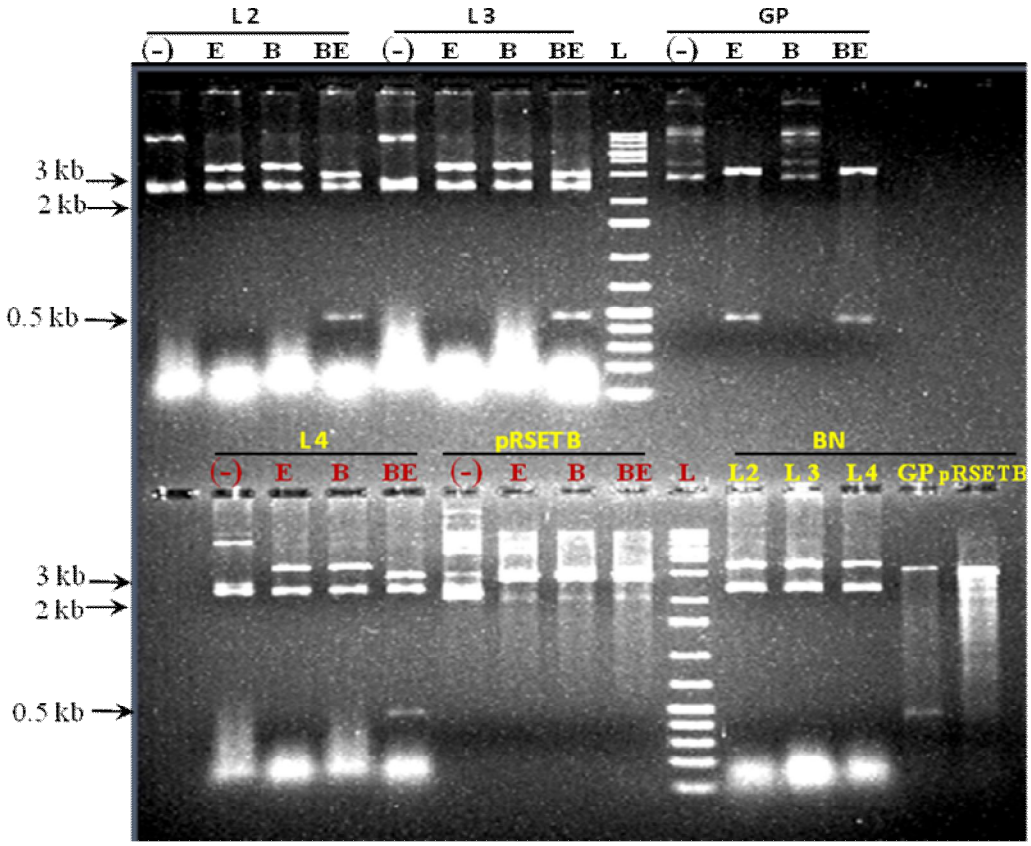

Figure 3.12 Restriction enzyme analysis of pRSET B/*Pflp* vector construct

Plasmids of the candidate pRSET B/*Pflp* clones (L2, L3 & L4), pGEM-T/ *Pflp* vector (GP) and empty vector pRSET B was digested with *Bam*HI, *Eco*RI and *Nco*I in single or double digests. Digestions with *Eco*RI (E), *Bam*HI (B), *Bam*HI + *Eco*RI (BE) and *Bam*HI + *Nco*I (BN) were set up for each vector along with the negative control reaction without addition of enzymes. Gene Ruler 1 kb plus DNA ladder was used (L).

Selection of pRSET B/T-*Pflp* was performed with *Hind*III and *Bam*HI digestions which result in 2.8 kb and 336 bp fragments. In Figure 3.13 the presence of the 2.8 bp fragments and the small fragments within 300 and 400bp at lane 8 and lane 15 suggests that these vectors are pRSET B/T-*Pflp* candidates. Negative controls including the digestions of pRSET B and pGEM-T Easy/T-*Pflp* which excluded restriction sites of *Hind*III and *Bam*HI showed no band below 1.5 kb. Plasmids of lanes 8, 10, 14 and 15 were chosen for PCR confirmation with T7 and T7 Reverse primers, of which amplification reactions were marked as Rd1 – Rd4 in Figure 3.14, respectively. As the schematic representation in Figure 3.14A the PCR product size of pRSET B/T-*Pflp* vector with T7 and T7 Reverse primers is 586 bp. Amplified products of Rd1, Rd3 and Rd4 have the sizes within the size rage of the predicted PCR product. The product size of Rd4 is a little bit smaller than those of Rd1 and Rd3. Amplification of the recombinant pRSET B vector which gave the negative result in *Hind*III and *Bam*HI digestions, Rd2, produced a 300 bp fragment as the PCR result of pRSET B. No bands were detected in the PCR reaction without template. The recombinant pRSET B vectors with the possible correct size of inserts - Rd1, Rd3 and Rd 4, were selected for sequencing.

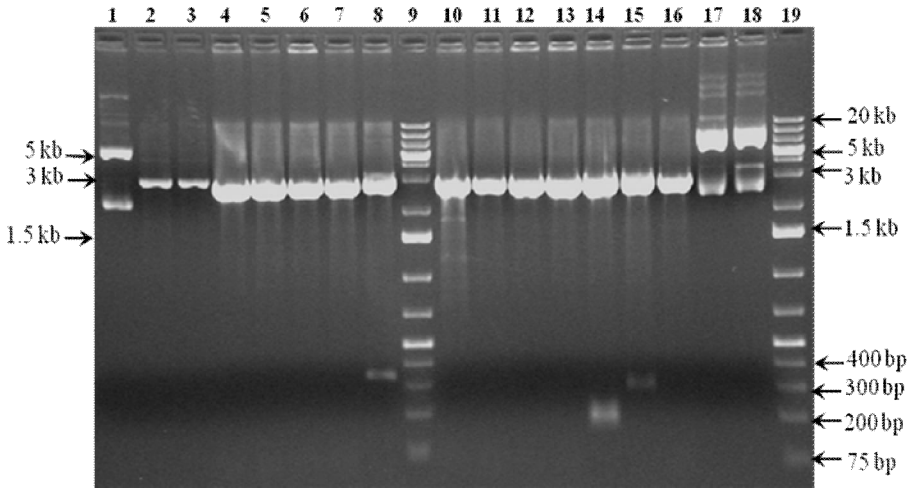

Figure 3.13 Digestions of pRSET B/T-*Pflp* candidate clones with *Hind*III and *Bam*HI

Screening of pRSET B/T-*Pflp* vectors with *Hind*III and *Bam*HI digestions, by which the right clones resulted in 2.8 kb and 336 bp bands on the agarose gel. Candidate pRSET B/T-*Pflp* vectors were digested with *Hind*III and *Bam*HI; lane 4 – 8, 10-16: putative pRSET B/T-*Pflp* + *BamH*I + *Hind*III. Digestions of pRSET B served as negative insert controls, lane 1: pRSET B in digestion mixture excluding restriction enzymes, lane 2: pRSET B + *Bam*HI, lane 3: pRSET B + *Hind*III. Containing no restriction sites of *BamH*I and *Hind*III digestions of pGEM-T Easy/T-*Pflp* appeared as intact plasmid; lane 17: pGEM-T Easy/T-*Pflp* in digestion mixture excluding restriction enzymes, lane 18: pGEM-T Easy/T-*Pflp* + *BamH*I + *Hind*III. Lane 9 & 19: 1 kb ladder.

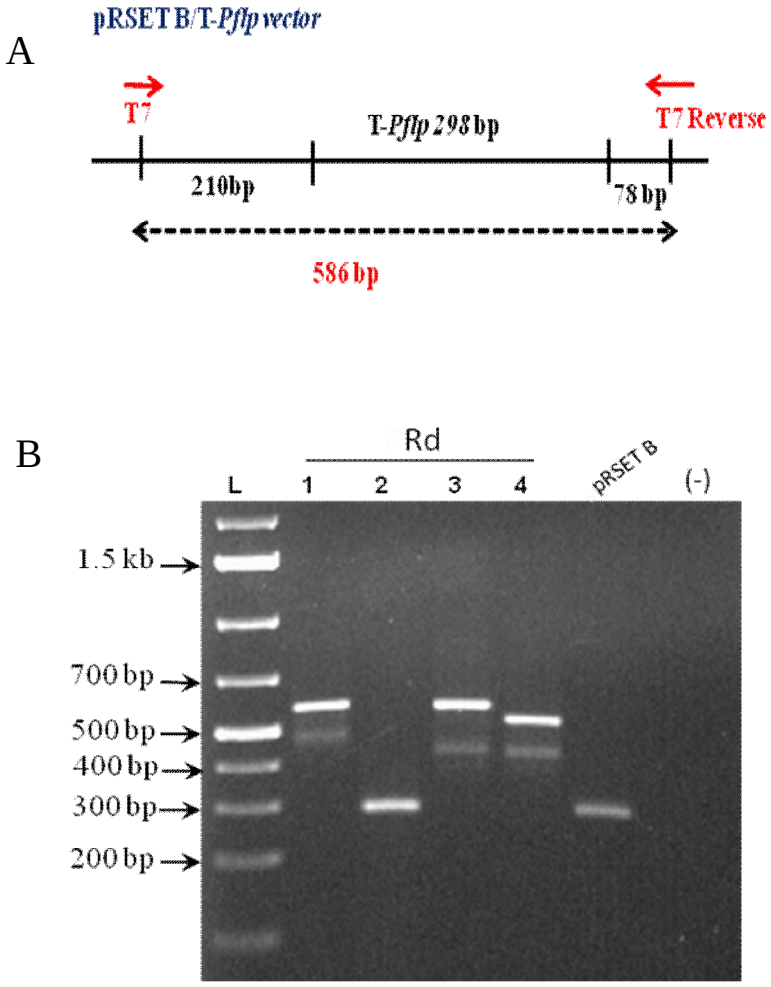

Figure 3.14 Confirmation of pRSET B/T-*Pflp* clones by PCR with T7 and T7 reverse primers

A. Schematic description for the size of PCR product amplified from pRSET B/T-*Pflp* with T7 and T7 Reverse primers which is 582 bp. B. Amplification of recombinant pRSET B selected from the restriction digestion analysis (Rd 1-4). Clones with positive results (Rd1, Rd3, Rd4) and negative result (Rd2) in *BamH*I + *Hind*III digestions were further analysed by PCR. Negative controls were the amplification of pRSET B and the reaction without DNA template (-). L: 1 kb ladder.

3.4.2 Sequence analysis

The multiple sequence alignments of the obtained *Pflp* and T-*Pflp* sequences were performed using BioEdit and ClustalW softwares. Each of the recombinant pRSET vector were sequenced with T7 and T7 reverse primers. The alignments with high percentage of identity with the published sequence are shown in Figure 3.15 and 3.16. There are one base pair difference between the subcloned sequences in pRSET B and the published data, which is the same as the *Pflp* and T-*Pflp* sequences derived from SP6 and T7 sequencing. The *Pflp* and T-*Pflp* inserts of the recombinant pRSET B vectors are in the correct orientation and in frame with the fusion protein preceded with 6x His sequences (Figure 3.17).

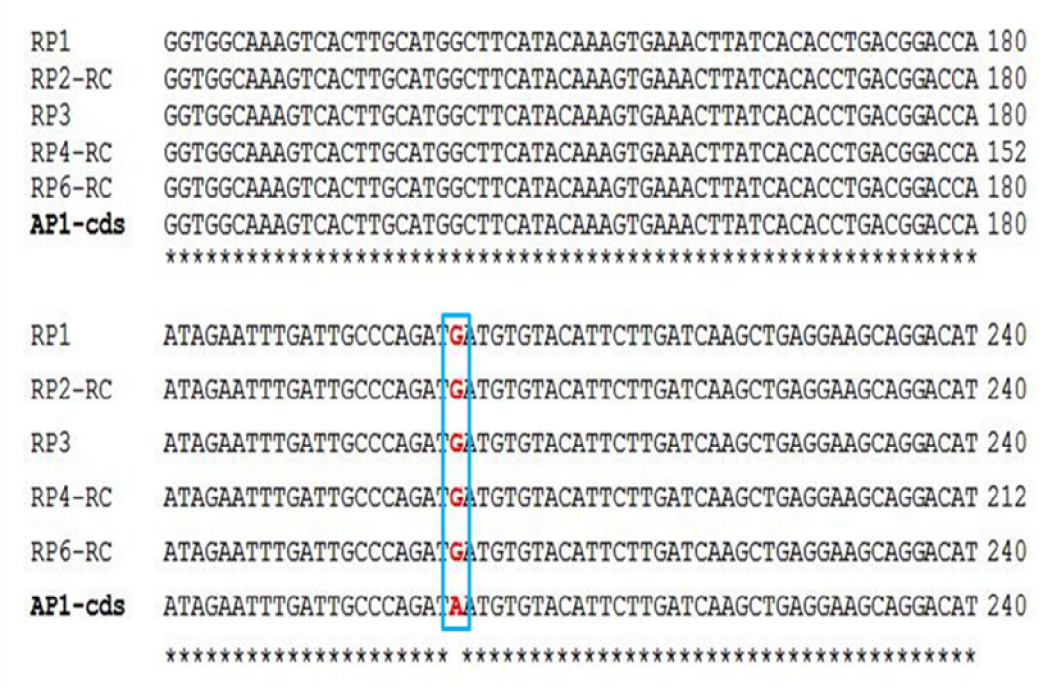

Figure 3.15 Alignment of *Pflp* sequences in pRSET B with the published AP1 sequence.

Each selected vector was sequenced with T7 and T7 reverse primers. Sequences obtained from T7 reverse primer sequencing were complimentarily reverted by BioEdit software prior to sequence alignment with ClustalW. Sequence profile for each of analysed vectors was indicated as follows: RP1/RP2-RC, RP3/RP4-RC and RP6-RC. The identical alignment is marked in asterisks and differences were indicated with red letters. There is one base pair difference between the *Pflp* sequences and the published sequence at nucleotide 202th in AP1 sequence, which is the same as the sequences of *Pflp* in pGEM-T Easy vector (blue rectangle).

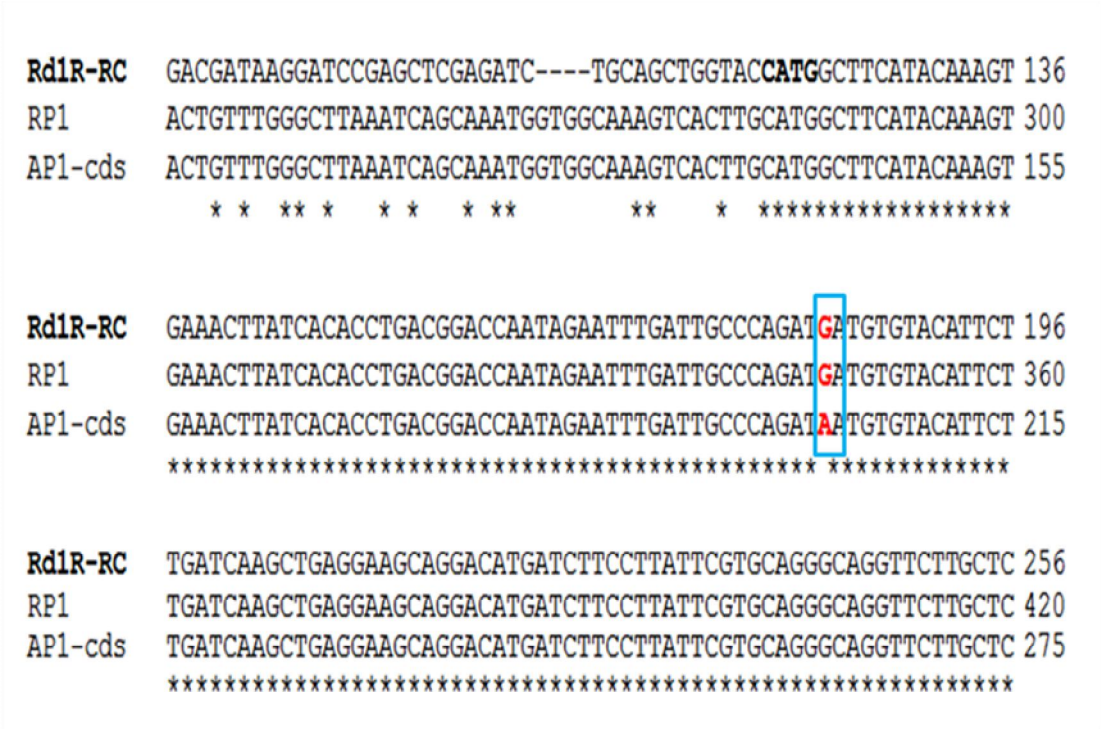

Figure 3.16 Alignment of T-*Pflp* sequences in pRSET B with the published AP1 sequence.

High homology with the published *Pflp* sequence (AP1) was obtained in clone Rd1. The Rd1 sequence with T7 reverse primer or Rd1R was complimentarily reverted by BioEdit software prior to sequence alignment with ClustalW and referredto as Rd1R-RC. The identical alignment is marked by asterisks and differences were indicated with red letters. The sequence of T-*Pflp* in pRSET B vector is started from the **bold nucleotide**, which is the same as *Pflp* sequence in pRSET B vector and the same identical percentage to the published sequence. The nucleotide difference occurs at the same position as the previous alignments. The size of T-*Pflp* insert in pRSET B vector is 298 bp**.**

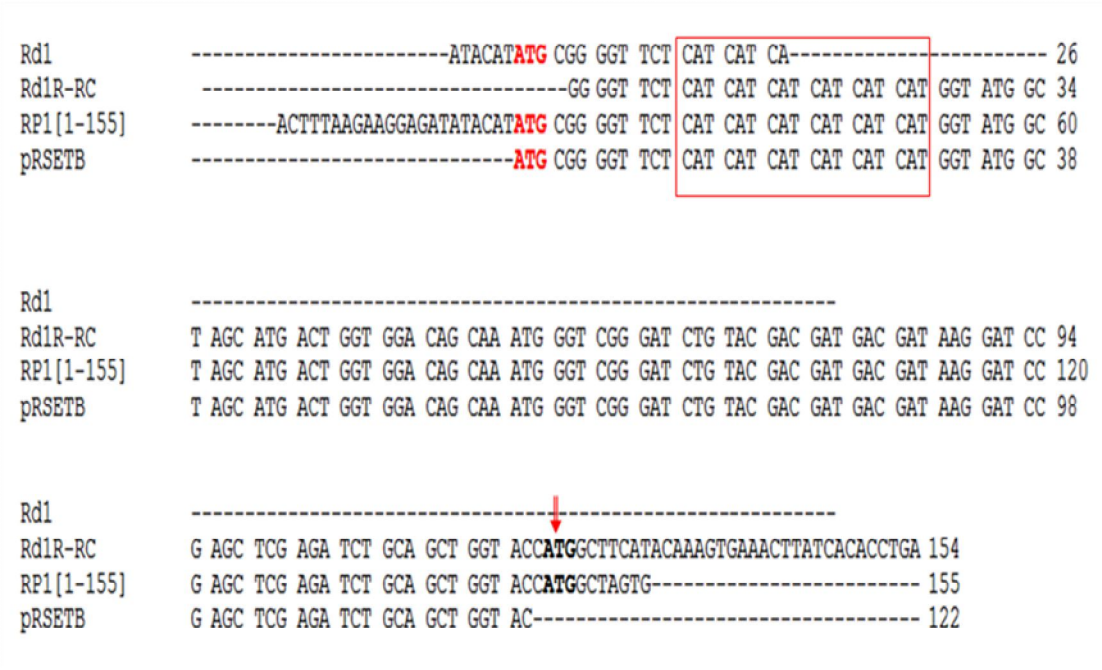

Figure 3.17 Alignment of the fusion regions of pRSET B/T-*Pflp* and pRSET/PFLP with the polyhistidine coding sequence of the vector.

The alignment of the fusion regions of the expression vectors of T-*Pflp* and *Pflp* with the 6xHis sequence of pRSET B vector was done to check if the inserted genes were in frame with the polyhistidine sequence. Sequence profiles of each vector derived from the sequencing with T7 and T7 reverse primers were combined for the analysis; Rd1 & Rd1R-RC of clone Rd1: pRSET/*T-Pflp* sequence, RP1: T7 primer derived sequence of pRSET/*Pflp*. The start codon of the fusion sequence in pRSET vectors was marked in red nucleotides and the 6xHis region was marked with the red rectangle. The insertion sites of *T-Pflp* and PFLP inserts were marked by the arrow.

3.5 Protein expression

The recombinant pRSET B vectors containing the inserts with correct sequences and orientation were transformed into BL21(DE3)pLysS. The transformants were subsequently selected on LB/Amp100 and LB/Amp100/Cm35 plates before protein expression with IPTG induction. The protein expression was analysed through samples collected from 0 to 6 hours during the induction. The positive control expression applied pQE 30 vector harboring 6x His *Gfp*. Protein expression of BL21(DE3)pLysS containing pRSET B vector was used as negative control for the expression of *Pflp* and T-*Pflp*. Samples of all time points were disrupted using "freeze-thaw" method. The clear supernatant and the pellet from the cell lysis were analysed on polyacrylamide gels with SDS-PAGE followed by Coomassie staining. The increase in protein expression observed in pellet and the clear lysate was consistent with the duration of IPTG induction. Sizes for 6x His GFP, 6x His PFLP and 6x His T-PFLP are 30, 20.2 and 13.5 kDa, respectively, which were estimated using Proteomics tools of ExPASy Proteomics Server (http://expasy.org). In the positive control the increased density of 6x His GFP in the soluble fraction (the clear lysate) of cell lyse was observed with the molecular weight of 30 kDa, which was distinct from the basal expression and the insoluble contents (Figure 3.18 A). The expression patterns of the negative control and the recombinant pRSET B clones were quite similar (Figure 3.18 B, C & D). There was no distinguishable bands of the polyhistidine fusion proteins in PFLP and T-PFLP expression (Figure 3.18 C & D). However, all of the samples at time point 6 resulted the best protein expression. Thus, 6 hour IPTG induction was applied for scaling up the protein extracts for purification.

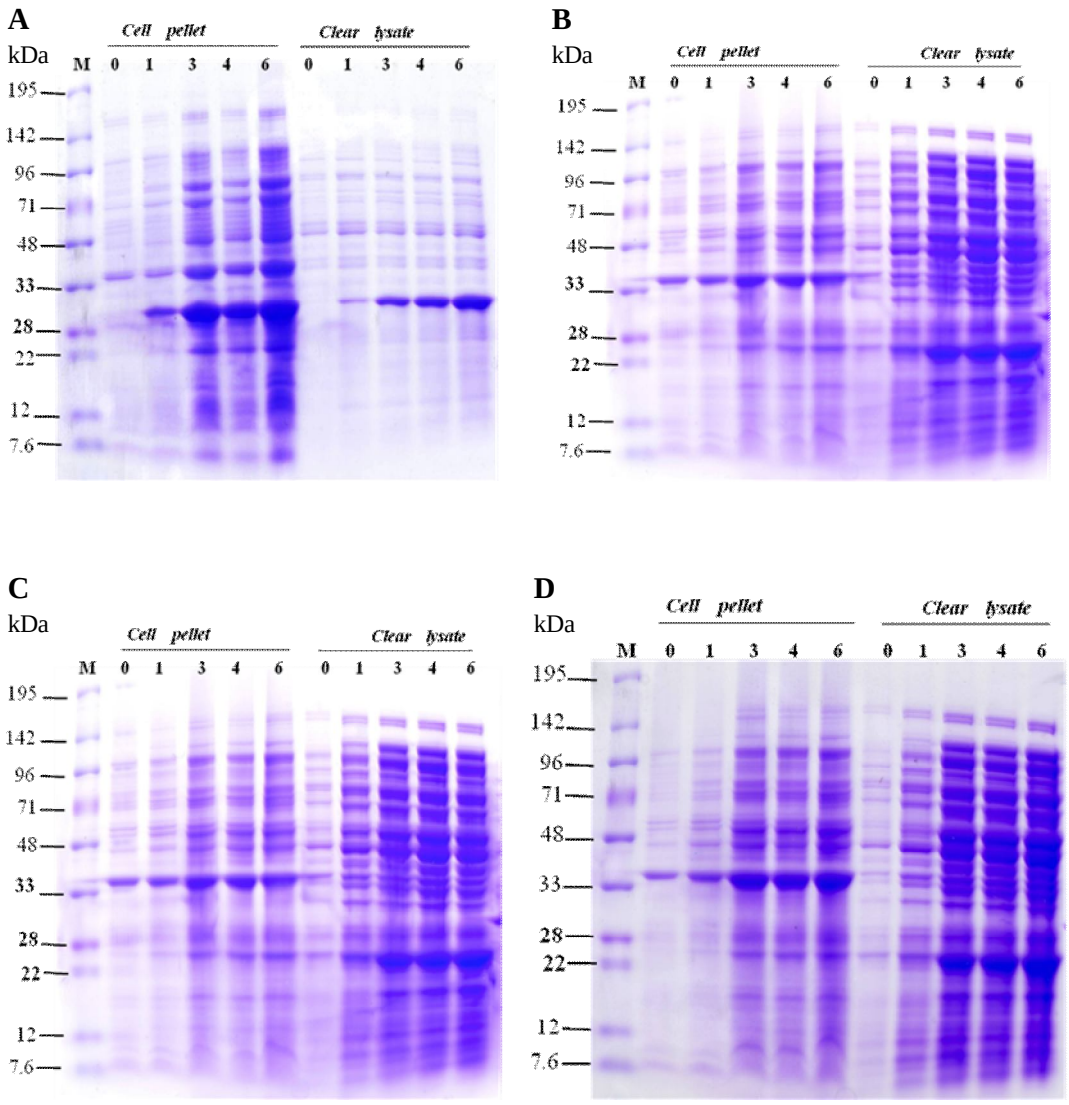

Figure 3.18 Time course expression of recombinant pRSET B

The protein expression in *E. coli* strains with IPTG induction in the duration from 0 to 6 hours. In each of the analysed expressions, the cell pellet and clear lysate from the cell lysis at each time point were collected and analysed on the same gel. **A**. Protein expression of BL21(DE3)pLysS containing pRSET B vector with *Gfp* gene insert, in which the molecular weight of expressed 6x His tagged GFP is 30 kD **B**. The protein expression of BL21(DE3)pLysS containing pRSET B **C.** The protein expression of BL21(DE3)pLysS with pRSET B haboring T-*Pflp*. **D**. The protein expression of BL21(DE3)pLysS with pRSET B haboring *Pflp*. (**M)** CLEAR PAGE Marker (C.B.S. Scientific, USA).

3.6 Protein purification

3.6.1 GFP purification

The clear lysate from the cell lysis after 6 hour culture with IPTG induction was introduced into PolyPrep columns containing 2 mL of equilibrated Ni-NTA agarose. Sodium buffers with increasing concentration of immidazole (20, 30, 200 and 250 mM) were subsequently added into the column. The flow-through fractions were collected at column ends and analysed by SDS-PAGE along with IPTG non-induced and induced controls. Western blotting with anti HisG antibody and HRP conjugates was applied to detect the target proteins in the collected fractions. Figure 3.19 A & B and suggest that most of the 6xHis GFP was eluted with 200 mM immidazole buffer (lane I200), while a small amount of the protein was present in the first flow through fraction (F), 20 mM and 30 mM immidazole fractions (lanes I20, I30). However, there was possibly more 6xHis GFP in the insoluble fraction of the cell lyse as more protein with the same molecular weight with the protein in lane I200 is observed in the pellet (IP) than in the lysate (IL). Additionally immunoblotting of the whole cell lysate showed the occurrence of GFP in both insoluble and soluble fractions (data not shown).

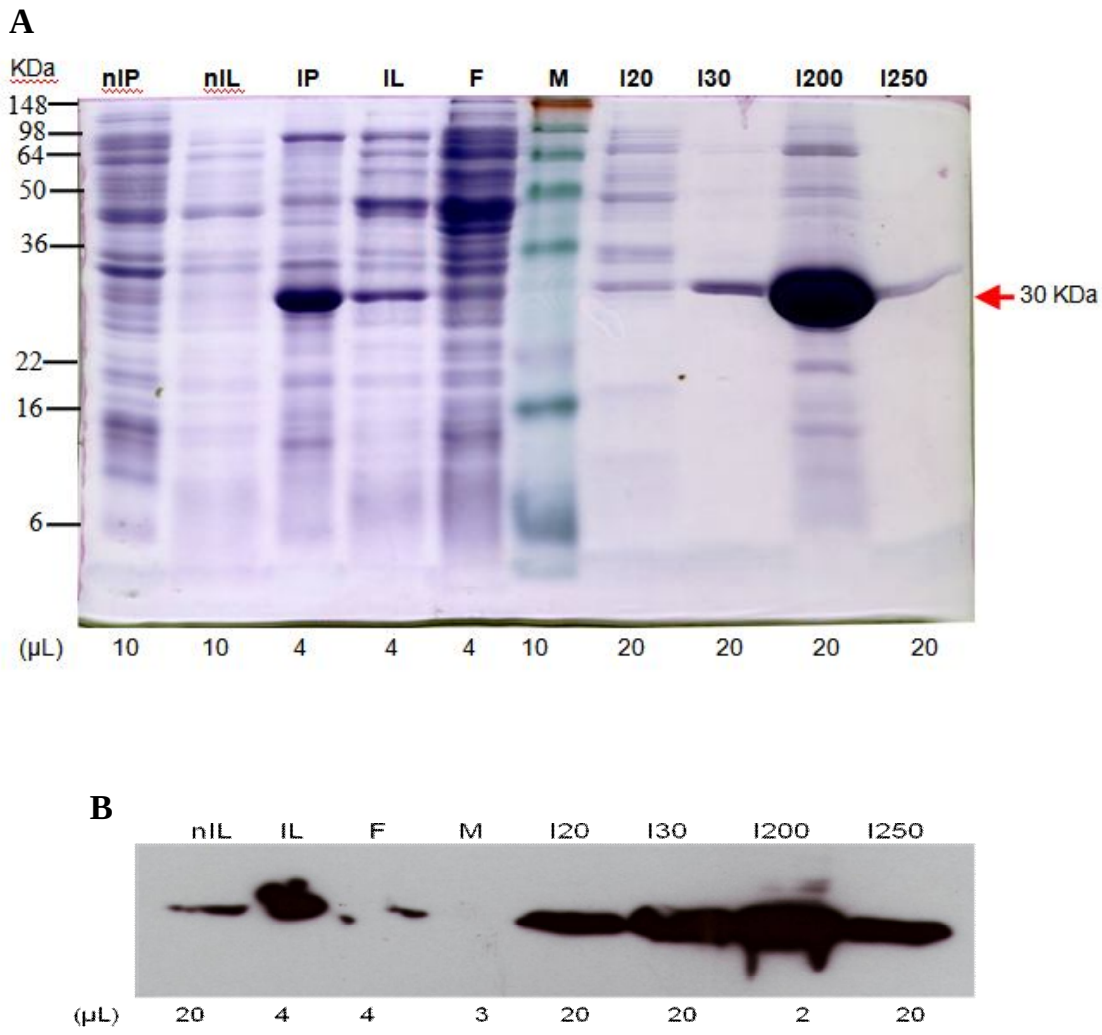

Figure 3.19 Purification of 6xHis GFP expressed in BL21(DE3)pLysS by Ni-NTA agarose

6x His tagged GFP expressed in BL21(DE3)pLysS was purified with Ni – NTA agarose (Qiagen) in Econo Poly Prep column and sodium buffers with varied concentrations of immidazole. **A**. The flow through collections after addition of the clear lysate of the cell lyses (F) and the buffers with increased concentrations of immidazole (20 – 250 mM or I20 – I250) were separated on 12.5% polyacrylamide gels. Lysed cell pellet and clear lysate samples of cell culture with or without IPTG induction were used to compare with the obtained purified proteins; nIP: non- IPTG induced pellet, nIL: non- IPTG induced lysate, IP: IPTG induced pellet, IL: IPTG induced lysate. M: SeeBlue pre-stained marker (Invitrogen). **B**. GFP was identified from the fractions of GFP purification by immunoblotting and chemiluminescent detection. The amount of each sample run on the gels as indicated.

3.6.2 T-PFLP purification

The clear lysate of T-PFLP extraction with the volume of 8 mL was passed through the equilibrated Ni-NTA column. The collected fractions were separated on 12.5% polyacrylamide gel and visualized with Coomassie staining as shown in Figure 3.20A. Multiple bands were present in the elution fractions with 200 mM immidazole buffer (lane I200.1 and I200.2, Figure 3.20A). However, only bands between 10 and 20 kDa were detected by immunoblotting with anti HisG antibody and chemiluminescent detection (Figure 3.20 B&C). The proteins were analysed on 12.5% glycine gel and electrophoretically transferred onto the membrane in Figure 3.20B, while 12% ClearPAGE (Tricine) gel and iBlot gel transfer system was used in Figure 3.20C. Identical protein pattern in the induced lysate (lane IL) and the unbound protein (lane F) fractions can be observed in Figure 3.20C. The amount of T-PFLP in the induced lysate was too low to be visible on the blots, but with higher concentration in elution fraction T-PFLP bands can be observed (lane I200, Figure 3. 20 B&C). By contrast, strong bands with the approximate molecular weight of 15 kDa was present in negative control lanes of both Western blottings. The protein bands of the negative controls are distinguishable on the immublots. The negative controls are whole cell lysate of BL21(DE3)pLysS bearing pRSET B which derived from the cell disruption by “freeze-thaw” (in Figure 3.20B) or sonication (in Figure 3.20C) method.

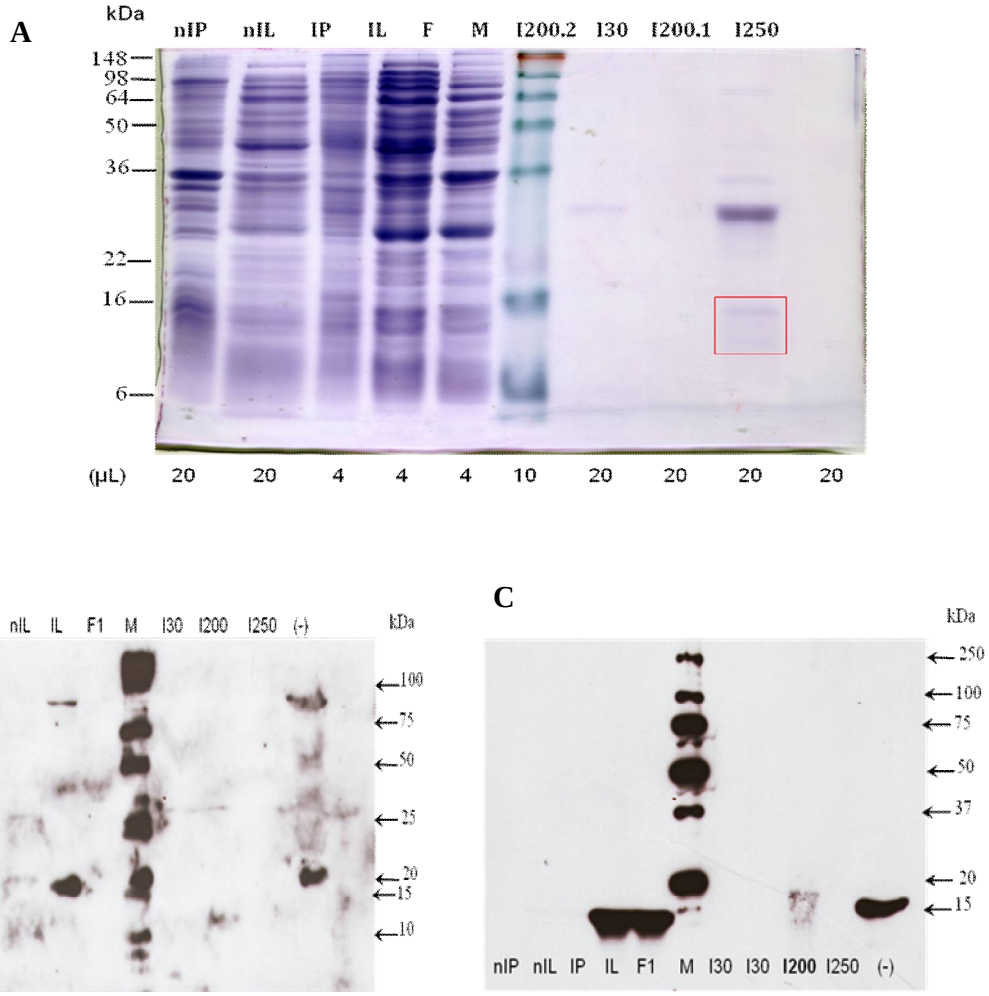

Figure 3.20 Purification of 6x His tagged T-PFLP expressed in BL21(DE3)pLysS

A. 6x His tagged T-PFLP were purified with Ni – NTA agarose (QIAGEN) and sodium buffers containing immidazole. The flow through samples after addition of the clear lysate of the cell lyses (F) and the buffers with increasing concentrations of immidazole (I_{30} – I_{250}) were analysed by SDS – PAGE. Lysed cell pellet and clear lysate samples of cell culture with or without IPTG induction were used to compare with the obtained purified proteins; nIP: non- IPTG induced pellet, nIL: non- IPTG induced lysate, IP: IPTG induced pellet, IL: IPTG induced lysate, M: SeeBlue pre-stained marker (Invitrogen). Predicted position of T-PFLP was marked with the red box. **B and C**. T-PFLP was identified by immunoblotting and chemiluminescent detection with CPS-3 substrate **(B)** or the solution of iodophenol, luminol and hydrogen peroxide (**C**). Each sample with the volume of 20 µL were run on 12.5% (**B**) or 12% (**C**) gels. Negative controls are cell lysate of BL21(DE3)pLysS containing pRSET B. (M) Precision Plus Protein standard

3.6.3 PFLP purification

The cell lysate of PFLP expression with the volume of 8 mL was passed through the equilibrated Ni-NTA column. The collected fractions were separated on 12.5% glycine gel as shown in Figure 3.21 A&B. It can be seen from the SDS-PAGE gel that most of the proteins were eluted with 100 mM immidazole buffer (lane I100.2) with the molecular weight range from 98 to 22 kDa. Lesser amount of the proteins below 16 kDa was visible. The highest amount of protein obtained between 36 and 22 kDa in the second fraction (or the second part of the elution volume) of 100 mM immidazole buffer (lane I100.2) and the first fraction of 200 mM immidazole buffer (I200.1). As the high basal expression in the IPTG induced samples it is impossible to distinguish PFLP band in the induced cell lysate. No protein bands were detected in the flow through sample of 250 mM immidazol buffer.

The fractions of PFLP purifications were separated on 12% ClearPAGE gels. Identification of PFLP in the loading samples was performed by immunoblotting and chemiluminescent detection with iodophenol, luminol and hydrogen peroxide. As shown in the immunoblot, Figure 3.22, the protein bands with the same approximate molecular weight of 25 kDa were obtained in the lanes of both induced and non-induced pellet (lanes nIP and IP) and the purified PFLP (lane I100). The appearance of the protein bands in the negative control, in the whole cell pellet and lysate and the unbound protein samples are quite similar. There was no His-tagged protein detected in the flow through fractions of 30 and 40 mM immidazole buffers. The His-tagged proteins present in lane I20 within 20 and 15 kDa might be the same those in the negative control.

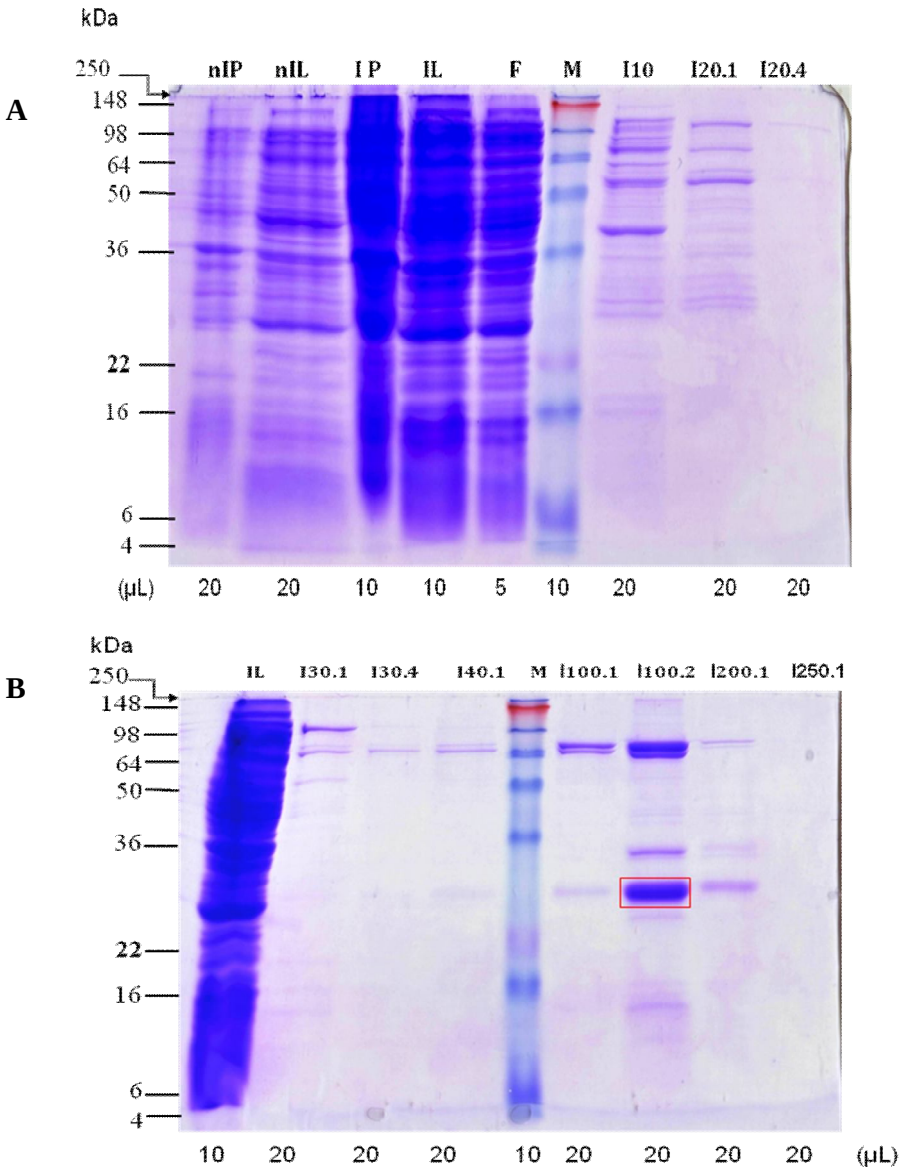

Figure 3.21 Purification of 6x His tagged PFLP expressed in BL21 (DE3)pLysS

The flow through samples after addition of the clear lysate of the cell lyses (F) and the buffers with increased concentrations of immidazole (I_{30} – I_{250}) were separated on 12.5% glycine gel by SDS-PAGE. Different flow-through fractions of the same immidazole concentration were also analysed. Lysed cell pellet and clear lysate samples of cell culture with or without IPTG induction were used to track the obtained purified proteins; nIP: non- IPTG induced pellet, nIL: non- IPTG induced lysate, IP: IPTG induced pellet, IL: IPTG induced lysate. M: SeeBlue pre-stained marker (Invitrogen). The estimated band of purified PFLP was marked with the red box.

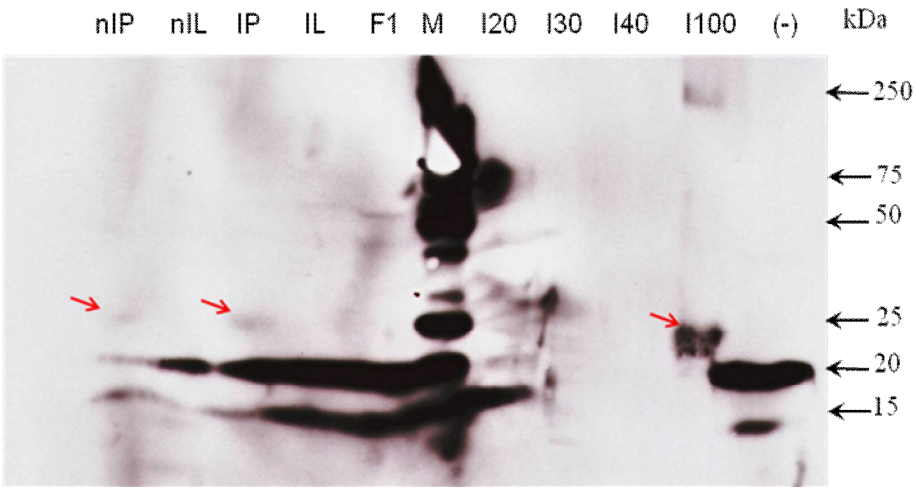

Figure 3.22 Western blot analysis of fractions from 6x His PFLP purification

The whole cell pellet and lysate without or with IPTG indution, respectively, and fractions collected from 6x His PFLP purification with the volume of 20 µL were analysed by SDS-PAGE with anti HisG antibody and HRP conjugates via chemiluminescent detection; 5 µL of Precision Plus Protein standard (M) was used to estimate the molecular weight of proteins. nIP: non- IPTG induced pellet, nIL: non- IPTG induced lysate, IP: IPTG induced pellet, IL: IPTG induced lysate. Samples with the volume of 20 µL was loaded to 12% ClearPAGE gel, F1: the flowthrough after lysate addition, I20-I40: washing fractions with indicated concentration immidazole. Elution of recombinant PFLP performed with 100mM immidazole buffer (I100) resulted in two bands at 250 kDa and 23 kDa. Negative control (-) which was the lysate from cell culture containing empty pRSET B vector showed 20 and 12 kDa bands. All of the analysed samples were collected from BL 21(DE3)pLysS cell culture. Precision Plus Protein Standard (Bio-Rad, M) was used to estimate molecular weight of the proteins. The position of the expressed PFLP was indidcated with the red arrows.

3.6.4 Comparision of purified T-PFLP, PFLP and GFP

Protein samples eluted from Ni-NTA columns were run on the same gel (12% ClearPAGE gel) to evaluate the protein purifications including fractions I100.2, I200.1, I200.1 of PFLP, T-PFLP and GFP purifications, respectively (Figure 3.23). The cell lysate for these purifications was obtained from the sonicated cell lyses as mentioned in section **2.17**. The purified PFLP derived from the cell lysate by "freeze-thaw" method was also analysed on the same gel along with the negative controls which are the cell lysate of BL 21(DE3)pLysS containing pRSET B achieved by sonication (SL) or "freeze-thaw" (FL) method. Quantification of the purified proteins via Bradford method using Bio-rad Protein Assay were performed prior to the Western blotting of the proteins. Aliquots of 2 μg protein, approximately, of each sample were separated on a 12% ClearPAGE gel. The electrophoresis was followed by the membrane transblotting, immunoblotting and X-ray film development with CPS-3 reagents (Sigma). As shown in Figure 3.23 the purified PFLP proteins derived from the cell lysis by either sonication method (PFLP 1) or "freeze-thaw" method have the same molecular weight of 20 kDa and PFLP1 has the higher concentration than that of PFLP2. The expressed T-PFLP is within 20 and 15 kDa which is quite similar PFLP bands. Multiple bands were detected in GFP lane at positions 150 kDa, 100 kDa, 75 kDa and 22 kDa. The same patterns of proteins observed in the negative controls lanes (SL and FL) which is identical to the negative controls. However, the bands in PFLP and T-PFLP lanes are distinct from the detected bands in the negative controls.

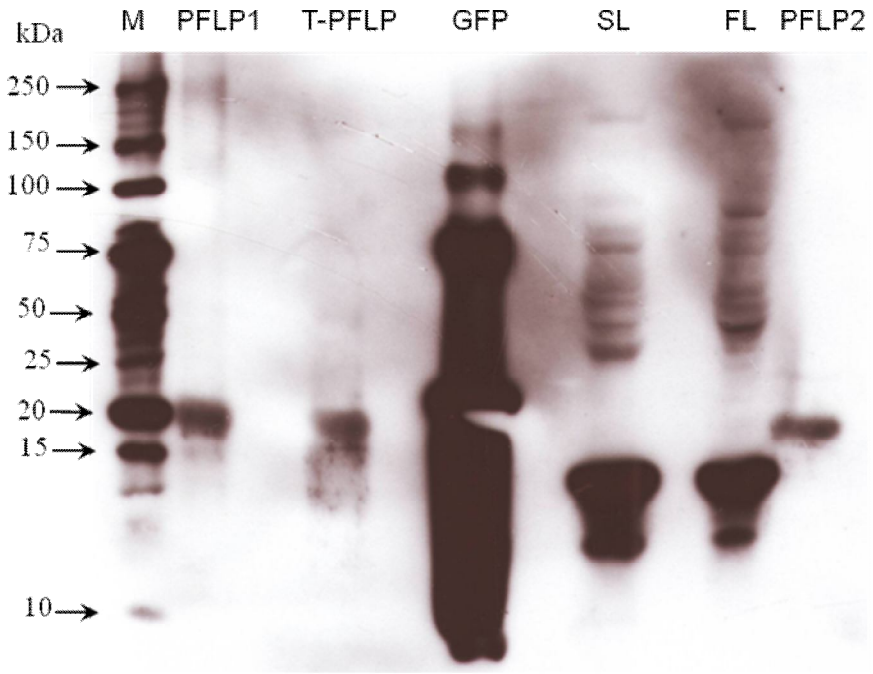

Figure 3.23 Western blot analysis of purified PFLP, T-PFLP and GFP

Purified PFLP, T-PFLP and GFP were run on the same gel along with the cell lysate of BL21(DE3)pLysS containing pRSET B as the negative controls. All of the analysed proteins were purified from sonicated cell lysate except PFLP2 derived from "free-thaw" extraction. The protein samples were separated on 12% ClearPAGE gel, transferred to nitrocellulose membrane for immunodetection with Anti HisG Antibody and HFP conjugates. The molecular weight values of PFLP1, PFLP2 and GFP are quite similar. Protein extract for the negative controls were achieved through different methods of cell disruption sonication (SL) or "Freeze-thaw" (FL) showed similar patterns and similar bands between 15 and 10 kDa.

Chapter 4 Discussion

4.1 Cloning of *Pflp* and T-*Pflp* from Capsicum

Pflp and T-*Pflp* were successfully isolated from Capsicum genomic DNA resulting in cloned DNA fragments. Upon sequence analysis a single base pair change (T-A to G-C) at position 202 compared to the coding region of the published sequence AF039662 was detected. This nucleotide change results in the presence of aspartic acid instead of asparagine in the deduced polypeptide from both the cloned *Pflp* and T-*Pflp* sequences. However, the deduced amino acid sequences of the isolated T-*Pflp* and *Pflp* excluding the signal sequence show 100% identity to Fd-I from *Capsicum annuum* var. *annuum* (Red pepper) (P83527).

Ferredoxin-based taxonomy research by Mino *et al.* (2003) found that there were 0-4 differences among ferredoxins from Solanaceae plants within the same genus whereas 14-40 differences occur between species from different families. Asparagine-aspartic acid substitution is known as a common amino acid change for the same protein from different organisms (Petsko & Ringe, 2004). It was reported that the replacement of asparagine at position 65 with aspartic acid in maize Fd-II increased the affinity of the protein with Fd-$NADP^+$ reductase (Matsumura, 1999). There is a possibility that the isolated ferredoxins (*Pflp* and T-*Pflp*) are structurally different from the ferredoxin encoded by AF039662 or Q9ZTS2 sequence and, thus, as a result they may have different activity and characteristics compared to the protein already reported by Dayakar *et al.* (2003).

The nucleotide difference between *Pflp* from Capsicum genomic DNA and from cDNA resulted in the substitution of a serine by a glycine at position 22 in the deduced polypeptide. This change located within the predicted transit peptide so it will have no effect on the tertiary structure and function of the mature functional protein. Alternatively, the difference detected may be an error in sequencing.

4.2 Expression vector constructions

The *Nco*I and *Eco*RI fragments of *Pflp* and T-*Pflp* were cloned, in frame, with the polyhistidine (6xHis) leader sequence of the pRSET B bacterial expression vector. As expected the single base pair change in the alignment of the cloned sequences in pRSET B vectors was consistent with the nucleotide difference observed in the previous sequencing results of *Pflp* and T-*Pflp* fragments that had been isolated. The molecular weight of 6xHis – tagged PFLP was predicted to be 20.2 kDa in the pRSET B system (Invitrogen) whereas it was reported to be 22.2 kDa in the pQE30 expression system (Qiagen) by Dayakar *et al*. (2003). As the Fd coding sequences in both cases have the same length and 99% identity, the discrepancy in molecular weight of the recombinant PFLP may be due to the different vectors and markers utilized. Moreover, the preparation of SDS polyacrylamide gels and samples for SDS-PAGE in both cases are also known to effect the migration of proteins.

4.3 Time course analysis of protein expression

Protein expression from *Pflp*/pRSET B and T-*Pflp*/pRSET B in the *E.coli* strain BL21(DE3)pLysS was carried out under similar conditions as those reported by Dayakar *et al.* (2003) in which 1 mM IPTG was used for the induction. Again, similar to Dayakat *et al.* (2003) the incubation was performed at 37^{o}C. The profile of total protein in the expression cultures increased significantly with the duration of IPTG induction (up to 6 h) as can be clearly seen on SDS polyacrylamide gels of the time course expressions. However, the levels of the expressed PFLP and T-PFLP appear indistinguishable from the basal levels of expression, which resemble that of the negative control. That is there appears to be no major induction of specific bands at the predicted size on the SDS gels. In contrast, however, expression of the GFP/pRSET is increased as can be clearly recognized by bands on the SDS gels of samples from the soluble fractions and, possibly, also in the insoluble fractions (Figure 3.18) clearly show. This low level of expression of the *Pflp* sequences may be due to the low concentration of the expressed Fd proteins. An alternate explanation may be that as the predicted molecular weight for the His-tagged forms of PFLP and T-PFLP is 19.6 and 15 kDa, respectively, the target proteins might appear at the same positions of the basal proteins between 22 and 12 kDa. With this is also the possibility of leaky expression from the T7 promoter leading to the increase of the basal expression, and low yield of the target proteins due to their toxicity to the host bacteria. This question was partly solved with protein purification followed by western blotting.

4.4 Evaluation of protein expression and purification by western blotting

Based on the affinity with nickel ions the 6xHis-tagged proteins expressed in *E.coli* were semi-purified by elution from affinity columns at high concentration of immidazole after the weakly bound proteins had been removed from the Ni-NTA matrix by washing. The 6xHis fused proteins were identified in samples pre- and post-purification with an Anti-His antibody and this in turn was bound with an Anti-mouse HRP conjugated antibody; these two acting as the primary antibody and secondary antibody respectively in a colourmetric detection assay. In all of the purifications less intense protein bands are detected in the elution fractions as observed after immunodetection compared to those in unpurified samples. Very low amounts of GFP and no Fd were detected in fraction washed with 250 mM imidazole (I250). This result suggests that all three of the His-tagged proteins (PFLP, T-PFLP and GFP) were mostly removed from the Ni-NTA columns with the introduction of the sodium buffers containing concentrations of immidazole between 100 mM and 200 mM. In addition to the His-tagged proteins some contaminants and cross-interacting proteins were also co-purified. There is also the possibility of polymerized forms of the same proteins which have molecular weights double or triple that of the protein original predicted weight being observed after SDS gel electrophoresis. This can be observed in the case of the 6xHis-tagged GFP (Figure 3.23). Polymerization seems to result in the appearance of a higher band in PFLP/I100 lanes at a position of approximately100 kDa (Figure 3.22) and at the position approximately 250 kDa (Figure 3.23).

The mis-folding forms of the proteins may be the cause of weak binding of the primary antibodies and the low density of the bands on the blots compared to the corresponding bands on the Coomassie stained gels. By contrast, high density of 6xHis-tagged proteins observed in insoluble and the first flow through fractions might be due to either inclusion bodies or cross-reactive aggregates in the samples. These aggregates could then be denatured prior to analysis by immunodetection, and as such then able to bind the Anti-His antibody, whereas as most were unable to bind Ni-NTA resins. Most of the expressed proteins might be present in inclusion bodies, thus, the obtained PFLP and T-PFLP in the elution fractions (I100/PFLP and I200/T-PFLP) was quite low (Figure 3.20C, 3.22). The 6xHis-GFP, by contrast, had high affinity with Ni-NTA as almost no GFP was detected in the first flow-through fraction, but was obtained at high amount in the elutate with 200 mM imidazole (I200). In addition, the GFP bands identified with anti–His antibody have the same molecular weight. The GFP in I20 and I30 fractions might be due to the insufficient capacity of the resins required for the binding of the amounts of protein present. Although the western blotting of GFP fractions lacking the insoluble samples, it is possible to infer from the blot that there is more GFP in the pellet than in the lysate from the induced cell lysate. This is additional evidence for the presence of inclusion bodies during the protein expression experiments.

.

4.5 Yield of the purified PFLP

4.5.1 Inclusion body formation during protein expression

Inclusion bodies result from over-expressed or mis-folded proteins that are segregate into insoluble aggregates (Bowden 1990; Baneyx 1999). Expression of foreign hydrophobic proteins was also reported to be toxic to the host bacteria and resulted in inclusion bodies

(Durbin, 1999; Shin, 2001). The His-tags of the proteins in the aggregates may have reduced exposure to the Ni resins that results in the low affinity bindings and their presence in the first flow through fraction. Denature purification is usually applied for these insoluble protein (QIAexpressionist). However, the presence of the target ferredoxins in the elution fractions suggests that the purifications under native conditions might be achieved by modifying the expression and purification conditions. Elimination of inclusion bodies might be achieved with protein expression procedure at lower temperature (rather than 37^{o}C), a shorter induction period with a lower concentration of IPTG and performing purification at 4^{o}C.

4.5.2 Protein polymerization

Another reason for the low yield of proteins may be polymerization. Disulfide bonds can be established among the target proteins (homologous) or in combination with host proteins (heterologous). Both polymerized forms of the protein can interact with Anti HisG antibody, though nickel resin affinity fluctuates in purifications under native conditions which might be due to the protein folding. An excess of IPTG used in the induction or insufficient reducing agent may cause discrepancy in bands on the immunoblots. The induced β-lactamase expression with 1 mM IPTG showed several bands in the polymerized form that cross-reacted with β-lactamase serum, which is absent when 0.0001-0.1 mM IPTG was used (Bowden, 1990). In addition to IPTG concentration in the induction, the introduction of BME into the cell lysis and sodium buffers for purifications is important in reducing disulfide bond formation. Although 20 mM BME was used in all purification buffers, polymerized proteins in homologous or heterologous forms were still present. This may due to BME evaporation during sonication and the prolonged washing steps. Additional BME should be added after cell lysis and the

purification steps need to be minimized and performed at 4^{o}C instead of room temperature. His-tagged proteins affinity for nickel ions should also be considered as it is affected at the higher concentration of BME (QIAexpressionist).

4.5.3 Inefficient expressions or protein toxicity?

Besides the inclusion body formation, low level expression of the target proteins is also a possible reason of their low yields. Plasmid loss was found in high density cultures, especially in cultures of plasmids bearing a gene encoding a protein toxic to the bacterial host (Baneyx, 1999). In the pRSET B system, similarly, gene expression of toxic proteins downstream of the T7 promoter limits the growth rate and may result in, cell death or plasmid instability. T7 lysozyme binds to T7 RNA polymerase and inhibits the transcription. However, as mentioned in previous section, PFLP and T-PFLP are iron-sulfur proteins and function in a variety metabolic processes as electron-transfer proteins. They are also components of several redox enzymes such as nitrite reductase, sulfite reductase, NADP reductase. In *E.coli,* Fd –NADP^{+} reductase (FNR) is the main regulator during the physiological switch between aerobic to anaerobic growth conditions (Mazoch, 2002; Kang, 2005). The ferredoxins within the Fd-FNR family are quite distinct from each other and the distribution of the cysteine residues functioning in iron biding in the polypeptide of bacterial Fd is different from that in plant Fd (Holden, 1999). The negative effect of Fd on bacterial growth has been reported (Huang, 2006), however, its mechanism is still a question. Changing the redox status of bacterial cell by the expressed PFLP and T-PFLP that decrease the growth rate of bacteria and the stability of the expression plasmids is possibly an answer for the low level expression of the target proteins. Optimization the protein expression and purification procedures to minimize the inclusion bodies will help answer the question.

4.6 Purified protein impurity

Contaminants were recognized in bands that are present in SDS polyacrylamide gels but absent in the immunoblots, but are unlikely to be polymerized forms of the target as they were not detected on the blots. These protein contaminants were co-purified along with the target proteins. Immidazole at the concentration of 10 mM was applied in the lysis buffer but it was inefficient to eliminate non-specific bindings. In this case, 20 mM immidazole can be used if it does not affect the bindings of the tagged proteins. Increasing the wash volume at 30 mM immidazole along with reducing bridging reactions with host proteins by BME may improve the protein purity. Moreover, nonspecific interactions with nickel ions can be reduced with Triton X-100 or Tween 20 (up to 2%) and high salt concentration (up to 2 M NaCl) (QIAexpressionist).

4.6 Immunodetection

Despite the recommended dilution for working solutions of the primary and secondary antibodies, their specificity and sensitivity need to be validated according to the obtained proteins. Western blottings of gradient protein amounts of which concentrations are estimated with the Bradford method along with a protein with known concentration (*e.g.* commercial BSA) need to be done to evaluate the sensitivity of the antibodies, especially the signal strength of the detection method. The immunoblotting were done using either CPS-3 reagent (Sigma) or the freshly prepared peroxidase substrate solution (pH 8.8). Different advantages were gained each kind of the substrate.

The commercial (ready- to -use) reagent was more sensitive, though, resulted rather in high backgrounds than the prepared substrate. In all of the performed blots, a low amount of protein were only detected with the addition of the CPS-3 substrate. The prepared substrate efficiently reduced the back ground signal but was incapable of detecting such low quantity of protein (Figure 3.20 B&C). The same protein patterns of the same blot developed with either substrate were only obtained within 20 minutes since the addition of the substrate. As similar molecular weights of PFLP, T-PFLP and GFP can be observed on the blot (Figure 3.23) the use of 15% SDS polyacrylamide gel for electrophoresis may offer well separated and distinct bands of each protein.

4.7 Future work

This study suggests higher recombinant protein yields are necessary before further experiments with the PFLP protein can be performed. These experiments may include bioassays using the purified proteins and potentially high level expression of these genes in transgenic plants. Improvement of protein yield and purity are suggested through adjustment of the protein expression and purification protocols. The protein induction with 0.01 - 0.5 mM IPTG will be investigated followed by the purifications performed at $4^{o}C$ and in more stringent conditions. Immunodetection protocols for His-tagged PFLP and T-PFLP will be standardized to evaluate the expression and purification of the target proteins. Besides, control expressions in which the protein content of the host cells as well as host cell with the empty pRSET vector will be taken into account to examine the basal expression of the host cell and the target proteins.

Possessing an iron binding domain, ferredoxins may compete with bacteria for iron utilization in iron defective media. The effect of purified PFLP and T-PFLP on growth of plant bacteria, both non-pathogenic and pathogenic, will be determined by bacterial inhibition bioassays. Moreover, as an electron transfer protein, Fd is a potential molecule involved in signal transmission in systemic acquired resistance. Although the interference of Fd in the early state of HR has been proved both *in vitro* and *in vivo* (Dayakar *et al.*, 2003; Huang *et al.*, 2004), the mechanism in which enhancement of HR and inhibition of bacterial growth was accomplished still remains poorly understood. The possible contribution of the transit sequence in antimicrobial activity needs to be considered when Fd is used for co-infiltration with pathogenic bacteria into plant leaves in HR assays.

When the mode of action of Fd towards increasing plant resistance against plant pathogenic bacteria is identified the application of the protein will be determined. It has been reported that transgenic plants of tomato and lili containing Capsicum *Pflp* have resistance against soft rot bacteria (Yip *et al.*, 2007; Huang *et al.*, 2007). If the ability to enhance plant defence of the isolated Capsicum Fd relies on the iron-binding domain and/or the transit sequence this characteristic can be extended to other ferredoxins types in the same genus and wider *Solanaceae* species . Tobacco would be a good model species for these studies.

4.8 Concluding remarks

In summary the research aimed to clone and express the gene encoding the Capsicum ferredoxin I. The Capsicum *Pflp* with and without signal sequence was isolated

and confirmed by comparison with the published sequence. The sequence analysis suggests the obtained Fd is different from the Fd identified by Dayakar *et al*. (2003), which may be due to the genetic variance within the same species.

Construction of expression vectors for *Pflp* and T-*Pflp* were accomplished with the identified proteins in purification. The protocols for purification of the His-tagged proteins has been established, though some modifications need to be done. The concentrations of the T-PFLP, PFLP and GFP eluates were 0.07, 0.1 and 1.1 mg/mL, respectively. It is evident that the protein yield and purity was affected by inclusion bodies, but the quality and quantity may be improved as indicated. Leaky expression of T7 polymerase and toxicity of the target proteins to the host should also be considered. Once production of PFLP and T-PFLP via *E. coli* is established, more knowledge on the interactions among the proteins, phytopathogenic bacteria and plants will be obtained.

References

Baker, C.J., Orlandi, E.W., and Anderson, A.J. (1997). Oxygen metabolism in plant cell culture/bacteria interactions: role of bacterial concentration and H_2O_2-scavenging in survival under biological and artificial oxidative stress. *Physiological and Molecular Plant Pathology* **51**(6): 401-415.

Baneyx, F. (1999). Recombinant protein expression in *Escherichia coli*. Current Opinion in Biotechnology **10**(5): 411-421.

Beattie, G.A., and Lindow, S.E. (1995). The Secret Life of Foliar Bacterial Pathogens on Leaves. *Annual Review of Phytopathology* **33**: 145-172

Beck, C.B. (2005). Periderm, rhytidome, and the nature of bark. *An Introduction to Plant Structure and Development.* Cambridge University Press.

Bent, A.F., and Mackey, D. (2007). Elicitors, Effectors, and *R* Genes: The New Paradigm and a Lifetime Supply of Questions. *Annual Review of Phytopathology* **45**: 399-436

Biruma, M., Pillay, M., Tripathi, L., Blomme, G., Abele, S., Mwangi, M., Bandyopadhyay, R., Muchunguzi, P., Kassim, S., Nyine., M., Turyagyenda, L., Eden-Green, S. (2007). Banana Xanthomonas wilt: a review of the disease, management strategies and future research directions. *African Journal of Biotechnology* **6**(8): 953-962

Blakeman, J.P. and Fokkema, N.J. (1982). Potential for Biological Control of Plant Diseases on the Phylloplane. *Annual Review of Phytopathology* **20**(1): 167-190.

Boudet, A.-M. (2003). Towards and understanding of the supramolecular organization of the lignified wall. *The Plant Cell Wall*. J. K. C. Rose. Ithaca, New York, Blackwell Publishing.

Bowden, G. A., and Georgiou, G. (1990). Folding and aggregation of beta-lactamase in the periplasmic space of *Escherichia coli*. Journal of Biological Chemistry **265**(28): 16760-16766.

Bubán, T. and Orosz-Kovács, Z. (2003). The nectary as the primary site of infection by *Erwinia amylovora* (Burr.) Winslow *et al.*: a mini review. *Plant Systematics and Evolution* **238**(1): 183-194.

Caetano-Anolles, G., Wall, L.G., De Micheli, A.T., Macchi, E.M., Bauer, W.D., and Favelukes, G. (1988). Role of motility and chemotaxis in efficiency of nodulation by *Rhizobium meliloti*. *Plant Physiology*. **86**(4): 1228-1235.

California Institute of Technology (2005). *Preparation of electrocompetent cells*. Retrieved November 15, 2009 from http://www.its.caltech.edu/~bjorker/Protocols/Prep_of_electocomp_cells.pdf

Chet, I., Zilberstein, Y., and Henin, Y. (1973). Chemotaxis of *Pseudomonas lachrymans* to plant extracts and to water droplets collected from the leaf surfaces of resistant and susceptible plants. *Physiologial Plant Pathology* **3**(4): 473-479.

Choudhary, D., A. Prakash, A., Johri, B. (2007). Induced systemic resistance (ISR) in plants: mechanism of action. *Indian Journal of Microbiology* **47**(4): 289-297.

Das, A. K. (2003). Citrus canker - A review. *Journal of Applied Horticulture* **5**(1): 52-60

Dayakar, B.V., Lin, H.-J., Chen, C.-H., Ger, M.-J., Lee, B.-H., Pai, C.-H., Chow, D., Huang, H.-E, Hwang, S.-Y., Chung, M.-C., Feng, T.-Y. (2003). Ferredoxin from sweet pepper (*Capsicum annuum* L.) intensifying harpinpss-mediated hypersensitive response shows an enhanced production of active oxygen species (AOS). *Plant Molecular Biology* **51**(6): 913-924.

Donaldson, L. A. (1992). Lignin distribution during latewood formation in *Pinus radiata*. *IAWA Bulletin n.s.* **12**.

Dow, J.M., Osbourn, A.E., Wilson, T.J.G., and Daniels, M.J. (1995). A locus determining pathogenicity of *Xanthomonas campestris* is involved in lipopolysaccharide biosynthesis. *Molecular Plant -Microbe Interactions* **8**(5): 768-777

Dow, M., Newman, M.-A., and von Roepenack, E. (2000). The induction and modulation of plant defense responses by bacterial lipopolysaccharides. *Annual Review of Phytopathology* **38**(1): 241-261.

Dube, S., Singh, L., and Alam, S.I. (2001). Proteolytic anaerobic bacteria from lake sediments of Antarctica. *Enzyme and Microbial Technology* **28**(1): 114-121.

Dulce, N.R.-N., Marta, S.D., José, E.R.-S. (2007). Attachment of bacteria to the roots of higher plants. *FEMS Microbiology Letters* **272**(2): 127-136.

Durbin, R. (1999). Gene expression systems based on bacteriophage T7 RNA polymerase. Gene Expression Systems. J. M. Fernandez, and J. P. Hoeffler. Academic Press, US.

Durner, J., Shah, J. and Klessig, D.F. (1997). Salicylic acid and disease resistance in plants. *Trends in Plant Science* **2**(7): 266-274.

Edlund, A.F., Swanson, R. and Preuss, D. (2004). Pollen and stigma structure and function: the role of diversity in pollination. *Plant Cell* **16**(suppl_1): S84-97.

Edreva, A. (2005). Pathogenesis-related proteins: Research progress in the last 15 years. *General and Applied Plant Physiology* **31**(1-2): 105-124.

Ellis, S. D., Boehm, M. J., and Coplin, D. 2008. Bacterial diseases of plants [Fact sheet]. Retrieved Feb 3, 2010 from http://ohioline.osu.edu/hyg-fact/3000/pdf/PP401_06.pdf

Everett, K.R., Hallett, I.C., Rees-George, J., Chynoweth, R.W., and Pak, H.A. (2008). Avocado lenticel damage: The cause and the effect on fruit quality. *Postharvest Biology and Technology* **48**(3): 383-390.

Forbes, G.A., Mizubuti, E.S.G., and Shtienberg, D. (2009). Plant disease epidemiology and disease management – Has science had an impact on practice? *Integrated Pest Management: Innovation-Development Process* **1:** 351-368.

Fromm, J., Rockel, B., Lautner, S., Windeisen, E., and Wanner, G. (2003). Lignin distribution in wood cell walls determined by TEM and backscattered SEM techniques. *Journal of Structural Biology* **143**(1): 77-84.

Frossard, R., and Oertli J.J. (1982). Growth and germination of fungal spores in guttation fluids of barley grown with different nitrogen sources. *Transactions of the British Mycological Society* **78**(2): 239-245.

Garrod, B., Lewis, B.G., Brittain, M.J. and Davies, W.P (1982). Studies on the contribution of lignin and suberin to the impedance of wounded carrot root tissue to fungal invasion. *New Phytologist* **90**(1): 99-108.

Ghuysen, J.M., and Hakenbeck, R., Eds. (1994). *Bacterial Cell Wall*. New Comprehensice Biochemistry, Elsevier.

Goatley, J.L., and Lewis, R.W. (1966). Composition of guttation fluid from rye, wheat, and barley seedlings. *Plant Physiol.* **41**(3): 373-375.

Gohre, V., and Robatzek, S. 2008. Breaking the Barriers: Microbial Effector Molecules Subvert Plant Immunity. *Annual Review of Phytopathology* **46**(1): 189-215.

Goodman, R.N. (1978). Inducible resistance responses in plants to plant pathogenic bacteria. *Mycopathologia* **65**(1): 107-113.

Hall, T. (2005). *BioEdit*. Retrieved October 20, 2009 from http://www.mbio.ncsu.edu/BioEdit/page2.html

Hallmann, J. (2001). Plant interactions with endophytic bacteria. *Biotic Interactions in Plant-Pathogen Associations*. M. J. Jeger and N. J. Spence. UK, CABI Publishing.

Hammerschmidt, R. (1999). Induced disease resistance: how do induced plants stop pathogens? *Physiological and Molecular Plant Pathology* **55**(2): 77-84.

Heil, M. (2001). Induced systemic resistance (ISR) against pathogens - a promising field for ecological research. *Perspectives in Plant Ecology, Evolution and Systematics* **4**(2): 65-79.

Heil, M., and Bostock, R.M. (2002). Induced Systemic Resistance (ISR) Against Pathogens in the Context of Induced Plant Defences. *Annals of Botany* **89**(5): 503-512.

Holden, H. M., Jacobson, B. L., Hurley, J. K., Tollin, G., Oh, B-.H., Skjedal, L., Chae, Y. K., Cheng, H. C., Xia, B., and Markley, J. (1994). Structure-function studies of [2Fe-2S] ferredoxins. *Journal of Bioenergetics and Biomembranes* **26**(1): 67-88.

Holtsmark, I., Eijsink, V.G.H., Brurberg, M.B. (2008). Bacteriocins from plant pathogenic bacteria. *FEMS Microbiology Letters* **280**(1): 1-7.

Huang, H.-E., Ger,M.-J., Cheng, C.-Y., Pandey, A.-K., Yip, M.-K., Chou, H.-W. and Feng, T.-Y. (2007). Disease resistance to bacterial pathogens affected by the amount of ferredoxin-I protein in plants. *Molecular Plant Pathology* **8**(1): 129-137.

Huang, H.-E., Liu, C.-A., Lee, M.-J., Kuo, C.-G., Chen, H.-M., Ger, M.-J., Tsai, Y.-C., Chen, Y.-R., Lin, M.-K., and Feng, T.Y. (2007). Resistance enhancement of transgenic tomato to bacterial pathogens by the heterologous expression of sweet pepper Ferredoxin-I protein. *Phytopathology* **97**(8): 900-906.

Huang, H.-E., Ger, M.-J., Cheng, C.-Y., Yip, M.-K., Chung, M.-C., and Feng, T.-Y. (2006). Plant ferredoxin-like protein (PFLP) exhibits an anti-microbial ability against soft-rot pathogen *Erwinia carotovora* subsp. *carotovora in vitro* and *in vivo*. *Plant Science* **171**(1): 17-23.

Huang, H.-E., Ger,M.-J., Yip, M.-K., Cheng, C.-Y., Pandey, A.-K., and Feng, T.-Y. (2004). A hypersensitive response was induced by virulent bacteria in transgenic tobacco plants overexpressing a plant ferredoxin-like protein (PFLP). *Physiological and Molecular Plant Pathology* **64**(2): 103-110.

Huang, J. (1986). Ultrastructure of Bacterial Penetration in Plants. *Annual Review of Phytopathology* **24**(1): 141-157.

Hueck, C.J. (1998). Type III protein secretion systems in bacterial pathogens of animals and plants. *Microbiology and Molecular Biology Reviews* **62**(2): 379-433.

Hutcheson, S.W. (1998). Current concepts of active defense in plants. *Annual Review of Phytopathology* **36**(1): 59-90.

Invitrogen (1998). pRSET Expression Systems. Product Manual. USA

Jane, R., and Linda, R., Eds. (2002). *Lab Ref.* A handbook of Recipes, Reagents, and other Reference Tools for Use at the Bench. New York, Cold Spring Harbor Laboratory Press.

Janse, J.D. (2005). *Phytobacteriology Principles and Practice*. CABI Publishing.

Kang, Y., Weber, K.D., Qiu, Y., Kiley, P.J., and Blattner, F.R. (2005). Genome-wide expression analysis indicates that FNR of *Escherichia coli* K-12 regulates a large number of genes of unknown function. *Journal of Bacteriology* **187**(3): 1135-1160.

Kelman, A., and Hruschka J. (1973). The role of motility and aerotaxis in the selective increase of avirulent bacteria in still broth cultures of *Pseudomonas solanacearum*. *The Journal of General Microbiology* **76**(1): 177-188.

Kenoyer, L.A. (1903). Winter condition of lenticels. *Transactions of the Kansas Academy of Science* **22**: 323-326.

Kloepper, J.W., Ryu, C.-M. and Zhang, S. (2004). Induced systemic resistance and promotion of plant growth by *Bacillus* spp. *Phytopathology* **94**(11): 1259-1266.

Kolattukudy, P.E., and Dean, B. B. (1976). Synthesis of suberin during wound-healing in jade leaves, tomato fruit, and bean pods. *Plant Physiology* **58**: 411-416.

Kolattukudy, P.E. (1980). Biopolyester membranes of plants: Cutin and Suberin. *Science* **208**: 990-1000.

Kolattukudy, P.E. (2001). Plant cuticle and suberin. *Encyclopedia of Life Sciences*, John Wiley & Sons, Ltd.

Langebartels, C., Wohlgemuth, H., Kschieschan, S., Grun, S., and Sandermann, H. (2002). Oxidative burst and cell death in ozone-exposed plants. *Plant Physiology and Biochemistry* **40**(6-8): 567-575.

Lippincott, B.B., and Lippincott, J.A. (1969). Bacterial attachment to a spesific wound site as an essential stage in tumor initiation by *Agrobacterium tumefaciens*. *Journal of Bacteriology* **97**(2): 620-628.

Loper, J.E. and Buyer, J.S. (1991). Siderophores in microbial interactions on plant surfaces. *Molecular plant -Microbe interactions* **4**(1): 5-13.

Macnab, R.M. and Aizawa, S.I. (1984). Bacterial motility and the bacterial flagellar motor. *Annual Review of Biophysics and Bioengineering* **13**(1): 51-83.

Maldonado, A.M., Doerner, P., Dixon, R.A., Lamb, C.J. and Cameron, R.K. (2002). A putative lipid transfer protein involved in systemic resistance signalling in Arabidopsis. *Nature* **419**(6905): 399-403.

Manson, M.D. (1990). Introduction to bacterial motility and chemotaxis. *Journal of Chemical Ecology* **16**(1): 107-118.

Matsumura, T., Kimata-Ariga, Y., Sakakibara, H., Sugiyama, T., Murata, H., Takao, T., Shimonishi, Y., and Hase, T. (1999). Complementary DNA cloning and characterizaton of ferredoxin localized in bundle-sheath cells of maize leaves. *Plant Physiology* **119**.

Mazzucchi, U., Bazzi, C., and Pupillo, P. (1979). The inhibition of susceptible and hypersensitive reactions by protein-lipopolysaccharide complexes from phytopathogenic

pseudomonads: relationship to polysaccharide antigenic determinants. *Physiological Plant Pathology* **14**(1): 19-30.

Mazzucchi, U., and Pupillo, P. (1976). Prevention of confluent hypersensitive necrosis in tobacco leaves by a bacterial protein-lipopolysaccharide complex. *Physiological Plant Pathology* **9**(2): 101-112.

McManus, P. S., and Stockwell, V. O. (2001). Antibotic use for plant disease management in the United States. *Plant Health Progress* (online journal). doi:10.1094/PHP-2001-0327-01-RV.

Mellick, A. S. and Rodgers, L., Eds. (2007). *Lab Ref.* A Handbook of Recipes, Reagents, and other Reference tools for use at the bench Vol.2. Cold Spring Harbor Laboratory Press, New York.

Melotto, M., Underwood, W. and He, S.Y. (2008). Role of stomata in plant innate immunity and foliar bacterial diseases. *Annual Review of Phytopathology* **46**(1): 101-122.

Melotto, M., Underwood, W., Koczan, J., Nomura, K. and He, S.Y (2006). Plant stomata function in innate immunity against bacterial invasion. *Cell* **126**(5): 969-980.

Meyer, J. (2001). Ferredoxins of the third kind. *FEBS Letters* **509**(1): 1-5.

Meyer, J. (2008). Iron–sulfur protein folds, iron–sulfur chemistry, and evolution. *Journal of Biological Inorganic Chemistry* **13**(2): 157-170.

Mino, Y., Hazama, T., and Machida, Y. (2003). Large differences in amino acid sequences among ferredoxins from several species of genus Solanum. *Phytochemistry* **62**(5): 657-662.

Mohan, R., Bajar, A.M. and Kolattukudy, P.E. (1993). Induction of a tomato anionic peroxidase gene (tap1) by wounding in transgenic tobacco and activation of tap1/GUS and tap2/GUS chimeric gene fusions in transgenic tobacco by wounding and pathogen attack. *Plant Molecular Biology* **21**(2): 341-354.

Molinari, S. and Loffredo, E. (2006). The role of salicylic acid in defense response of tomato to root-knot nematodes. *Physiological and Molecular Plant Pathology* **68**(1-3): 69-78.

Montesinos, E., Bonaterra, A., Badosa, E., Francés, J., Alemany, J., Llorente, I. and Moragrega, C. (2002). Plant-microbe interactions and the new biotechnological methods of plant disease control. *International Microbiology* **5**(4): 169-175.

Montesinos, E. and Vilardell, P. (2001). Effect of bactericides, phosphonates and nutrient amendments on blast of dormant flower buds of pear: a field evaluation for disease control. *European Journal of Plant Pathology* **107**(8): 787-794.

Mortenson, L.E., Valentine, R.C. and Carnahan, J.E. (1962). An electron transport factor from. *Biochemical and Biophysical Research Communications* **7**(6): 448-452.

Mugira, F. (2009). Uganda loses $8bn to banana disease, African News.

Nawrath, C., Métraux, J.-P. and Genoud, T. (2006). Chemical signals in plant resistance: salicylic acid. *Multigenic and Induced Systemic Resistance in Plants***:** 143-165.

Neish, P.G., Drinnan, A.N. and Ladiges, P.Y. (1995). Anatomy of leaf-margin lenticels in *Eucalyptus denticulata* and three other Eucalypts. *Australian Journal of Botany* **43**(2): 211-221.

Newman, M.-A., Daniels, J.M. and Dow, J.M. (1995). Lipopolysaccharide from *Xanthomonas campestris* induces defense-related gene expression in *Brassica campestris*. *Molecular Plant -Microbe Interactions* **8**(5): 778-780.

Newman, M. A., Dow, J. M. and Daniels, M. J. (2001). Bacterial lipopolysaccharides and plant-pathogen interactions. *European Journal of Plant Pathology* **107**(1): 95-102.

Norelli, J.L., Holleran, H.T., Johnson, W.C., Robinson, T.L. and Aldwinckle, H.S. (2003). Resistance of geneva and other apple rootstocks to *Erwinia amylovora*. *Plant Disease* **87**(1): 26-32.

O'Neill, M.A., and York, W.S. (2003). The composition and structure of plant primary cell walls. *The Plant Cell Wall*. J. K. C. Rose. Ithaca, New York, Blackwell Publishing.

Ogle, H., and Dale, M. (1997). Disease management: Cultural Practices. *Plant Pathogens and Plant Disease*. J. F. Brown and H. J. Ogle. Australia, Rockvale Publications.

Ottow, J.C.G. (1975). Ecology, physiology, and genetics of fimbriae and pili. *Annual Review of Microbiology* **29**(1): 79-108.

Panopoulos, N.J. and Schroth, M.N. (1974). Role of flagellar motility in the invasion of bean leaves by *Pseudomonas phaseolicola*. *Phytopathology* **64**(11): 1389-1397.

Petsko, G. A., and Ringe, D. (2004). Protein structure and Function. New Science Press Ltd. UK

Promega (2000). pGEM-T and pGEM-T Easy vector. Technical Manual.USA

Qiagen (2000). *Ni-NTA Spin Handbook*

Qiagen (2003). *The QIAexpressionist.*

Rajan, S. S. (2003). *Physiology of transport in plants*. New Delhi, Anmol Publications PVT. Ltd.

Rico, A., Jones, R. and Preston, G.M. (2009). Adaptation to the plant apoplast by plant pathogenic bacteria. *Plant Pathogenic Bacteria: Genomics and Molecular Biology*. R. W. Jackson, Caister Academic Press.

Romantschuk, M. (1992). Attachment of plant pathogenic bacteria to plant surfaces. *Annual Review of Phytopathology* **30**(1): 225-243.

Romantschuk, M., Nurmiaho-Lassila, E.-L., Roine, E. and Suoniemi, A. (1993). Pilus-mediated adsorption of *Pseudomonas syringae* to the surface of host and non-host plant leaves. *The Journal of General Microbiology* **139**(9): 2251-2260.

Saleem, M., Arshad, M., Hussain, S. and Bhatti, A. (2007). Perspective of plant growth promoting rhizobacteria (PGPR) containing ACC deaminase in stress agriculture. *Journal of Industrial Microbiology and Biotechnology* **34**(10): 635-648.

Sambrook, J. and Russell , D.W. (2001). *Molecular Cloning: A Laboratory Manual*, Cold Spring Harbor Laboratory Press.

Sbragia, R.J. (1975). Chemical control of plant diseases: an exciting future. *Annual Review of Phytopathology* **13**(1): 257-269.

Scholthof, K.-B.G. (2007). The disease triangle: pathogens, the environment and society. *Nature Review Microbiology* **5**(2): 152-156.

Schulze-Lefert, P. and Robatzek, S. (2006). Plant pathogens trick guard cells into opening the gates." *Cell* **126**(5): 831-834.

Shin, H.-C. (2001). Protein folding, misfolding, and refolding of therapeutic proteins. *Biotechnology and Bioprocess Engineering* **6**(4): 237-243.

Shoda, M. (2000). Bacterial control of plant diseases. *Journal of Bioscience and Bioengineering* **89**(6): 515-521.

Sigee, D.C. (1993). *Bacterial Plant Pathology: Cell and Molecular aspects*, Cambridge University Press.

Singh, S., Singh, T.N., and Chauhan, J.S. (2009). Guttation in rice: occurrence, regulation, and significance in varietal improvement. *Journal of Crop Improvement* **23**(4): 351 - 365.

Staub, T., and Williams, P.H. (1972). Factors influencing black rot lesion development in resistant and susceptible cabbage. *Phytopathology* **62**(2): 722-728.

Sticht, H., and Rösch, P. (1998). The structure of iron-sulfur proteins. *Progress in Biophysics and Molecular Biology* **70**(2): 95-136.

Strange, R.N. (2003). *Introduction to Plant Pathology*. London, John Wiley & Sons Ltd.

Tagawa, K. and Arnon, D. (1962). Ferredoxin as electron carriers in photosynthesis and in the biological production and consumption of hydrogen gas. *Nature* **195**: 537-543.

Taguchi, F., Suzuki, T., Takeuchi, K., Inagaki, Y., Toyoda, K., Shiraishi, T. and Ichinose, Y. (2009). Glycosylation of flagellin from *Pseudomonas syringae* pv. *tabaci* 6605 contributes to evasion of host tobacco plant surveillance system. *Physiological and Molecular Plant Pathology* **74**(1): 11-17.

The American Phytopathological Society (2010). *Plant Disease management Strategies*. Retrieved February 11, 2010 from http://www.apsnet.org/education/AdvancedPlantPath/Topics/Epidemiology/ManagementStrategies.htm

Titarenko, E., López-Solanilla, E., García-Olmedo, F. and Rodríguez-Palenzuela, P. (1997). Mutants of *Ralstonia (Pseudomonas) solanacearum* sensitive to antimicrobial peptides are altered in their lipopolysaccharide structure and are avirulent in tobacco. *Journal of Bacteriology* **179**(21): 6699-6704.

Torii, K. U. (2006). *Stomatal development*. Retrieved January 30, 2010 from http://faculty.washington.edu/ktorii/stomata.html

Turnbull, G.A., Morgan, J.A.W., Whipps, J.M. and Saunders, J.R. (2001). The role of bacterial motility in the survival and spread of *Pseudomonas fluorescens* in soil and in the attachment and colonisation of wheat roots. *FEMS Microbiology Ecology* **36**(1): 21-31.

van der Zwet, T. (1993). Present distribution of fire blight and its mode of dissemination - a review. *Acta Horticulturae (ISHS)* **367**.

van der Zwet, T. and Bonn, W.G. (1999). Recent spread and current worldwide distribution of ffire blight. *Acta Horticulturae (ISHS)* **489**.

van Loon L.C., Geraats, B.P.J., and Linthorst, H.J.M. (2006). Ethylene as a modulator of disease resistance in plants. *Trends in Plant Science* **11**(4): 184-191.

van Loon, L.C. (1997). Induced resistance in plants and the role of pathogenesis-related proteins. *European Journal of Plant Pathology* **103**(9): 753-765.

van Loon, L.C., Bakker, P.A.H.M. and Pieterse, C.M.J. (1998). Systemic resistance induced by rhizosphere bacteria. *Annual Review of Phytopathology* **36**(1): 453-483.

van Loon, L.C. and van Strien, E.A. (1999). The families of pathogenesis-related proteins, their activities, and comparative analysis of PR-1 type proteins *Physiological and Molecular Plant Pathology* **55**(2): 85-97.

Vesprini, J.L., Nepi, M. and Pacini, E. (1999). Nectary structure, nectar secretion patterns and nectar composition in two *Helleborus* species. *Plant Biology* **1**(5): 560-568.

Vesper, S.J. and Bauer, W.D. (1986). Role of pili (fimbriae) in attachment of *Bradyrhizobium japonicum* to soybean Roots. *Applied Environmental Microbiology* **52**(1): 134-141.

Vidaver, A.K. (1976). Prospects for control of phytopathogenic bacteria by bacteriophages and bacteriocins. *Annual Review of Phytopathology* **14**: 451-465.

Watanabe, N. and Lam, E. (2006). The hypersensitive response in plant disease resistance. *Multigenic and Induced Systemic Resistance in Plants***:** 83-111.

Waheed (2007). Ni-NTA Agarose from QIAGEN. Retrieved November 30, 2009 from http://www.biocompare.com/Articles/ProductReview/825/Ni-NTA-Agarose-From-Qiagen.html..

Whetten, R. and Sederoff , R. (1995). Lignin biosynthesis. *The Plant Cell* **7**: 1001-1013.

Young, D.H., Stemmer, W.P.C. and Sequeira, L. (1985). Reassembly of a fimbrial hemagglutinin from *Pseudomonas solanacearum* after purification of the subunit by preparative sodium dodecyl sulfate-polyacrylamide gel electrophoresis. *Applied Environmental Microbiology* **50**(3): 605-610.